AFFDL-TR-76-67

AD A031403

A JOINT ARMY/AIR FORCE INVESTIGATION OF REFLECTION COEFFICIENTS AT C AND Ku BANDS FOR VERTICAL, HORIZONTAL AND CIRCULAR SYSTEM POLARIZATIONS

IIT RESEARCH INSTITUTE
CHICAGO, ILLINOIS

JULY 1976

FINAL REPORT FOR PERIOD NOVEMBER 1975 to FEBRUARY 1976

Approved for public release; distribution unlimited

Prepared For
AIR FORCE FLIGHT DYNAMICS LABORATORY
AIR FORCE WRIGHT AERONAUTICAL LABORATORIES
AIR FORCE SYSTEMS COMMAND
WRIGHT-PATTERSON AIR FORCE BASE, OHIO 45433

AVIONICS LABORATORY
US ARMY ELECTRONICS COMMAND
FORT MONMOUTH, NEW JERSEY 07703

DDC
RECEIVED
NOV 1 1976
B

NOTICE

When Government drawings, specifications, or other data are used for any purpose other than in connection with a definitely related Government procurement operation, the United States Government thereby incurs no responsibility nor any obligation whatsoever; and the fact that the government may have formulated, furnished, or in any way supplied the said drawings, specifications, or other data, is not to be regarded by implication or otherwise as in any manner licensing the holder or any other person or corporation, or conveying any rights or permission to manufacture, use, or sell any patented invention that may in any way be related thereto.

This report was submitted by IIT Research Institute, Chicago, Illinois, under Contract F33615-76-C-3044, with the AF Flight Dynamics Laboratory, Wright-Patterson Air Force Base, Ohio. Mr. Terry J. Emerson, AFFDL/FGT was the Air Force Program Manager. Mr. Walter Melnick, AFFDL/FGT was the Air Force Project Engineer, and Mr. Paul S. Demko, ECOM/DRSEL-VL-G was the Army Project Engineer. Mr. George W. Palmer, AFFDL/FGT was the Contract Monitor.

This report has been reviewed by the Information Office (OI) and is releasable to the National Technical Information Services (NTIS). At NTIS, it will be available to the General Public, including foreign nations.

This technical report has been reviewed and is approved for publication.

Walter Melnick
WALTER MELNICK
AF Project Engineer

Paul S. Demko
PAUL S. DEMKO
Army Project Engineer

FOR THE COMMANDER

Edward L. Heft
EDWARD L. HEFT, LT COL, USAF
Chief, Terminal Area Control Br
Flight Control Division

Copies of this report should not be returned unless return is required by security considerations, contractual obligations, or notice on a specific document.

AIR FORCE - 1 OCTOBER 76 - 125

UNCLASSIFIED

SECURITY CLASSIFICATION OF THIS PAGE (When Data Entered)

REPORT DOCUMENTATION PAGE	READ INSTRUCTIONS BEFORE COMPLETING FORM
1. REPORT NUMBER: AFFDL-TR-76-67	2. GOVT ACCESSION NO.
3. RECIPIENT'S CATALOG NUMBER	
4. TITLE (and Subtitle): A JOINT ARMY/AIR FORCE INVESTIGATION OF REFLECTION COEFFICIENTS AT C AND KU BANDS FOR VERTICAL, HORIZONTAL AND CIRCULAR SYSTEM POLARIZATIONS.	5. TYPE OF REPORT & PERIOD COVERED: Final rept. Nov 1975-Feb 1976
	6. PERFORMING ORG. REPORT NUMBER
7. AUTHOR(s): A. E. Brindley, L. C. Calhoun, T. N. Patton	8. CONTRACT OR GRANT NUMBER(s): F33615-76-C-3044 NEW
9. PERFORMING ORGANIZATION NAME AND ADDRESS: IIT Research Institute, 10 West 35th Street, Chicago, Illinois 60616	10. PROGRAM ELEMENT, PROJECT, TASK AREA & WORK UNIT NUMBERS: AF-404L0124
11. CONTROLLING OFFICE NAME AND ADDRESS: AF Flight Dynamics Laboratory (AFFDL/FGT), Air Force Wright Aeronautical Laboratories, Wright-Patterson Air Force Base, Ohio 45433	12. REPORT DATE: July 1976
	13. NUMBER OF PAGES: 149
14. MONITORING AGENCY NAME & ADDRESS (if different from Controlling Office): Avionics Laboratory, US Army Electronics Command, Fort Monmouth, New Jersey 07703	15. SECURITY CLASS. (of this report): Unclassified
	15a. DECLASSIFICATION/DOWNGRADING SCHEDULE

16. DISTRIBUTION STATEMENT (of this Report)

Approved for Public Release; Distribution Unlimited

160p.

17. DISTRIBUTION STATEMENT (of the abstract entered in Block 20, if different from Report)

18. SUPPLEMENTARY NOTES

19. KEY WORDS (Continue on reverse side if necessary and identify by block number)

Multipath
Reflection Coefficient
Polarization
Ground Illumination
Fresnel Zone
Grazing Angles
Spectra

20. ABSTRACT (Continue on reverse side if necessary and identify by block number)

This report describes an experimental effort to measure the reflection coefficients of typical airport structures at C-Band (5000 MHz) and Ku Band (15,000 MHz) for vertical (VP), horizontal (HP), and circular (CP) system polarizations. The choice of polarization is of vital concern in the implementation of microwave landing systems since it offers the designer an opportunity to minimize multipath reflections - the most critical factor limiting system performance.

DD FORM 1 JAN 73 1473 EDITION OF 1 NOV 65 IS OBSOLETE

UNCLASSIFIED

SECURITY CLASSIFICATION OF THIS PAGE (When Data Entered)

175350

The measurements were made on buildings along the flight lines of Areas B and C at Wright-Patterson AFB, Ohio.

The rationale for the test procedure is outlined, the test sites are described and the test results are presented in both detail and summary forms.

It is shown for sixteen different combinations of frequency, grazing angle and reflecting surface that vertical polarization produced more severe specular reflections than either horizontal or circular radiation in every case. The HP measurements showed an advantage of at least 3 db over VP for 81% of the cases and in 88% of the cases the CP exhibited a similar advantage over VP.

This combination of multi-frequency, multi-polarization data at the same sites represents a unique contribution of information to the MLS community.

FOREWORD

This document describes the work performed by IIT Research Institute, Chicago, Illinois, under Contract F33615-76-C-3044, Program Element 404L0124, for the Air Force Flight Dynamics Laboratory during the period November 1975 to February 1976. The work was supported by funds and technical assistance from the U.S. Army Electronics Command, Fort Monmouth, New Jersey.

The technical results show convincing evidence that horizontal and circular system polarizations offer significant potential advantages over vertically polarized systems in reducing the level of multipath interference to landing guidance signals in typical airport environments. The principal IITRI contributors to the program were Dr. T. N. Patton, L. C. Calhoun and A. E. Brindley (Program Manager). The Air Force Project Engineer was Mr. Walter Melnick. The Army Project Engineer was Mr. Paul Demko. The report was submitted by the authors February 1976.

The authors wish to express their appreciation to the U.S. Army Electronics Command for the support provided during this effort. Special thanks are due to Mr. Paul Demko whose personal participation and high level of enthusiasm for the work were a major factor in its success.

Thanks are also due to the staff of the Air Force Flight Dynamics Laboratory, notably Mr. Virgil Weinder (AFFDL/FGT) and SSgt Dan Martin (AFFDL/FGT) whose patience during long hours of field testing was exemplary.

TABLE OF CONTENTS

	PAGE
I. INTRODUCTION	
1.1 Purpose	1
1.2 Background	2
1.3 Summary of Program	3
1.3.1 Summary of Basic Technique	3
1.3.2 Measurement of Corrugated Surface Reflections	5
1.3.3 Comparison of Short Range Measurements with Operational Geometry Test	6
1.4 Report Organization	6
II. PROGRAM DESCRIPTION	
2.1 Technical Considerations and Constraints	7
2.1.1 Choice of Experimental Parameters	8
2.1.2 Problem Areas	13
2.2 Basic Experiments	22
2.2.1 Short Range Experiments	23
2.2.2 Long Range Experiments	32
2.2.3 Supporting Measurements	37
III. EXPERIMENTAL RESULTS - REFLECTION COEFICIENTS VS POLARIZATION	
3.1 Survey Data	39
3.2 Reflection Data for Nominally Flat Surfaces	39
3.3 Reflection Data for Corrugated Surfaces	58
3.3.1 Field Test Data	58
3.3.2 Comparison with Scale Model Measurements	71
3.4 Results of Long Range Test on Building 206	72

	PAGE
IV. EXPERIMENTAL RESULTS - GROUND ILLUMINATION EFFECTS	
4.1 Purpose	75
4.2 Experimental Technique	75
4.3 Observations	80
4.4 Conclusions	80
V. CONCLUSIONS AND RECOMMENDATIONS	
5.1 Comments on Data	82
5.2 Summary Conclusions	88
5.3 Recommendations	89
REFERENCES	91
APPENDIX A - Site Surveys	92
APPENDIX B - Geometric Considerations	139

LIST OF ILLUSTRATIONS

Figure No.	Title	Page
1	General Experimental Geometry	9
2	Ground Reflection Geometry	11
3a	Surface Illumination - C Band	14
3b	Surface Illumination - Ku Band	15
4	Direct Path View Showing Placement of ECCOSORB	17
5	Reflect Path View Showing Placement of ECCOSORB	18
6	Basic Instrumentation	24
7	Short Range Reflection Loss Measurement	25
8	Reflecting Region and Detail Structure of Building 1	28
9	Reflecting Region and Detail Structure of Building 485	29
10	Building 206 - Area C - Wright-Patterson AFB	30
11	Reflecting Region and Detail Structure of Building 22	31
12	Antenna Mounts for Measurement of Corrugated Surface of Building 22	33
13	Long Range Test Geometry Area C, WPAFB, Building 206	35
14	Expanded Test Geometry - Area C, WPAFB Building 206	36
15	Site Map - Area B - Long Range Test Geometry	38
16 (a-p)	Patterns for Scientific-Atlanta Parabolic Antennas at C and Ku Band	41-57
17	Photo of C Band Transmitting Antenna	77
18	Signal Profile With and Without Ground Illumination on Transmit Path	79

Figure No.	Title	Page
A1	Initial Set Up Geometry	120
A2	Site Survey Geometry	121
A3	Area B Site Map	122
A4	Building 1 Site Contour	123
A5	Building 1 Plan	124
A6	Building 1 Front Elevation	125
A7	Building 6 Site Contour	126
A8	Building 6 Plan	127
A9	Building 6 Front Elevation	128
A10	Building 22 Site Contour	129
A11	Building 22 Plan	130
A12	Building 22 Front Elevation	131
A13	Building 22 Site Contour	132
A14	Section Through Building 22	133
A15	Building 485 Site Contour	134
A16	Building 485 Section Characteristics	135
A17	"Ghost" Site Contour at end of Area B runway	136
A18	"Ghost" Site Contour Between Buildings 1 and 485	137
A19	Building 206 Site Contour	138
B1	Spot and Fresnel Zone Bounds (FT)	148

LIST OF TABLES

Table No.	Title	Page
1	Table of Polorization Combinations	26
2	Summary of Experimental Configurations - Short Range	27
3	Reflection Coefficients in db below zero	40
4	Recorded Data Bldg 1 C Band 20°	59
5	Recorded Data Bldg 1 C Band 30°	59
6	Recorded Data Bldg 1 C Band 40°	60
7	Recorded Data Bldg 1 Ku Band 20°	60
8	Recorded Data Bldg 206 C Band 35°	61
9	Recorded Data Bldg 206 Ku Band 35°	61
10	Recorded Data Bldg 486 C Band 10°	62
11	Recorded Data Bldg 485 C Band 20°	62
12	Recorded Data Bldg 485 C Band 30°	63
13	Recorded Data Bldg 485 C Band 40°	63
14	Recorded Data Bldg 485 Ku Band 10°	64
15	Recorded Data Bldg 485 Ku Band 20°	64
16	Recorded Data Bldg 485 Ku Band 30°	65
17	Recorded Data Bldg 485 Ku Band 40°	65
18	Bldg 22 Data Summary C Band	66
19	Bldg 22 Data Summary Ku Band	67
20	Recorded Data Bldg 22 C Band 40° (Specular)	69
21	Recorded Data Bldg 22 C Band 40° (Space Harmonic 57°)	69
22	Recorded Data Bldg 22 Ku Band 40° (Specular)	70

Table No.	Title	Page
23	Recorded Data Bldg 22 Ku Band 40° (Space Harmonic 52°)	70
24	Recorded Data Bldg 22 Ground Illumination Test	78
A1	Building 1 Survey Data	101
A2	Building 1 Height and Range	102
A3	Building 6 Survey Data	103
A4	Building 6 Height and Range	104
A5	Building 22 (Concrete) Survey Data	105
A6	Building 22 (concrete) Height and Range	106
A7	Building 22 (Corrugated) Survey Data	107
A8	Building 22 (Corrugated) Height and Range	108
A9	Building 485 Survey Data	109-110
A10	Building 485 Site Height and Range	111
A11	First "Ghost" Site Survey Data	112
A12	First "Ghost" Site Height and Range	113
A13	Second "Ghost" Site Survey Data	114
A14	Second "Ghost" Height and Range	115
A15	Building 206 Site Survey Data	116
A16	Building 206 Height and Range	117

I. INTRODUCTION

1.1 Purpose

The purpose of the technical effort described here is the measurement of the reflectivity at microwave frequencies of structural surfaces found at typical airports. Although reflection coefficient measurements have been made by a number of experimenters (See references), the work described here is believed to be unique insofar as it includes

- Measurement at the same site(s) of reflection coefficients for vertical, horizontal and circular polarizations and
- Measurements at the same site(s) of reflection coefficients for both 5 GHz and 15 GHz (C-Band and Ku-Band) signals at each polarization.

The choice of frequencies was predicated upon the use of these bands for future microwave landing guidance systems. The MLS currently under development by FAA will operate at C-Band for instance; the Marine Remote Area Advanced Landing System (MRAALS) and the Tactical Landing SYstem (TLS) are both designed for Ku-Band.

The choice of polarization for this experimental work was likewise based upon those which are likely candidates for future landing-guidance systems. There are two principal technical issues which affect the choice of polarization.

1. Which polarization offers the greatest protection to the integrity of the guidance signal by virtue of minimizing interference from multipath reflections?

2. Does the choice of system polarization allow the implementation of airborne antennas having adequate coverage volume?

The second of these issues is being addressed by several technical bodies such as NASA/Langley, the U.S. Army and Ohio State University, through theoretical studies and measurements on both full scale and small scale models. It is the potential multipath advantage available through proper choice of polarization which is the motivation for the effort described here.

1.2 Background

Previous experimental work[6,9] conducted for the Air Force Flight Dynamics Laboratory by IIT Research Institute has revealed a number of interesting features concerning multipath at C-Band with vertically polarized equipment. This work was conducted at Wright-Patterson AFB, Ohio, an installation exhibiting flight-line features not untypical of many airports. The previous work was aimed at exploring the general characteristics of multipath reflections in rather a broad way, primarily to compare reflections from actual structures with reflections from flat screen reflectors. The present study is more specific in that it addresses the polarization and wavelength dependencies of the reflections from real structures. Even within that narrow mandate the resources available for the effort allowed only limited cases to be studied, namely four building types, two frequencies, three polarizations and four or five angles of incidence. The results obtained here represent the result of less than five man-months of contractual effort.

1.3 Summary of Program

1.3.1 Summary of Basic Technique

The basic experimental technique employed in this effort was a bi-static measurement using pure CW transmissions at C-Band and Ku-Band between narrow beam antennas mounted on adjustable ground-based tripods.

The transmitter for C-Band was the exciter portion of the Doppler hardware used previously by AFFDL and IITRI (Ref 6,9). The transmitter was capable of at least 40 dbm output. At Ku the transmitter was an H-P 628 signal generator capable of at least +10 dbm output. The narrow beam antennas were Scientific-Atlanta dishes equipped with switchable polarizers permitting rapid changes from linear to either left hand or right hand circularly polarized radiation. The mounting tripods provided a capability to aim the dishes very precisely in azimuth and elevation, as well as providing height adjustment and the capability to rotate the antennas about their boresight axis to facilitate the change from vertical to horizontal polarization.

Prior to measurement at any one location a survey was conducted to determine the terrain profile in front of the structure under investigation. A suitable point on the reflecting surface was nominated as the desired specular reflection point and a series of points spaced every 10° was located on a semicircle of radius 190 feet in front of the building. Appendix A describes this procedure in greater detail. It is estimated that these ground locations are accurate to within one inch in range and angles better than six minutes of arc.

Knowledge of the terrain profile allowed the heights of the transmit and receive antennas to be computed so that their phase centers and the point of specular reflection lay in a horizontal plane for each set of measurements. The tilts of the building surfaces were also measured to determine the allowance to be made for skewing of the reflected ray due to this effect.

The four-foot diameter C-Band dishes were provided with peep-sites which were aligned with the optical boresights using the sun as a source of parallel light rays. At Ku-Band the feed waveguide on the two-foot diameter dishes were found to be a reliable sight for aiming.

At each test location the transmit and receive antennas were set up at the predetermined locations for specular reflection, the operators adjusting height, level and aiming angles to ensure specular geometry. The transmitter power was adjusted to the desired level and the reflected signal level measured on either a power meter or sensitive calibrated receiver connected directly to the reciving dish feedline. Measurements were repeated with the polarization set at vertical, circular and horizontal by switching the polarizers and rotating the dishes about their boresight axes. Ground reflections were reduced to negligible levels by (a) the choice of measurement geometry so that ground illumination through elevation sidelobes was at least 16 db down on the boresight signal and (b) the placement of vertical sheets of RF absorbing material on the ground at the ground reflection points.

Following the measurement of the reflected signal the dishes were aimed towards each other and the direct path signal level was measured for each polarization in turn.

This basic procedure was repeated for grazing angles of 10, 20, 30, and 40 degrees wherever physically possible. Since the illuminated spot size was arranged to be of the order of the size of the first Fresnel zone, the difference in the direct and reflected signals (appropriately compensated for the range difference) provides a good estimate of the effective reflection coefficient of the surface under test.

1.3.2 Measurement of Corrugated Surface Reflections

Considerable interest has been aroused in the technical community concerning reflections from corrugated surfaces. An FAA survey of ten civilian airports revealed that such surfaces are quite common. The U.S. Army has conducted a number of theoretical and practical studies of RF scattering from such surfaces. Experiments were conducted during this effort to (a) compare the reflection coefficients of corrugated surfaces at VP, HP and CP in the specular region at C and Ku Band and (b) spot-check the Army's theoretical model for selected non-specular reflections. The corrugated surface of Building 22 at Wright-Patterson AFB unfortunately begins at a height of about five feet from the ground, necessitating that the antenna tripods be elevated some 4-5 feet in order to maintain useable geometric conditions. This was accomplished by conducting the experiments from the back of stake trucks at the receiver and transmitter sites. The non-rigid nature of the truck beds presented some challenging experimental problems in maintaining aiming angles of the narrow beam antennas and a recommendation is offered to would-be workers in this type of experiment to avoid such techniques. Despite these problems a very good match of predicted and measured signal levels was made at C-Band. The match of predicted and

measured signal levels at Ku-Band was less satisfying but may be attributable to the fact that some experimental parameters lay outside the areas of validity of the Army's theoretical model. Further work on this is proceeding at USAECOM. The measured signal levels at Ku-Band did, however, agree within better than one to three db with measurements made by the Army on a scale model surface machined to model the dimensions of the Building 22 corrugations for illumination in a laboratory set-up at 70 GHz. Thus, an excellent match of scale and real life measurements appears to exist (see Paragraph 3.3.2).

1.3.3 Comparison of Short Range Measurements with Operational Geometry Test

In the previous testing of the Doppler MLS at Wright-Patterson AFB (Ref 6, 9) strong multipath reflections from a large hangar (Building 206) were experienced in the vicinity of the touchdown point on Runway 23, (C-Band, VP guidance signal). Tests were run on this hangar, first using the basic CW technique for short range measurements for a grazing angle of 35 degrees (the actual angle pertaining to a guidance transmitter located on the overrun to Runway 23). The transmitting test equipment was then relocated to the overrun and signals beamed at Building 206. A pickup truck carrying a receiver and wide beam horn was then used to probe the reflected signal in the vicinity of the expected specular region on the runway. This test was repeated for the direct path signal. Both C and Ku were tested with VP and HP signals.

1.4 Report Organization

Section II of the report contains a full explanation of the test philosophy and implementation, descriptions of the structures studied and

some of the experimental difficulties which had to be overcome.

The test results themselves are presented in Sections III & IV with both detailed breakdowns of the individual measurements and summary sheets showing the overall situation in a few concise tables.

The conclucions and a number of recommendations are to be found in Section V.

Two Appendices are included. Appendix A contains a description of the sites and the details of the surveys. Appendix B contains a mathematical discussion of the geometrical aspects of the test procedure.

II. PROGRAM DESCRIPTION

2.1 Technical Considerations and Constraints

The intent of the present experiments was to obtain estimates of the magnitude of reflection coefficients of typical airport building surfaces at Wright-Patterson AFB. This means, of course, that reflections must be obtained, as nearly as possible, from homogeneous segments of the surfaces of real buildings in a practical experimental environment - that of the Area B flight line. Ideally, one would make such measurements on an infinite plane reflecting surface, of uniform composition, in the absence of a ground plane, and of physical obstructions to transmission. In practice, one is confronted by buildings (having relatively small sections of uniform composition) situated on a ground surface which is not necessarily planar and which is used for both vehicular traffic and parking. The experimental problem was to make some reasonable use of this real environment to estimate the magnitude of the desired reflection coefficients. This problem is discussed

briefly, in the paragraphs which follow, in terms of general experimental technique and of a specific set of experiments. The originally projected experiments fall into three general categories. These included: (1) supporting measurement, (2) short range static measurements, and (3) long range operational-like measurements. Resource limitations precluded completion of all projected experiments.

The reflection from a building can be considered in terms of the size of the first Fresnel zone (i.e., the zone within which specular path length differentials will be less than one half wavelength) at the building reflecting surface. Assuming purely specular reflection with unity reflection coefficient, the ratio of reflected signal voltage to incident signal voltage is approximately equal to one if both the semi-major and semi-minor axes of the Fresnel ellipse are less than the corresponding dimensions of the reflecting surface. (See Figure 1).

Hence, if $H > F$ and $W > \frac{F}{\sin \phi}$ the desired condition is met. This is essential, of course, since otherwise the estimate of reflection coefficient would be influenced by building dimensions as well as material. It is not the only consideration, however.

2.1.1 Choice of Experimental Parameters

The experimental arrangements are intended to assure that: (1) a sufficiently large* homogeneous surface is available as reflector, (2) this reflector is in the nominal far field of the transmitting antenna, (3) the incident energy is concerntrated in the homogeneous portion of the surface (i.e. primarily within the first Fresnel zone), and (4) the interference

*"Large" is meant in the sense that the dimensions of the homogeneous portion of the surface are comparable to the dimensions of the first Fresnel zone.

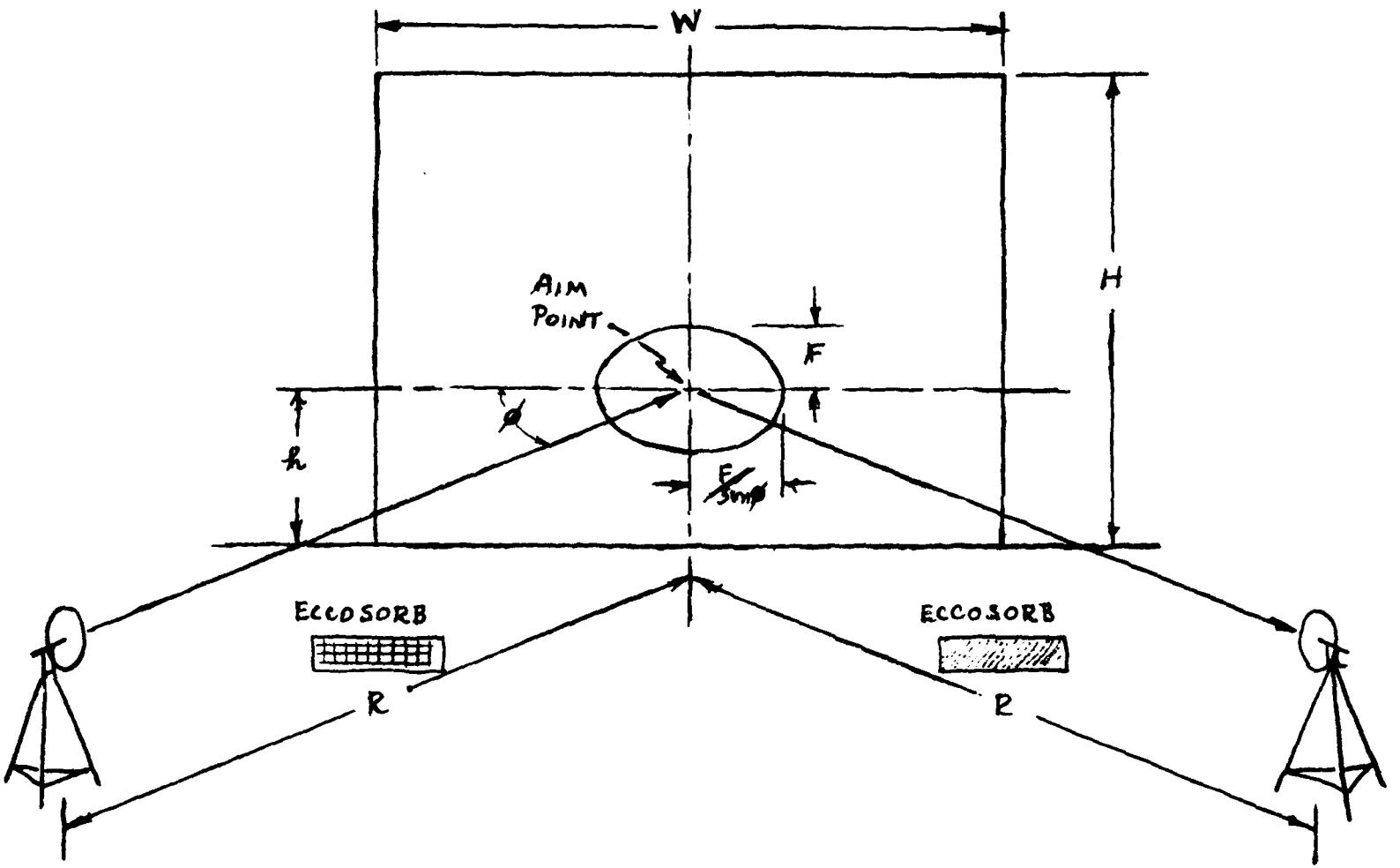

Figure 1 General Experimental Geometry

effects of ground reflections are minimized. For a given set of antennas, then, the parameters to be controlled are spot size, Fresnel zone size, and ground lobing. It is assumed that, with reasonable Fresnel zone size, sufficiently large homogeneous surfaces can be found. The parameters which may be adjusted include antenna heights, aim angles, distances, aim points, and, of course, general experimental geometry.

These basic elements are shown in Figure 2. The nominal "far field range" for the antennas depends on frequency band. For C Band it is approximately 167 feet and for Ku-Band it is approximately 126 feet. A basic range of 190 feet was chosen for the legs of the transmission path. This range provides assurance that the reflector is well into the far field region of the two antennas; and also provides that, for the desired antenna height of about 7 feet, pertinent ground illumination will be attenuated (due to antenna pattern) by about 16 db with respect to the direct path signal.

Restriction of ground illumination in this fashion is of considerable importance if the ideal experimental situation is to be approximated at all. For, if signals reflected from the ground surface are permitted to interfere on both the incident and reflected paths, non-uniform illumination patterns result at both the reflecting surface and the receiving antenna. Such non-uniformity, a pattern of maxima and minima in the vertical direction, is inevitable in the presence of ground reflection, but may be reduced if care is taken in the experimental setup. The lobing pattern itself exhibits extrema for alternate values of n when

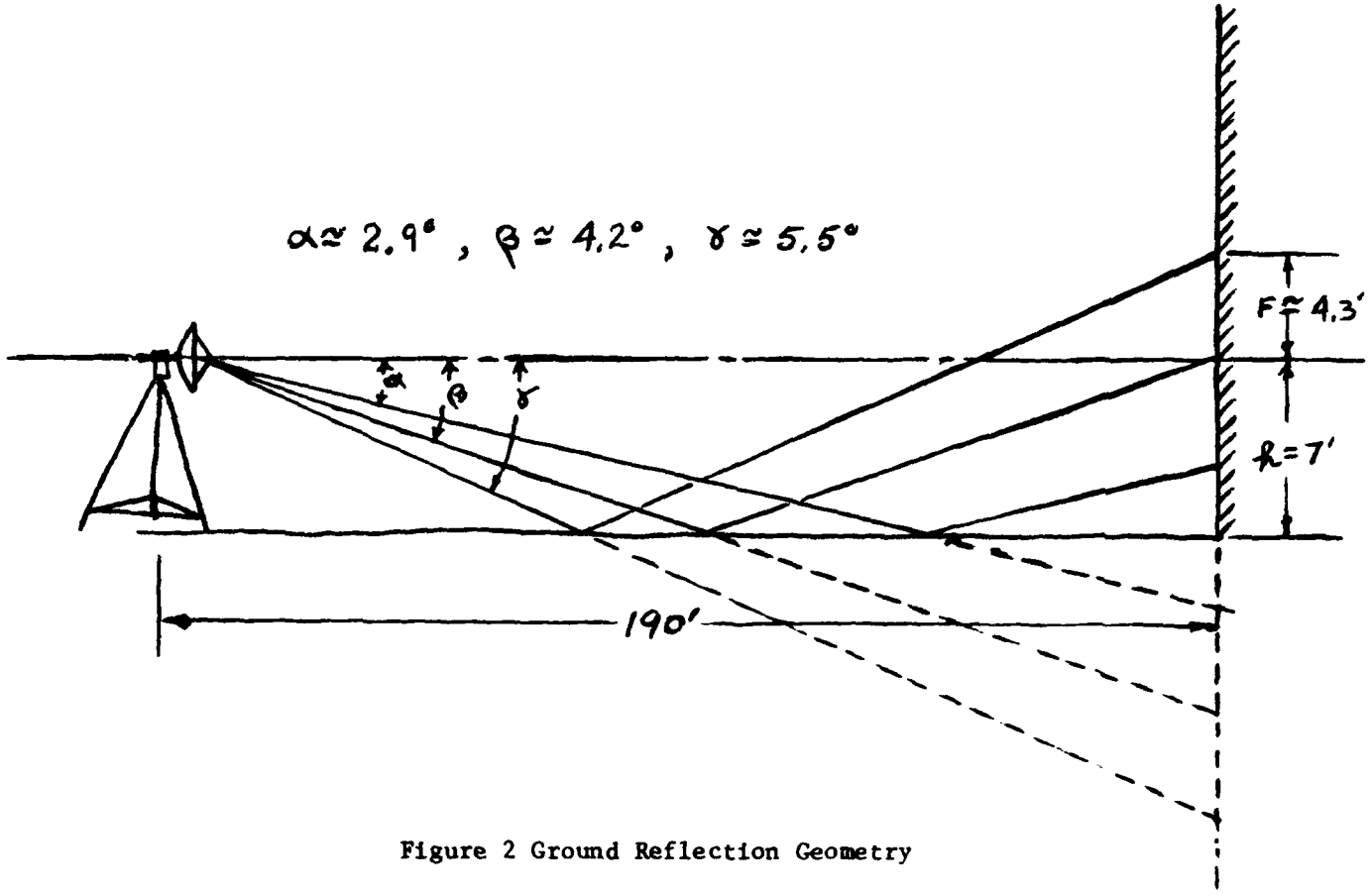

Figure 2 Ground Reflection Geometry

$$h_2 = \frac{nR\lambda}{4h_1}$$

h_2 is height of receiving antenna or point on reflecting surface,

h_1 is height of transmitting antenna,

R is distance between the antennas, and

λ is the wave length.

For the present case, h_1 = 7' and R = 190'. Also, at the C Band frequency, λ_c = 5.8 cm; and at Ku Band, λ_k = 1.9 cm. This means the minima, at C Band, occur at spacings of about 2.6 feet while those at Ku Band occur at spacing of about 0.9 feet. Maxima occur halfway between the minima. Spacing of extrema for all values of h_1 employed throughout the experiments are given in the following table.

	Spacing of Extrema in Feet	
h_1 (ft)	C Band	Ku Band
5.5	3.31	1.10
6.0	3.04	1.01
7.0	2.60	0.86
12.0	1.52	0.50

Additional means of limiting ground reflection phenomena are discussed in a subsequent section.

Spot size, the remaining item to be controlled, is nicely managed at 190 feet too. If the spot is defined as being bounded by the cone on which antenna gain is down 3 db, then the spot would be very nearly circular at normal incidence and would have radius S.

$$S = R \tan \frac{BW}{2}$$

The Fresnel zone dimensions may also be calculated to provide a complete picture of the situation at the reflecting surface. At normal incidence these zones are also circular with radius F.

$$F = \frac{\lambda R_1 R_2}{R_1 + R_2}$$

λ is wave length

R_1 and R_2 are the lengths of the legs on the reflected path.

In this case $R_1 = R_2 = 190$ feet.

Band	Wavelength λ (ft)	Fresnel Radius (ft)
C	0.192	4.3
Ku	0.064	2.5

These items, ground lobe spacing, spot size, and Fresnel zone size, are shown together in Figure 3 for a transmitting antenna height of 7', and, of course, normal incidence. In practice, no measurements were planned for normal incidence. All measurements were taken at grazing angles less than or equal to 40°. At shallow grazing angles the horizontal axes of both Fresnel zone and illumination spot become elongated. Also there is a shift in the center of the intersection between the 3 db cone and the reflecting surface. At all of the angles used, however, the Fresnel zone remains roughly centered and within the illumination spot.

2.1.2 Problem Areas

It was not possible to fully realize ideal experimental conditions. The buildings were not, for example, situated on a horizontal, plane ground.

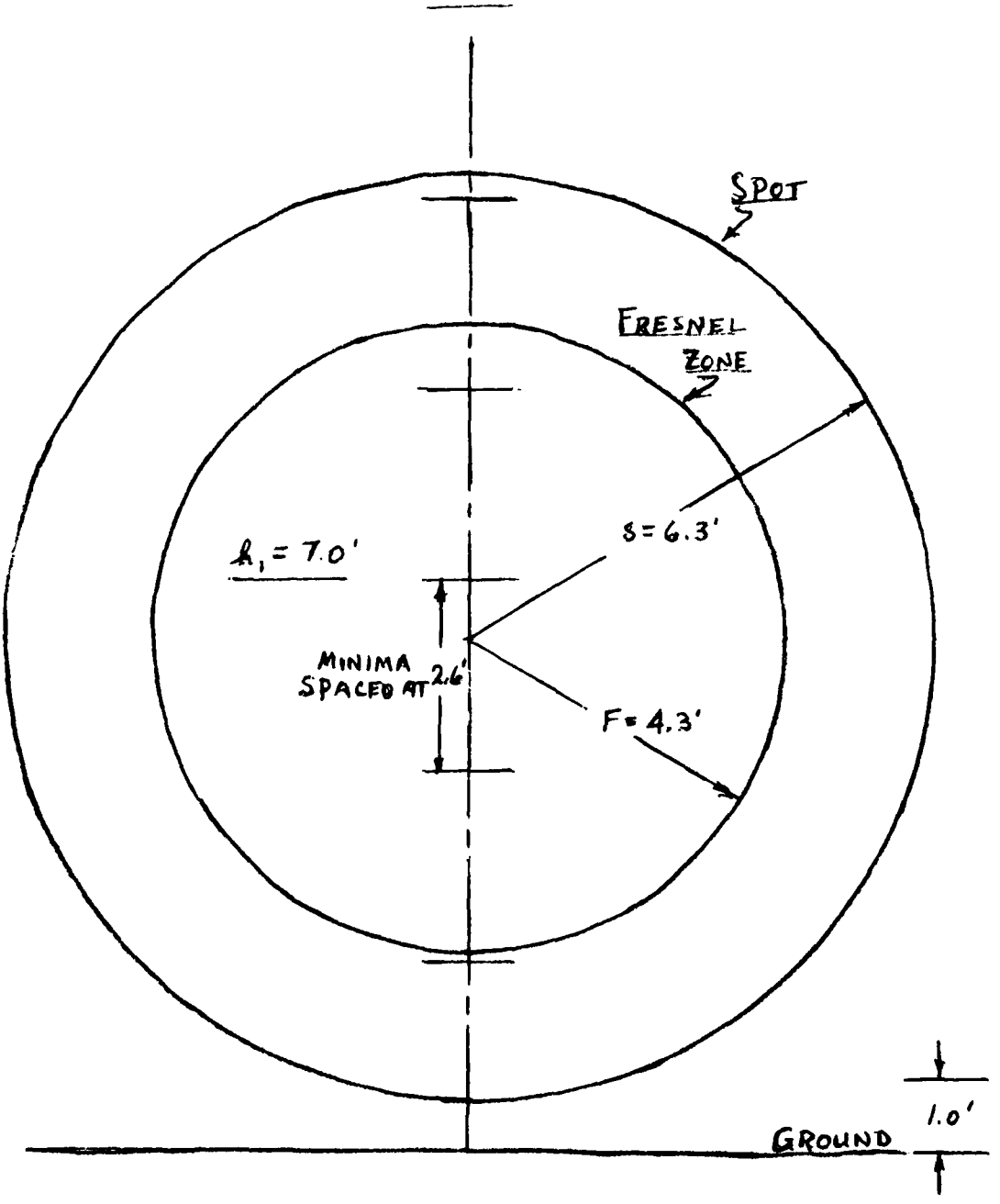

Figure 3a Surface Illunimation
C-Band

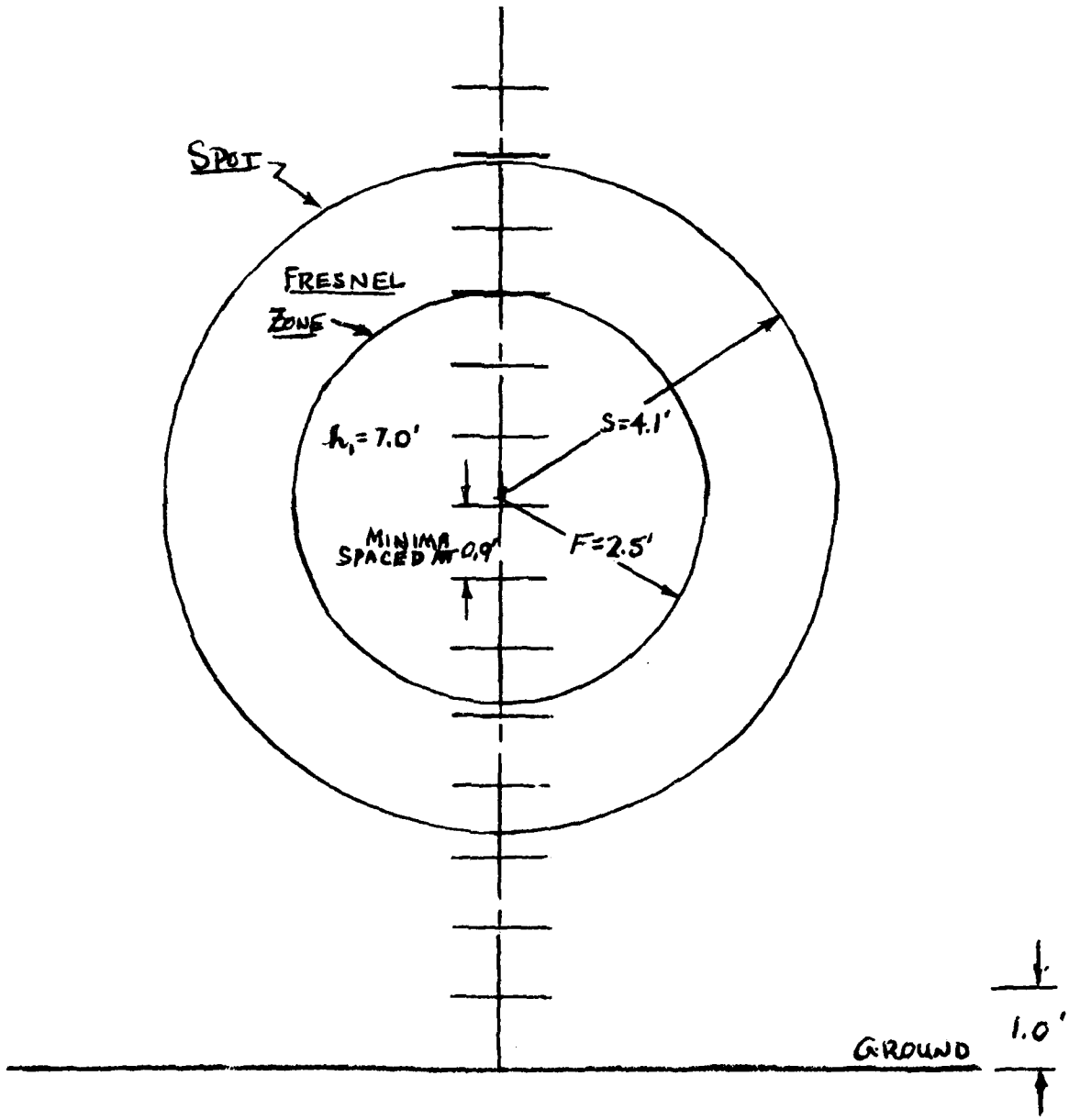

Figure 3b Surface Illumination
Ku-Band

Also, at some angles, the desired transmission paths were obstructed. And, even with the pencil beam antennas, ground reflection phenomena were measurable. Building 22 presented a unique problem in that the bottom of the desired surface was elevated by roughly five feet above the ground.

Of these various problems the most potentially serious was that of ground reflections. To determine its severity the C Band transmitting antenna was set at a height of seven feet, and a standard gain horn was used to probe the vertical pattern at a range of 190 feet over a paved surface. A peak to null ratio of 8 db was observed. This was considered to be unacceptable; and an ECCOSORB barrier ten feet wide and two feet high was set up at the halfway point of the ground path. The probe was then repeated. This time the signal strength variations observed were about $\pm$ 1db. This amounts to about a nine to one signal strength advantage on the direct path; and was considered acceptable. A second ECCOSORB barrier of the same dimensions was obtained. All subsequent measurements were made with these barriers in place halfway between each antenna and the reflector; no further vertical probes were made at C Band. The two foot barrier is almost of perfect height to block all specular ground paths from antenna center to the Fresnel zone. A higher barrier would tend to cut down still further on interfering rays outside the Fresnel zone, but it also begins to cut down on direct path transmission to the wall.

Figures 4 and 5 show the ECCOSORB placement for the direct path and reflected path measurements respectively. It has also been noted that not all ground surfaces emp.oyed were planar and horizontal over the whole

Figure 4
Direct Path View Showing
Placement of ECCOSORB

Figure 5
Reflected Path View Showing
Placement of ECCOSORB

experimental range. They generally tended to be convex upward and to fall as one moved away from the reflecting surfaces. They did, however, tend more closely to the horizontal planar as the reflecting surface was approached. Time did not permit probes of illumination function at all reflecting surfaces. However, the 2 db max to min ratio alluded to earlier, is believed to be representative. Building 485 presented the greatest difficulty of all the reflecting surfaces because of ground irregularities. For this surface, it was necessary to use a smaller value of h_1. This necessity arose from the fact that the antenna tripods provided for heights roughly between 5 and 8 feet above local ground, while local ground at some of the test points fell two or more feet below the base of the reflecting surface. In order to use the same aim point for all measurements it was necessary to choose an aim point which was low enough to be accessible from all test points. A height of 5.5 feet satisfied this criterion.

Building 22 presented a related but different problem. The corrugated surface of that building does not extend all the way to the ground. In fact, in order to have the same kind of relationship between reflecting surface, Fresnel zone, and illuminated spot as that achieved on the other surfaces, it is necessary to use an aim point 12.0 feet above the ground.

Still another class of problem experienced during the measurement program has to do with obstructions to transmission along desired paths. One may distinguish between permanent and operational difficulties of this type. An example of the first type is provided by the small outboard structures at the bases of the concrete piers of Building 1. Because of

these structures it was impossible to make measurements at a grazing angle of 10°. The operational type of difficulty is typified by the parking lot which overlays the whole experimental range for Building 22. Because of this parking lot, it was necessary to choose a time when the lot was empty, to make measurements on Building 22.

As an ordinary matter of course, in the conduct of experimental operations, one assesses the realibility of his data in terms of its repeatability. In fact, during the present experiments an effort was made to repeat each measurement a number of times to reduce the impact of random features of the experimental arrangement. It was not practical, however, to repeat the measurements in the sense that the entire experiment was dismantled and then set up again from the beginning. Consequently, those steps of erecting, and leveling the antenna tripods, aiming the antennas, and changing polarization were not repeated a number of times at each test point. It is certain, however, that the survey of test points is accurate to within an inch or so. Furthermore, by means of plumb bob, tape, and level, the antennas could be placed to within an inch of their desired position. The same is true of the location of the aim point, which is a surveyed point. The aim point was denoted by a mylar target affixed to the structure at the intended point of reflection. The antennas were then oriented on the aim point by means of a "peep sight" arrangement so arranged that the axis of the sight is parallel to antenna boresight (optical and electrical) but offset by about 1.5 feet. A field check of the alignment showed the RF boresight of the dish to be within a foot or so of the peep

boresight at the operating range, Best present extimate of the capability of the peep sight is that sighting can be done to within about 1/4°. This aiming accuracy is well within the antenna beamwidths of about 3° for the C Band antennas and 2° for the Ku Band antennas. It is believed, therefore, that the experiments are inherently reliable. Their only feature which would seem to contribute any substantial error lies in interaction between the aiming process and the mechanics of changing polarization. While the offset of the peep sights may cause a lateral offset of real aim point from apparent aim point, there is no relative aiming error and the actual reflecting surface is not changed in any significant sense. Initial aiming was always done in this way, with the antennas in the vertically polarized position. The circularly polarized cases were then treated without re-aiming. In order to change to horizontal polarization it was necessary to rotate the entire dish about boresight. After this change the sights had necessarily moved to a new position, but still remained parallel to the electrical boresight. Re-aiming, therefore, would have given rise to a shift in optical aim point, but no significant shift in the electrical aim point. Also, the sights, after rotation, were almost inaccessible. For these reasons, it was not thought desirable to re-aim after changing to horizontal polarization. But there was a real threat that, in making the change, there would be a disturbance of aim. The data themselves, however, indicate a real consistency in aiming both the C and Ku Bands antennas. This indication is apparent in the consistency of direct path data (See Section III).

2.2 Basic Experiments

A family of experiments was designed including sets of measurements aimed directly at the production of reflection coefficient data, as well as measurements which are best described as supporting measurements. These latter measurements were considered as desirable but expendable, if the pressures of time and funds were too severe, or if additional data were desired from the production runs. An essential condition for dropping the supporting measurements was that the data were behaving more or less as expected. If they were not, of course, that might be construed as evidence that the experiments were out of control; and the extra measurements would have to be made. In fact, the data did behave more or less well. A number of the supporting measurements were made on an ad hoc basis; but the full set of supporting measurements was not completed.

The production measurements were of two general types, and were performed in two areas (Area B and Area C) of Wright-Patterson AFB. Geometry distinguished the types of experiment. A short range, symmetric geometry was employed for the bulk of the measurements; but a number of data points were taken at ranges of the order of a mile in an operationally real geometry. The short range tests were intended to give precise estimates of reflection loss for a variety of reflecting surfaces. The long range tests were intended to show that the manifestations of reflection phenomena at long ranges were qualitatively similar to those observed at short ranges. It was not anticipated that they would be quantitatively similar because there was to be no effective control of ground illumination at long range. The

reflector, in this case Bldg 206, is still large with respect to the Fresnel zone; but the transmitting antenna is only at about six feet. Consequently, only the upper half, roughly, of the Fresnel zone falls on the reflecting surface.

One distinctive test was programmed to examine the impact of reduced ground illumination on fine grain spatial variations of reflected signals. These phenomena were observed and reported during the previous program but data were not conclusive in identifying the mechanism which produced them. The ground reflection effect was suggested by Lincoln Labs and was simply added to the present experimental effort. The results are included in section IV of this report.

2.2.1 Short Range Experiments

The short range test program is patterned on that implemented by the Royal Aircraft Establishment. Instrumentation is shown in block form in Figure 6. Geometrically, transmitting antenna, receiving antenna and main reflecting region* are centered on a horizontal plane at a nominal height of seven feet as discussed earlier and shown in Figure 2. A measurement is made first on the reflected path and then on the direct path and the reflection loss is equal to their ratio appropriately compensated for difference in total path length. (See Figure 7)

$$\frac{1}{P} = \frac{P_D \cos^2 \phi}{P_R}$$

Note that ϕ is a grazing angle rather than an incidence angle. Ideally, at

* First Fresnel Zone

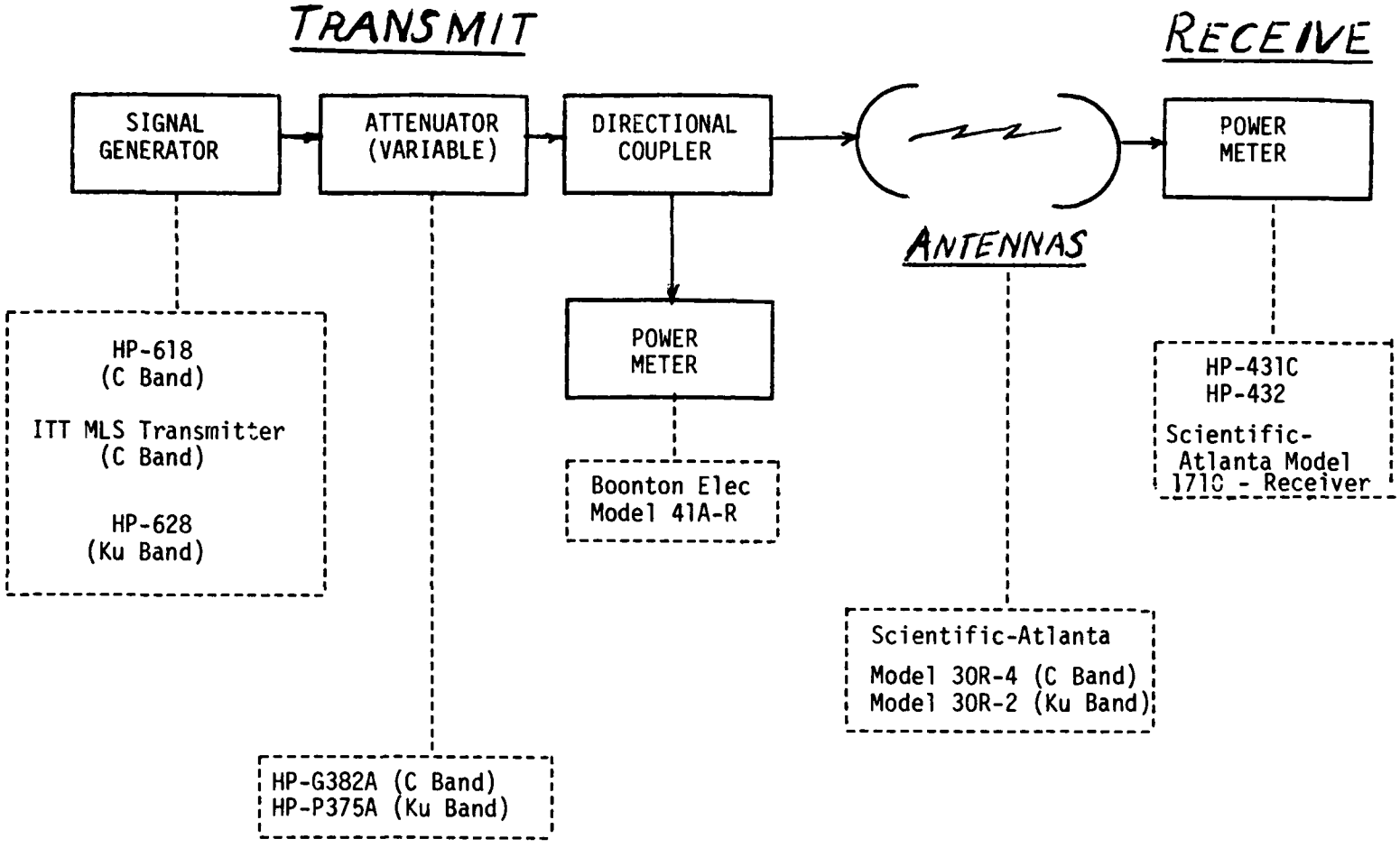

FIGURE 6 - BASIC INSTRUMENTATION

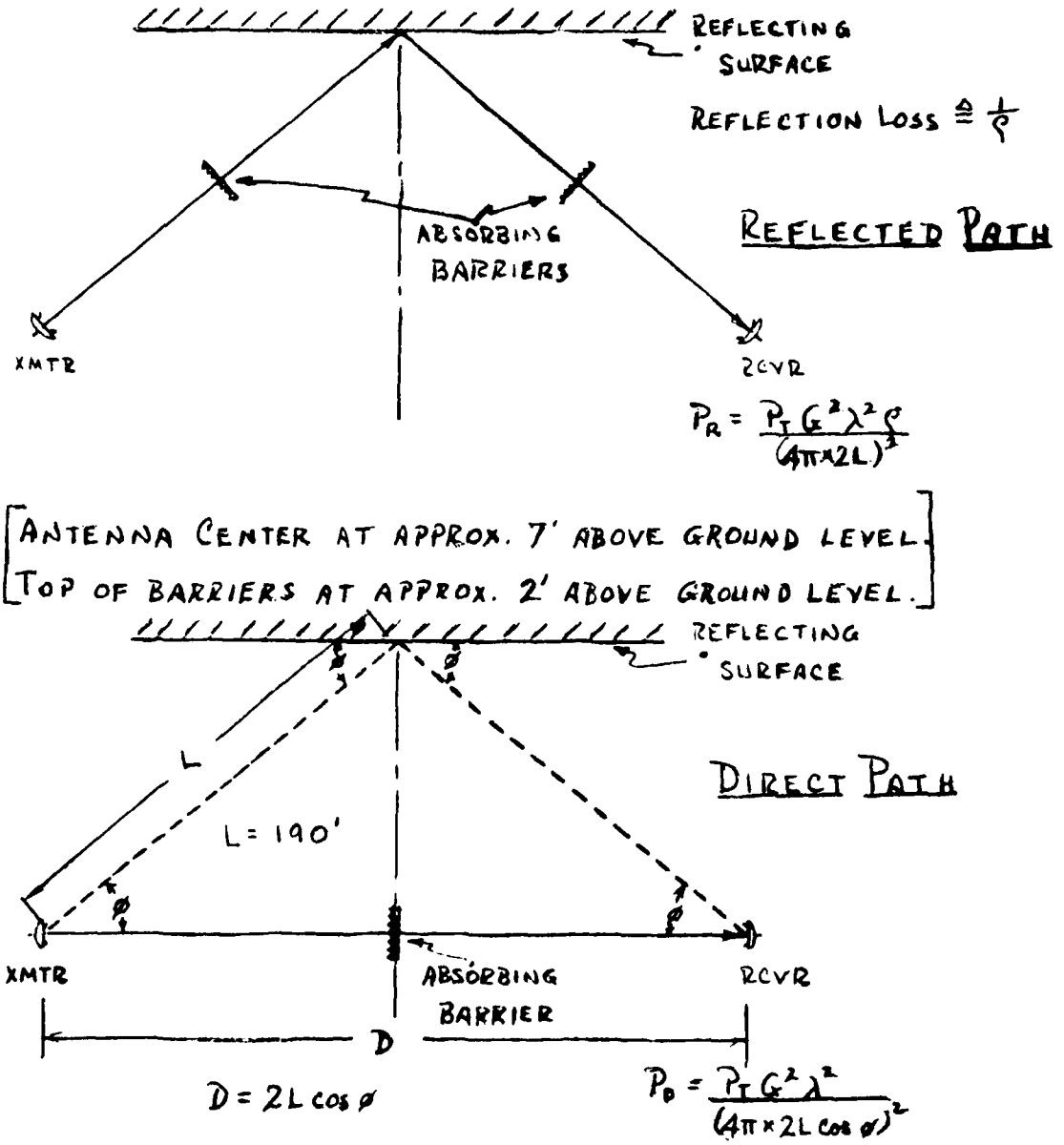

Figure 7 Short Range Reflection Loss Measurement

each reflecting surface measurements would be made at both frequencies, at all desired polarizations, at each of a number of selected grazing angles. Resource limitations rendered it impractical to make Ku Band measurements for all cases but the full range of C Band measurement was made for all except Building 206. For a given building/reflector, grazing angle, and frequency it was found desirable to record direct path signal power, P_D and reflected path signal power P_R for each of the following polarization combinations.

TABLE 1. Table of Polarization Combinations

	Tx Ant	Rc Ant
1	Vert	Vert
2	LH Circ	LH Circ
3	RH Circ	RH Circ
4	LH Circ	RH Circ
5	RH Circ	LH Circ
6	HORIZ	HORIZ

While the two cross-polarized combinations (4 and 5) were not checked on the bulk of the experimental configurations, the complete set of polarization combinations is desirable (for later computational purposes) and data for the full set were recorded for the corrugated reflecting surface of Building 22.

The actual set of experimental configurations employed is shown in Table 2.

TABLE 2. Summary of Experimental Configurations - Short Range

Building #	Grazing Angle				
	10	20	30	35	40
1	-	X	X**	-	X**
22*	-	-	-	-	X
206	-	-	-	X	-
485	X	X	X	-	X

At each of these building/angle combinations, direct and reflected path measurements were made at both frequencies***, and at least the polarization combinations 1, 2, 3, and 6.

Building 1 and 485 were examined at most of the angles. They typify many of the building reflecting surfaces at Wright-Patterson AFB. The main reflecting region for 1 (see Figure 8) consisted of metal clad hangar doors having wire-reinforced windows. The diameter of the mesh of this wire is roughly one inch. The corresponding region for 485 consisted of a rough surface concrete slab (see Figure 9). Short range measurements on 206 (Figure 10) were intended to support a long range experiment on the reflecting surface which produced such a serious multipath problem at C Band, vertical polarization, during the MLS Concept Validation Program (MLSCVP). Measurements were made only at the grazing angle, 35°, to be used for an operational geometry experiment.

Building 22 represents a totally different sort of reflecting surface (Figure 11). Its main composition is of a sort of asbestos shingle material

---

* For Bldg 22 the experiment also included a serach for one space harmonic at each frequency
** Measurements made at C Band only
*** C Band measurements only were made at 30° and 40° grazing angles on Bldg 1

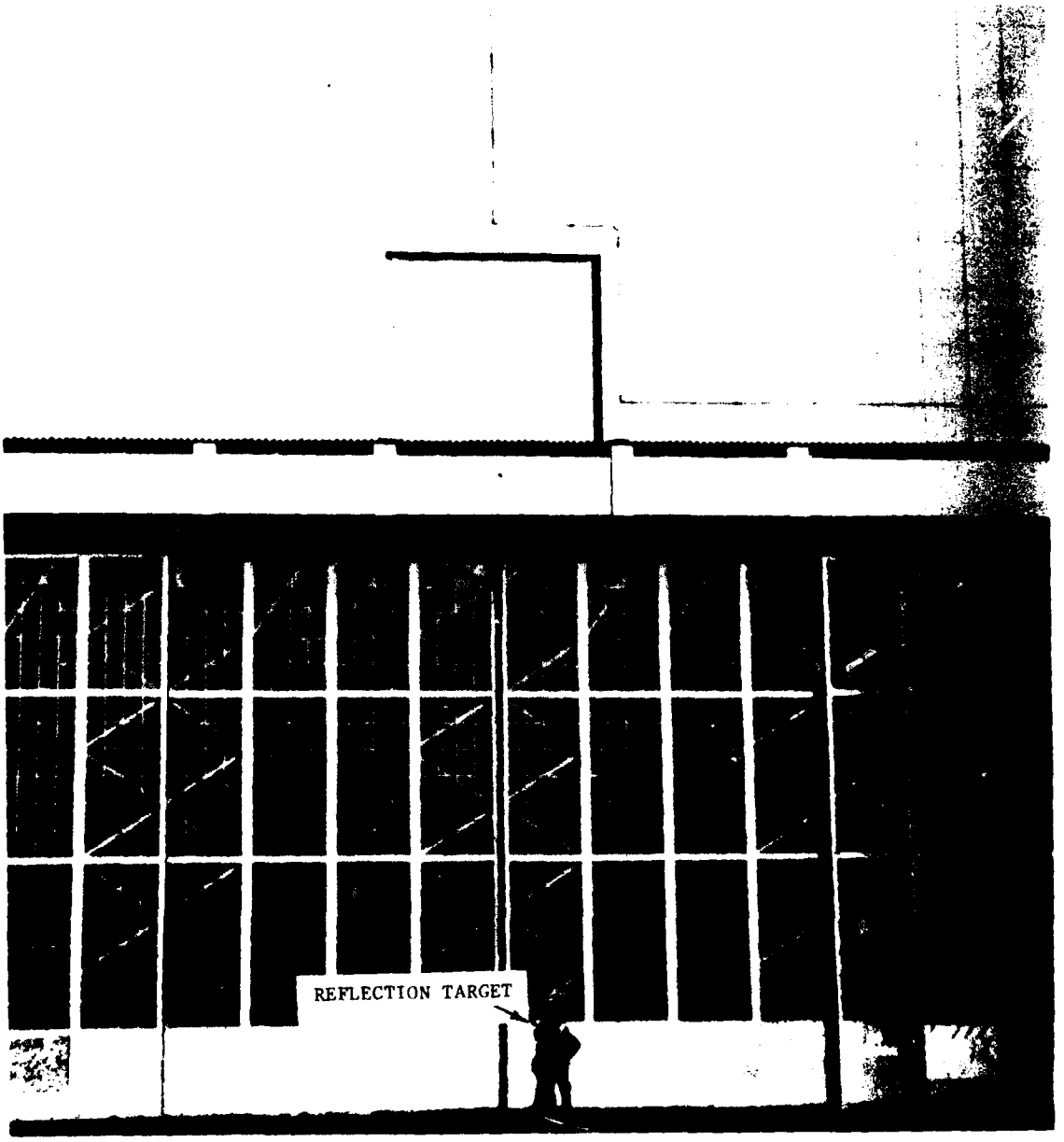

Figure 8
Reflecting Region and
Detail Structure of Bldg 1

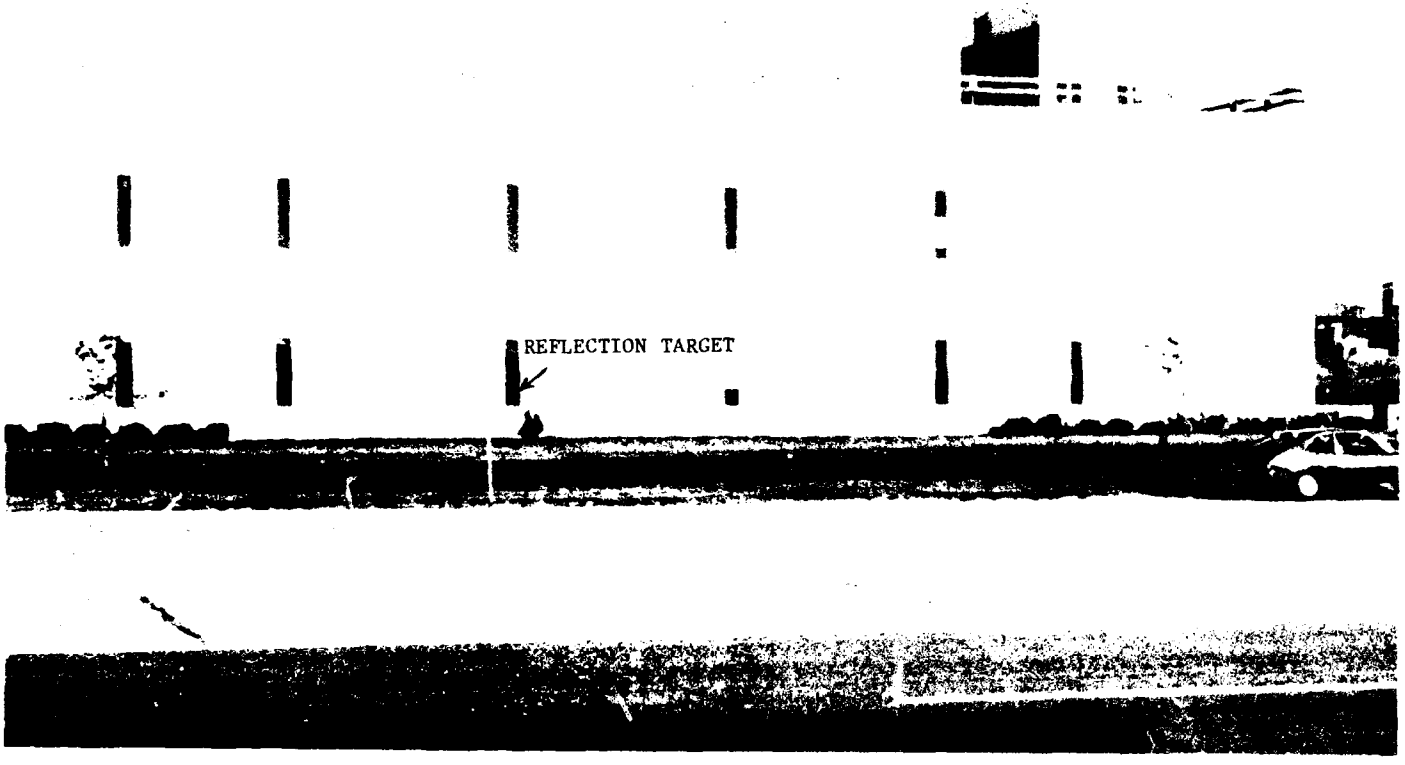

Figure 9
Reflecting Region and
Detail Structure of Bldg 485

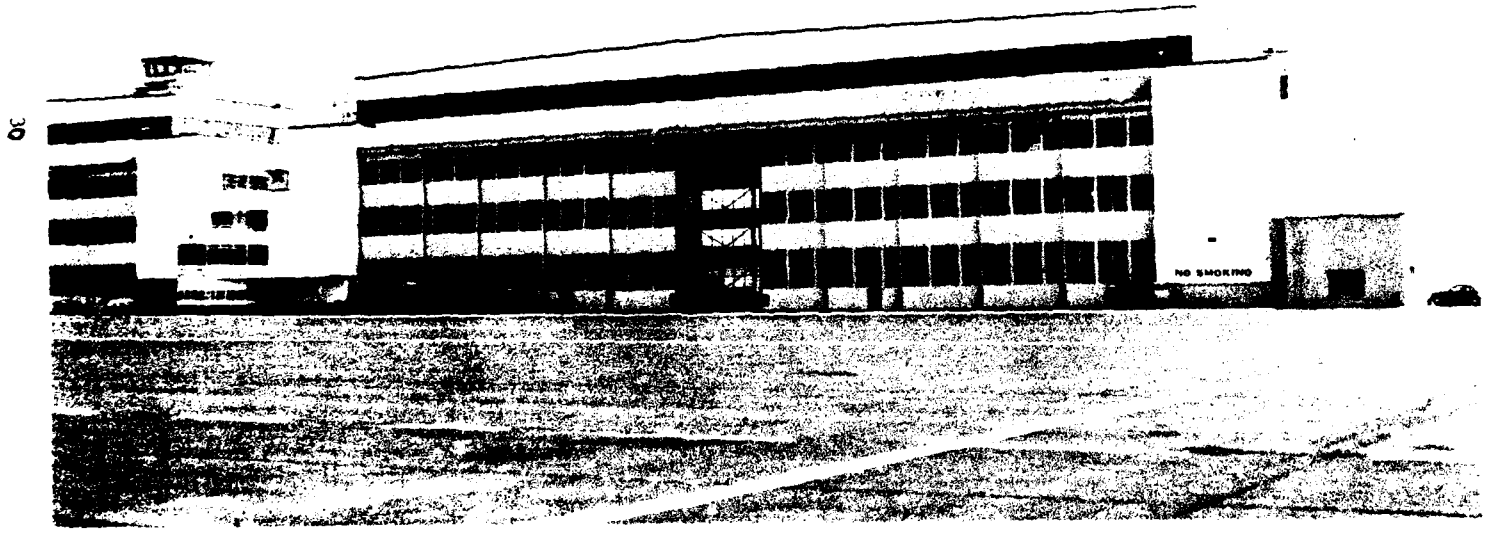

Figure 10
Photo of South Section of
Bldg 206 Area C, WPAFB

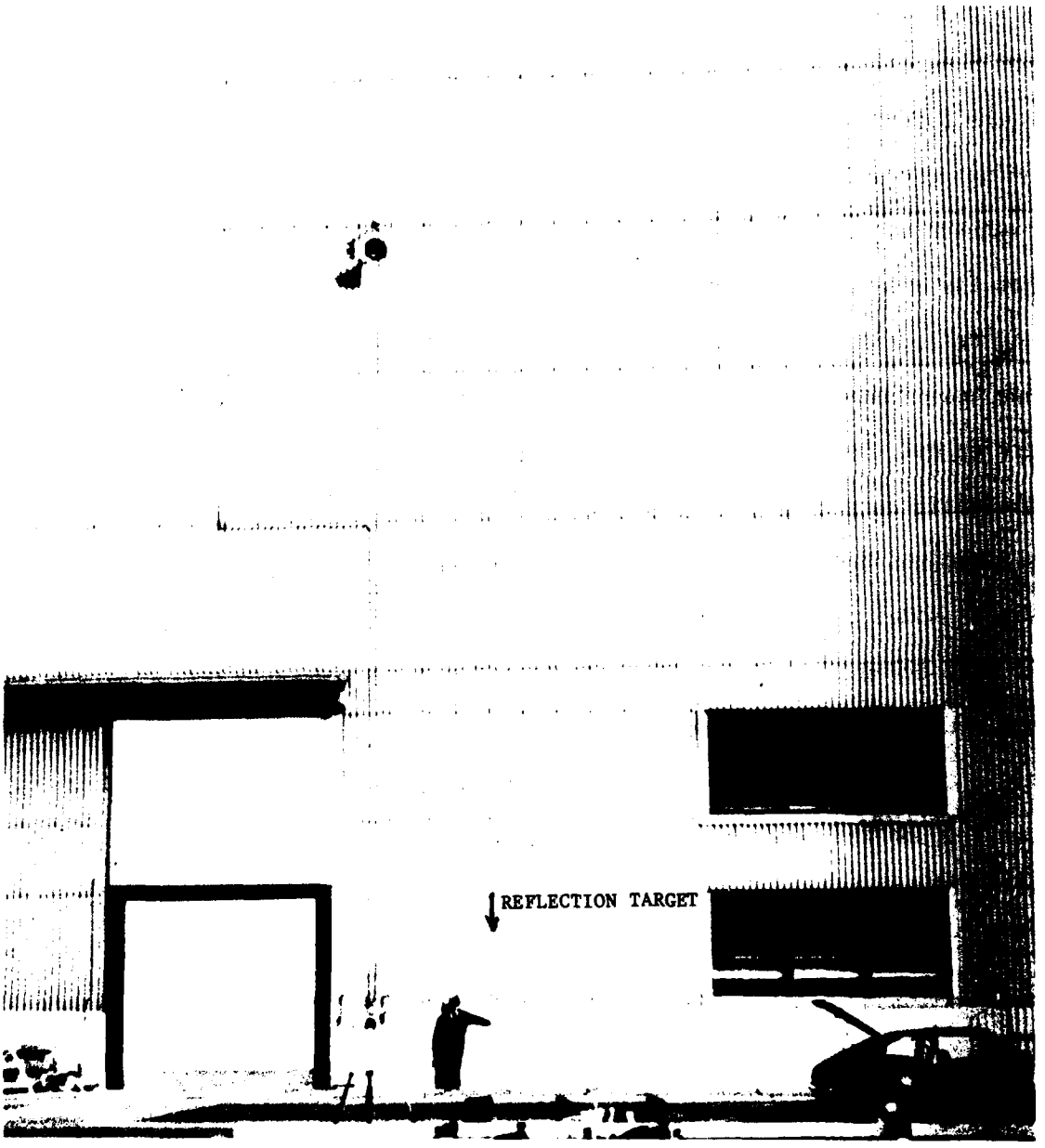

Figure 11
Reflecting Region and
Detail Structure of Bldg 22

which presents a vertically ridged, corrugated surface to the flight line. (The corrugations are sinusoidal of wavelength 5 1/4" and peak-peak depth of 1 3/4"). This surface is coated with several layers of paint containing some sort of metallic pigment. Except for some small, random irregularities in the sheets of surface material and in their placement on the face of the building, this surface provides the only easily accessible periodically rough surface available at Wright-Patterson AFB. Even this building required that the antennas be raised to a height of 12 feet in order to place the main reflecting region totally on the corrugated surface (Figure 12). The same measurement procedures as in the other short range measurements were carried out, but in addition an attempt was made to locate a spatial harmonic of significant magnitude at each of the two frequencies. The choise of harmonic was based on a reflection pattern computed by Dr. J. Mink of USAECOM using a model developed at New York University. British experimenters at RAE have achieved results which correspond closely with predictions from this model. Because of the added complication of the spatial harmonics only a single grazing angle of 40° was examined for this reflecting surface. Both frequencies were employed, of course, as was the full range of polarization combinations.

2.2.2 Long Range Measurements

Although basic data collection was intended to be done in the short range work, some questions remained which could only be dealt with at long range. First there was substantial interest in the serious multipath condition due to Building 206 and observed during MLSCVP. The only measurements made

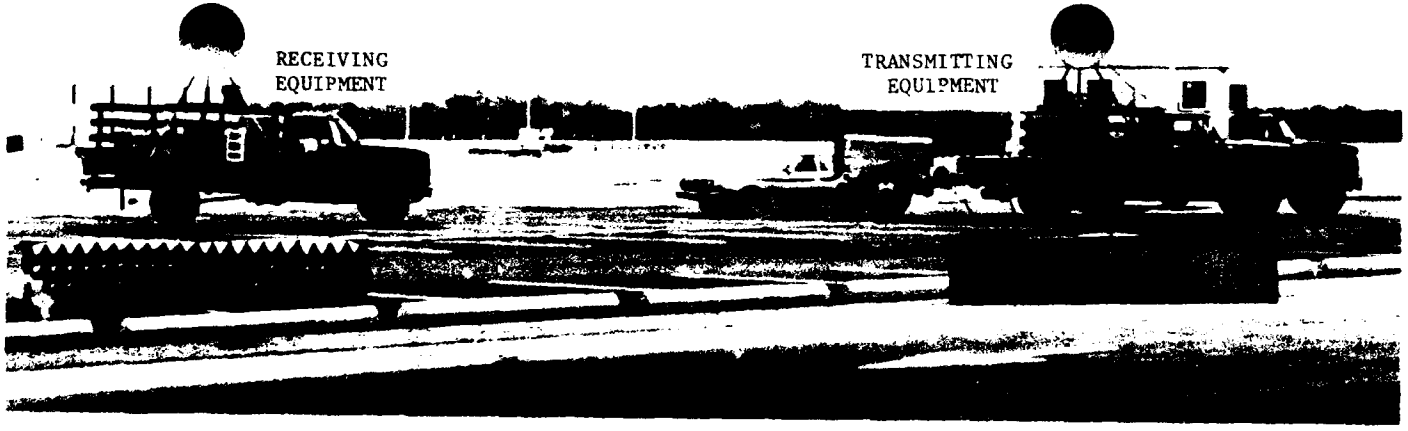

Figure 12
Antenna Mounts for Measurement
of Corrugated Surface of Bldg 22

during that program were made at C Band and with vertical polarization. It is of interest to know how much different the multipath condition might have been if the polarization had been horizontal. Also, it is of interest to know the relative multipath condition at Ku Band. Consequently, using the same transmitting site as MLSCVP and a receiving antenna at about six feet above local ground (in the bed of a pickup truck) data pertaining to these questions were collected. Figure 13 shows the geometry of these tests in the large while Figure 14 shows an expansion of the region about the specular reflection ray. The procedure, at each frequency and polarization*, was to make a measurement of the signal reflected from Building 206 and then to aim the transmitting antenna along the runway and measure the "direct"** path signal to approximately the specular point.

The second long range test also has it origins in earlier experimental work. Very fine grain measurements of reflected energy from the faces of buildings along the flight line in Area B of Wright-Patterson AFB had shown substantial variations as the receiving antenna was moved through distances of only a few inches along the runway (i.e. Loop Road). These variations were thought to be due to the configuration of the faces of the buildings and attempts were made to reject a number of alternate hypotheses. Since the completion of that measurement program it has been suggested that the variations arose from phenomena associated with excessive illumination of the ground from the antennas which were employed. The antennas available

---

* Circular polarization was not employed during these measurements for no appropriate receiving antenna was available

** It should be noted that the direct path is somewhat obstructed by a hump in the runway.

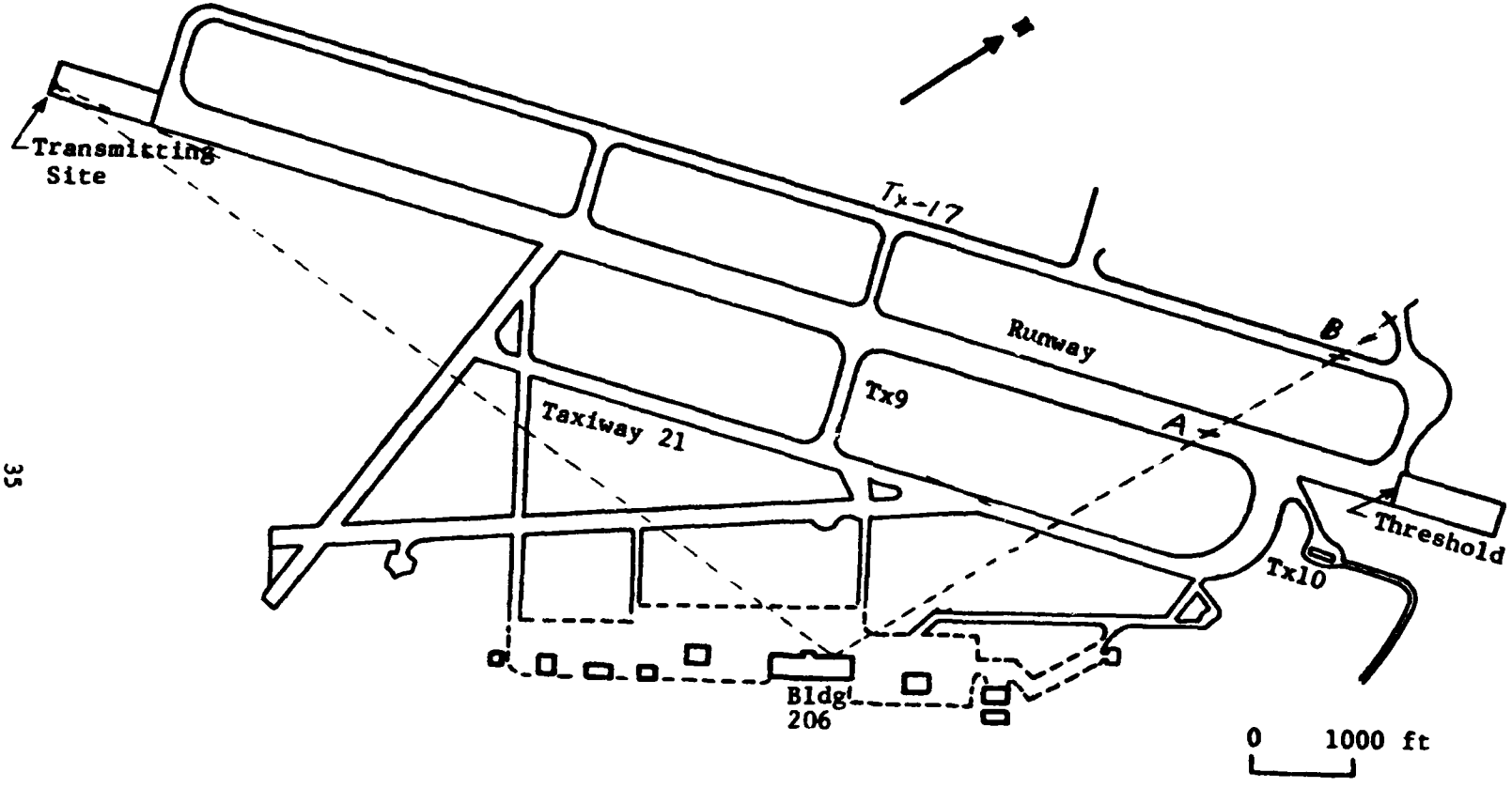

Figure 13
Long Range Test Geometry
Area C, WPAFB, Bldg 206

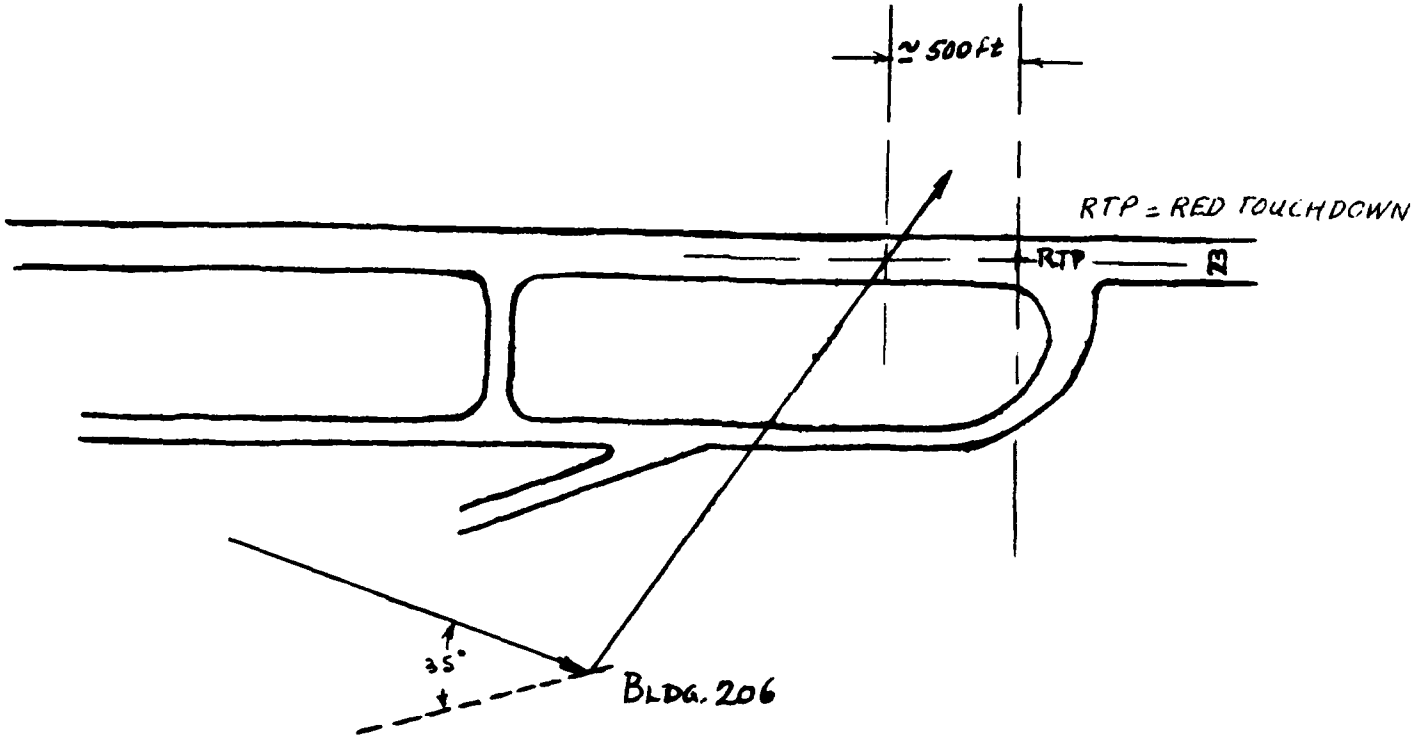

Figure 14

Expanded Test Geometry
Area C, WPAFB, Bldg 206

for the present measurement provide a pencil beam. It is consequently feasible to approximate the ground illumination conditions foreseen for MLS by tilting the transmitting antenna upwards until the rolloff of direct path antenna gain at the horizon is about 10 db per degree. Then, employing the same geometry as in previous experiments (Figure 15) the spatial variation may be checked. One major difference between the present measurements and the earlier ones is that no automatic data recording and processing equipment are now available. For this reason the actual measurements required a sequence of static measurements taken at intervals of only a few inches over short sections of Loop Road. Only spatially relative levels are of interest so no attempt was made to relate present power readings to the ones made earlier. The result of this experiment is reported in Section IV.

2.2.3 Supporting Measurements

In addition to these general data collection experiments, three supporting experiments were also defined. Their intent was to provide aid in carrying out the main experimental sequence and in interpreting the data. These experiments included a series of vertical probes to assess the probable effects of ground reflection with and without an absorbing barrier, a series of reflection measurements with no reflector to assess experimentally the effect of side lobe leakage along the direct path, and a series of actual short range reflection measurements all using the same basic geometry but with differing leg lengths on the reflected path to assess the effect on received power of changing the distribution of power on the reflector. Of

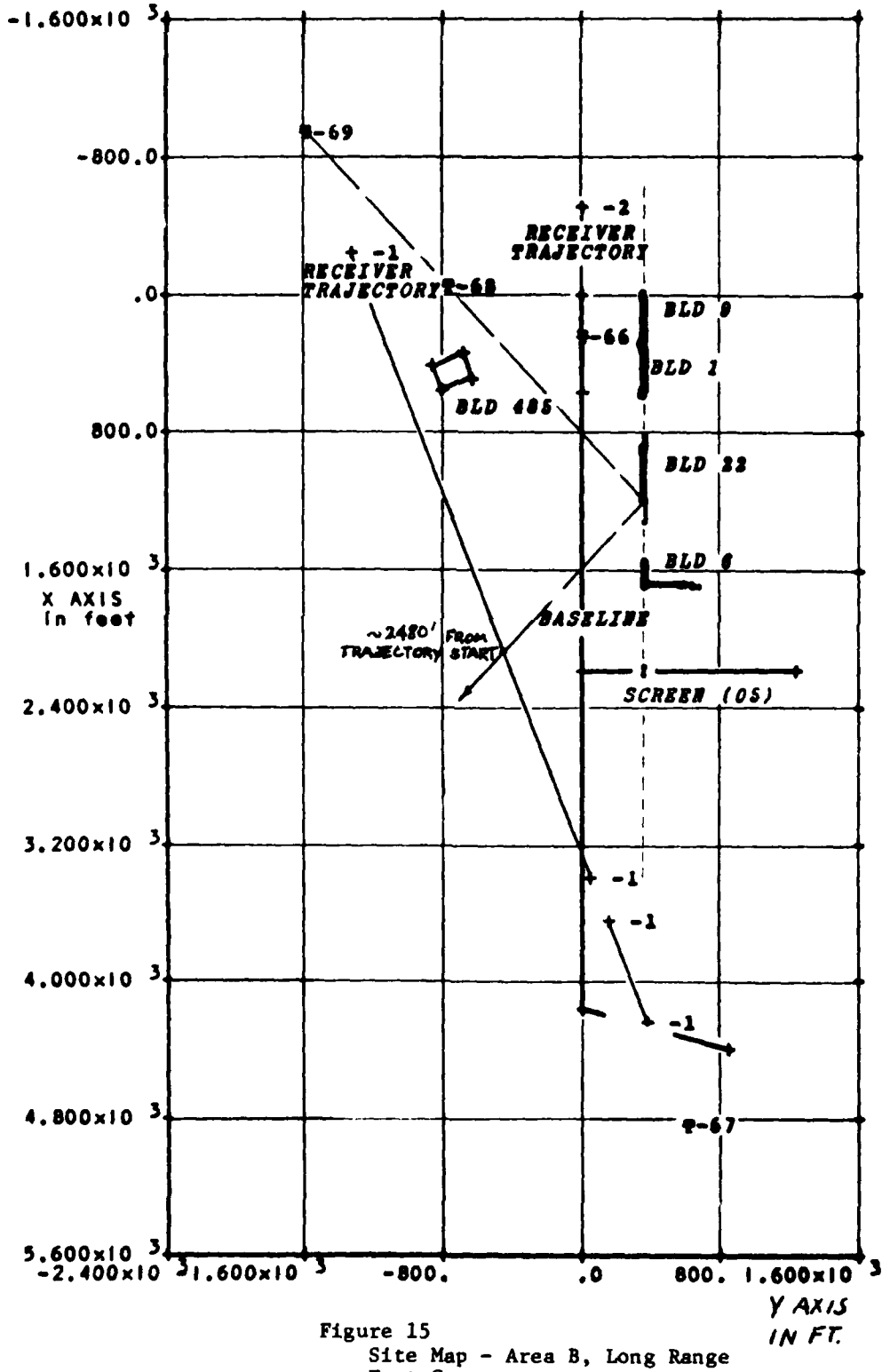

Figure 15
Site Map - Area B, Long Range
Test Geometry

the three only the first was actually performed and that in an ad hoc fashion in an actual short range set up for Building 1. The second was not run at all but this is not thought to be a serious lack since comprehensive patterns are available on all antennas. The third and last of these projected supporting experiments was conceived as having low priority and was simply dropped in favor of more desired results.

The measured patterns for the dishes are shown in Figure 16.

III. EXPERIMENTAL RESULTS - REFLECTION COEFFICIENTS VS POLARIZATION

3.1 Survey Data

The site surveys were conducted with precision instrumentation (theodolite and electronic DME) and the locations for transmitter and receiver are known within an inch or so. This error is negligible when it is remembered that the reciving antenna aperture is two feet at Ku Band and four feet at C Band. Upon completion of each site survey the lengths of the chords from adjacent 10° survey points were checked with a tape measure, confirming the high accuracy expected. It may be noted from the contours of the ground in front of Bldgs 1 and 22 that the surfaces are reasonably planar; however, in the case of Bldg 485 the grassy surface exhibits departures of several feet from a plane. In the case of Bldg 206 the pavement appears to have about the same degree of flatness as do the Bldg 1 and 22 sites, but the small amount of actual survey data collected (35° grazing only) precludes a more definitive statement.

3.2 Reflection Data for Nominally Flat Surfaces

Table 3 summarizes the results of basic test conducted on Bldg 1, 206, and 485 for the polarization, wavelength and grazing angle combinations

Table 3

REFLECTION COEFFICIENTS IN DB BELOW ZERO

Bldg	Pol	10°	20°	30°	40°	10°	20°	30°	40°
1	V		3.25	4.84	15.46		10.95		
	H		12.65	9.44	15.76		28.45		
	LHC		12.7	17.84	24.16		19.45		
	RHC		12.35	-			14.45		
206	V			7.55				6.05	
	H			11.95	35°			14.25	35°
	LHC			16.65				15.95	
	RHC			19.85				12.25	
485	V	2.77	2.36	5.44	6.46	3.47	8.46	11.24	5.16
	H	11.07	19.86	21.14	14.26	9.07	23.96	36.24	18.16
	LHC	5.17	7.16	12.84	16.96	5.37	12.46	17.74	13.16
	RHC	5.07	6.86	12.24	15.16	5.47	12.96	16.24	8.66
		C				Ku			

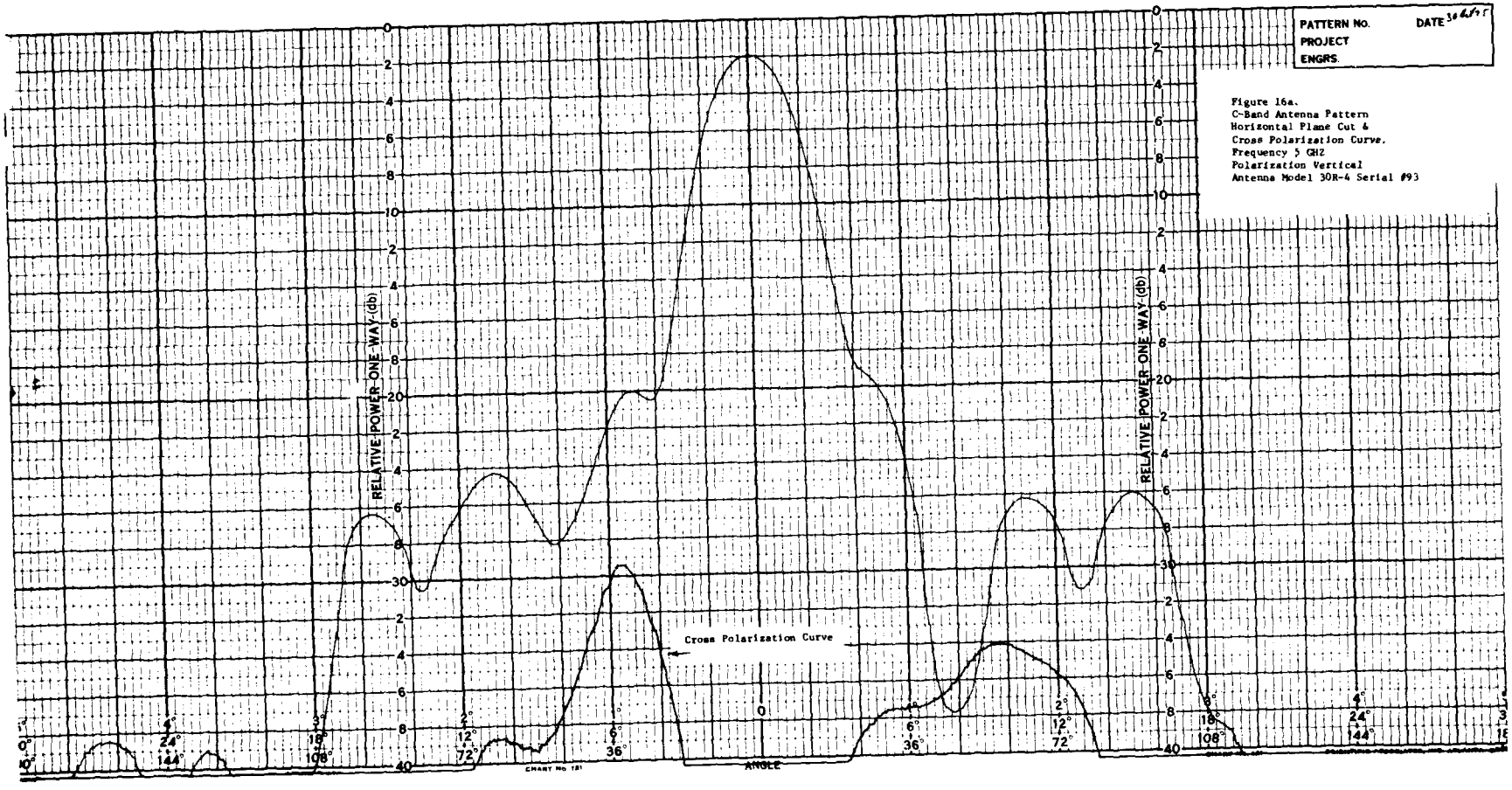

Figure 16a.
C-Band Antenna Pattern
Horizontal Plane Cut &
Cross Polarization Curve.
Frequency 5 GHZ
Polarization Vertical
Antenna Model 30R-4 Serial #93

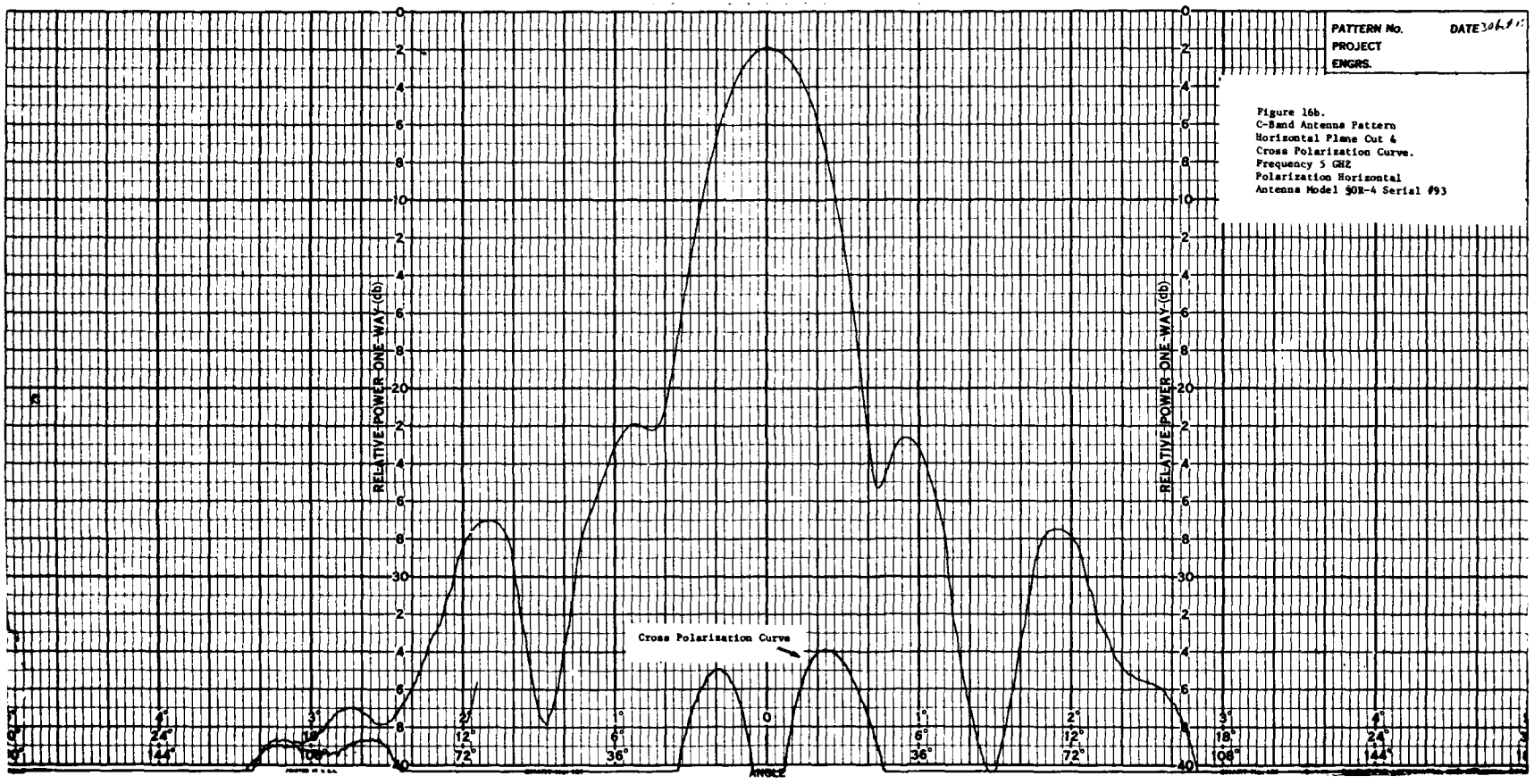
PATTERN No.
DATE
PROJECT
ENGRS.
Figure 16b.
C-Band Antenna Pattern
Horizontal Plane Cut &
Cross Polarization Curve.
Frequency 5 GHZ
Polarization Horizontal
Antenna Model 90R-4 Serial #93
RELATIVE POWER ONE-WAY (db)
Cross Polarization Curve
ANGLE
0
2
4
6
8
10
20
30
40
4°
24°
144°
3°
18°
108°
2°
12°
72°
1°
6°
36°

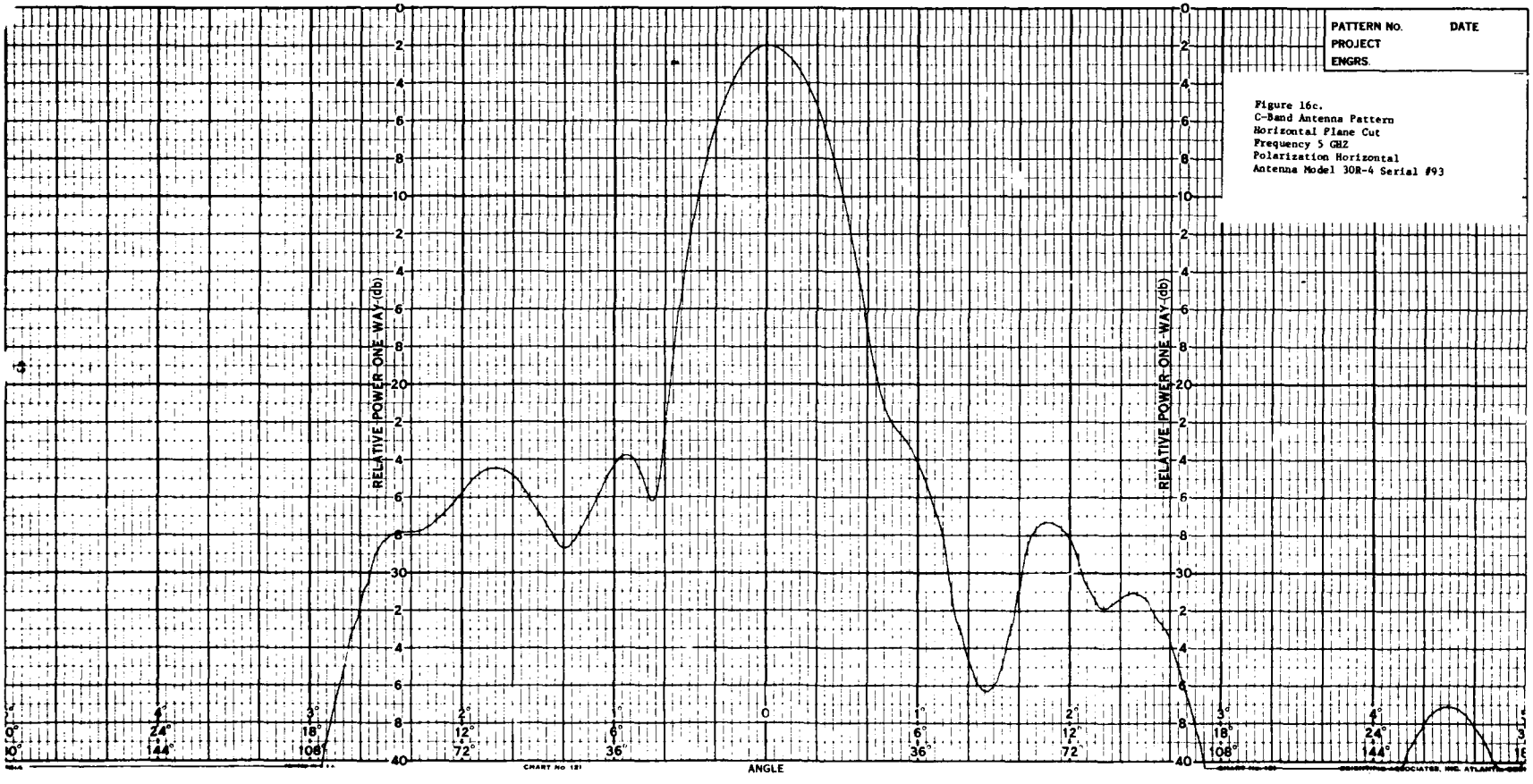
PATTERN NO.
DATE
PROJECT
ENGRS.
Figure 16c.
C-Band Antenna Pattern
Horizontal Plane Cut
Frequency 5 GHZ
Polarization Horizontal
Antenna Model 30R-4 Serial #93
RELATIVE POWER-ONE WAY-(db)
ANGLE
0
2
4
6
8
10
20
30
40
4°
24°
144°
3°
18°
108°
2°
12°
72°
1°
6°
36°
0

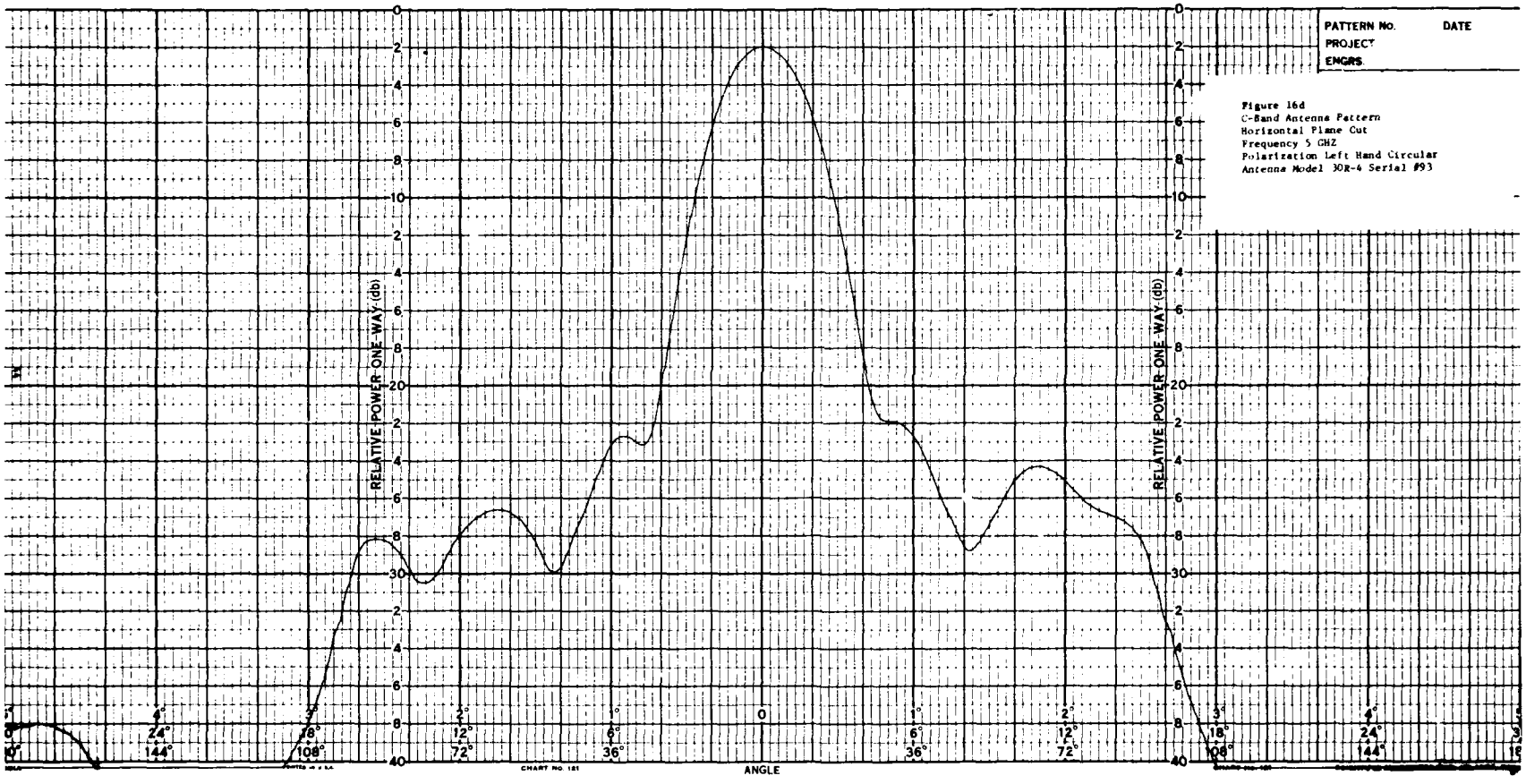
PATTERN NO.
DATE
PROJECT
ENGRS.
Figure 16d
C-Band Antenna Pattern
Horizontal Plane Cut
Frequency 5 GHZ
Polarization Left Hand Circular
Antenna Model 30R-4 Serial #93
RELATIVE POWER ONE-WAY (db)
RELATIVE POWER ONE-WAY (db)
ANGLE
0
2
4
6
8
10
20
30
40
3°
18°
108°
2°
12°
72°
1°
6°
36°
0
1°
6°
36°
2°
12°
72°
3°
18°
108°
4°
24°
144°

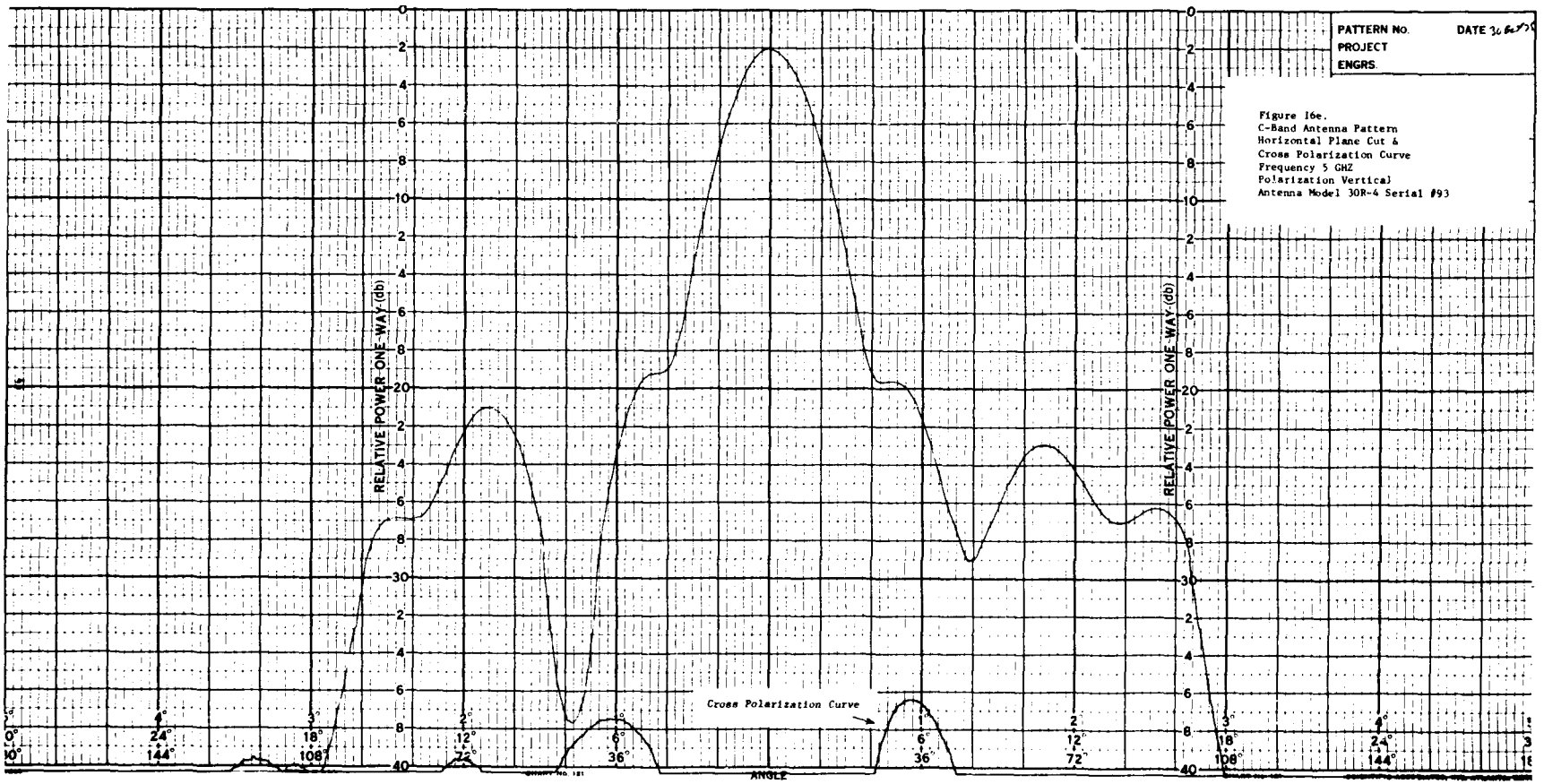
PATTERN NO.
DATE
PROJECT
ENGRS.
Figure 16e.
C-Band Antenna Pattern
Horizontal Plane Cut &
Cross Polarization Curve
Frequency 5 GHZ
Polarization Vertical
Antenna Model 30R-4 Serial #93
RELATIVE POWER ONE WAY (db)
Cross Polarization Curve
ANGLE

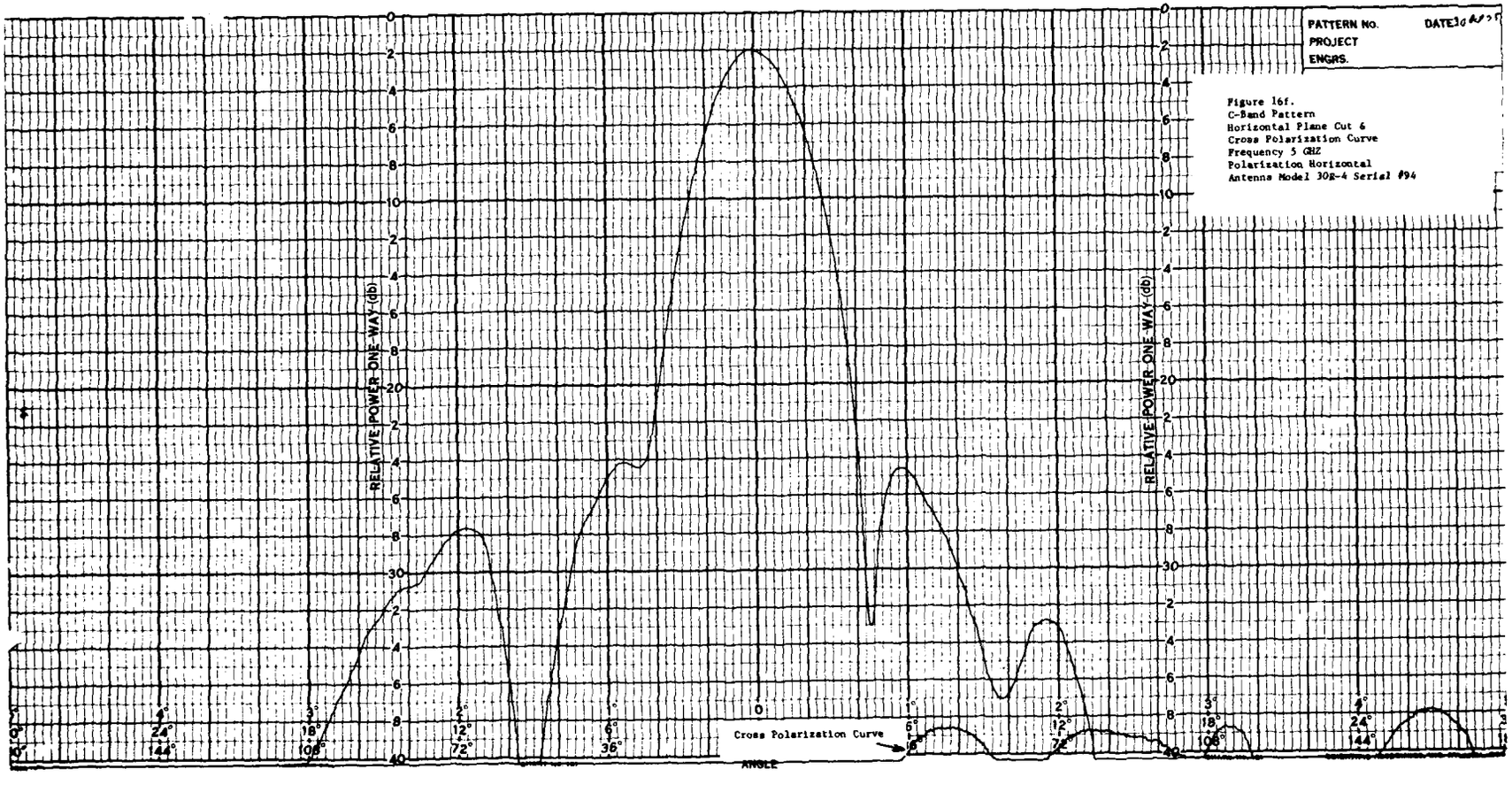
PATTERN NO.
DATE
PROJECT
ENGRS.
Figure 16f.
C-Band Pattern
Horizontal Plane Cut &
Cross Polarization Curve
Frequency 5 GHZ
Polarization Horizontal
Antenna Model 30R-4 Serial #94
RELATIVE POWER ONE-WAY (db)
Cross Polarization Curve
ANGLE

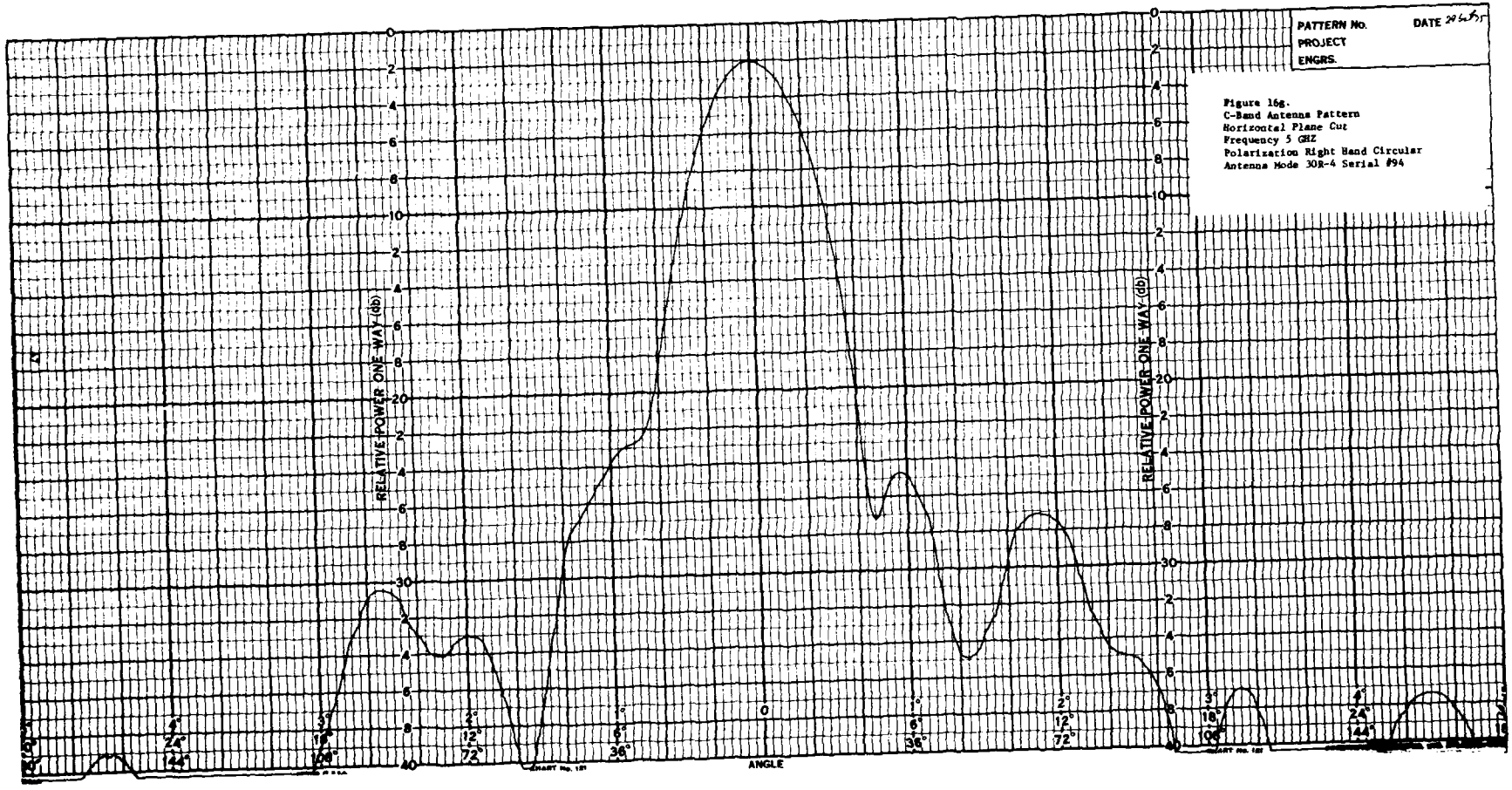
PATTERN No.
DATE
PROJECT
ENGRS.
Figure 16g.
C-Band Antenna Pattern
Horizontal Plane Cut
Frequency 5 GHZ
Polarization Right Hand Circular
Antenna Mode 30R-4 Serial #94
RELATIVE POWER ONE-WAY (db)
ANGLE
0
2
4
6
8
10
20
30
40
3°
18°
108°
2°
12°
72°
1°
6°
36°
1°
24°
144°

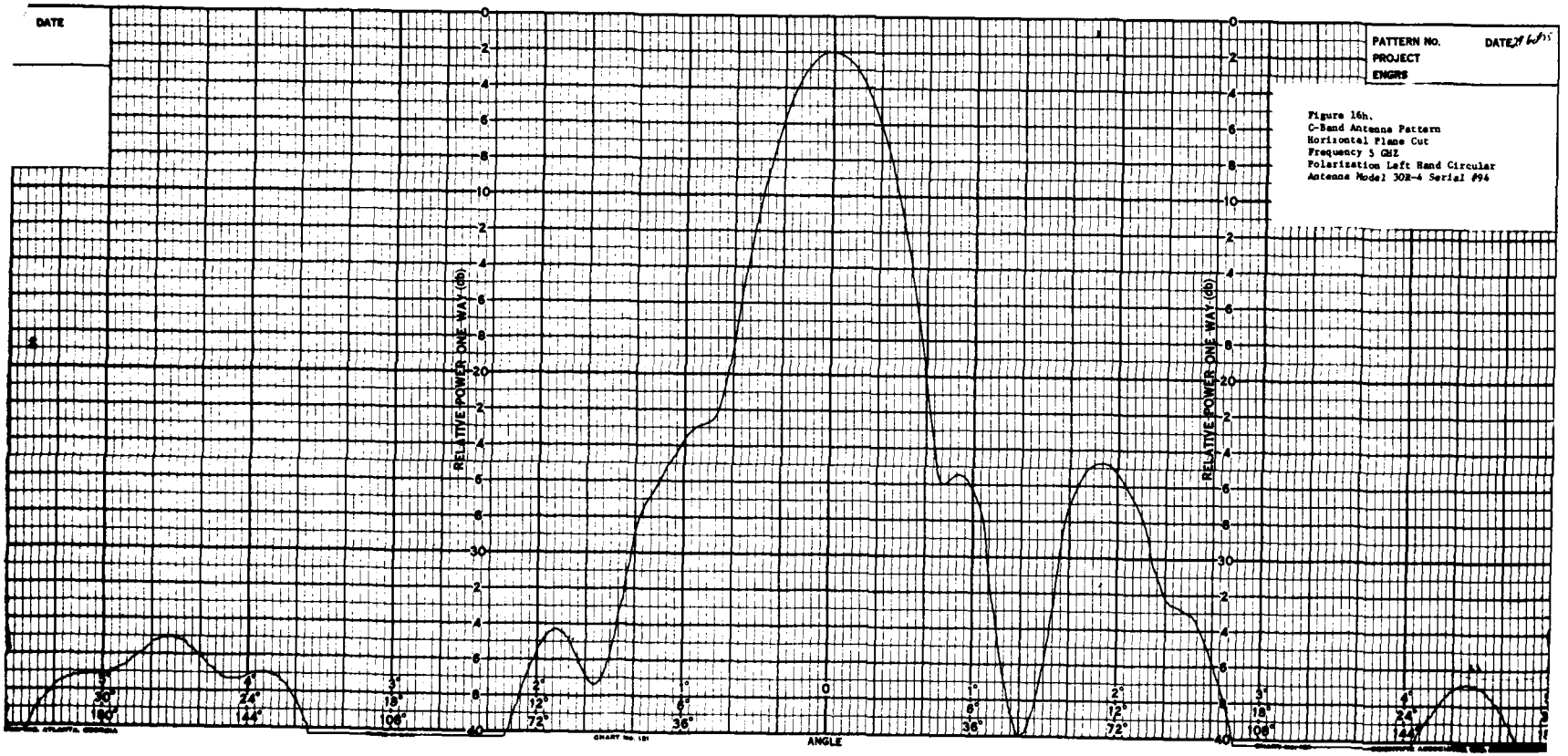
DATE
PATTERN No.
PROJECT
ENGRS
Figure 16h.
C-Band Antenna Pattern
Horizontal Plane Cut
Frequency 5 GHZ
Polarization Left Hand Circular
Antenna Model 302-4 Serial #94
RELATIVE POWER ONE WAY (db)
ANGLE

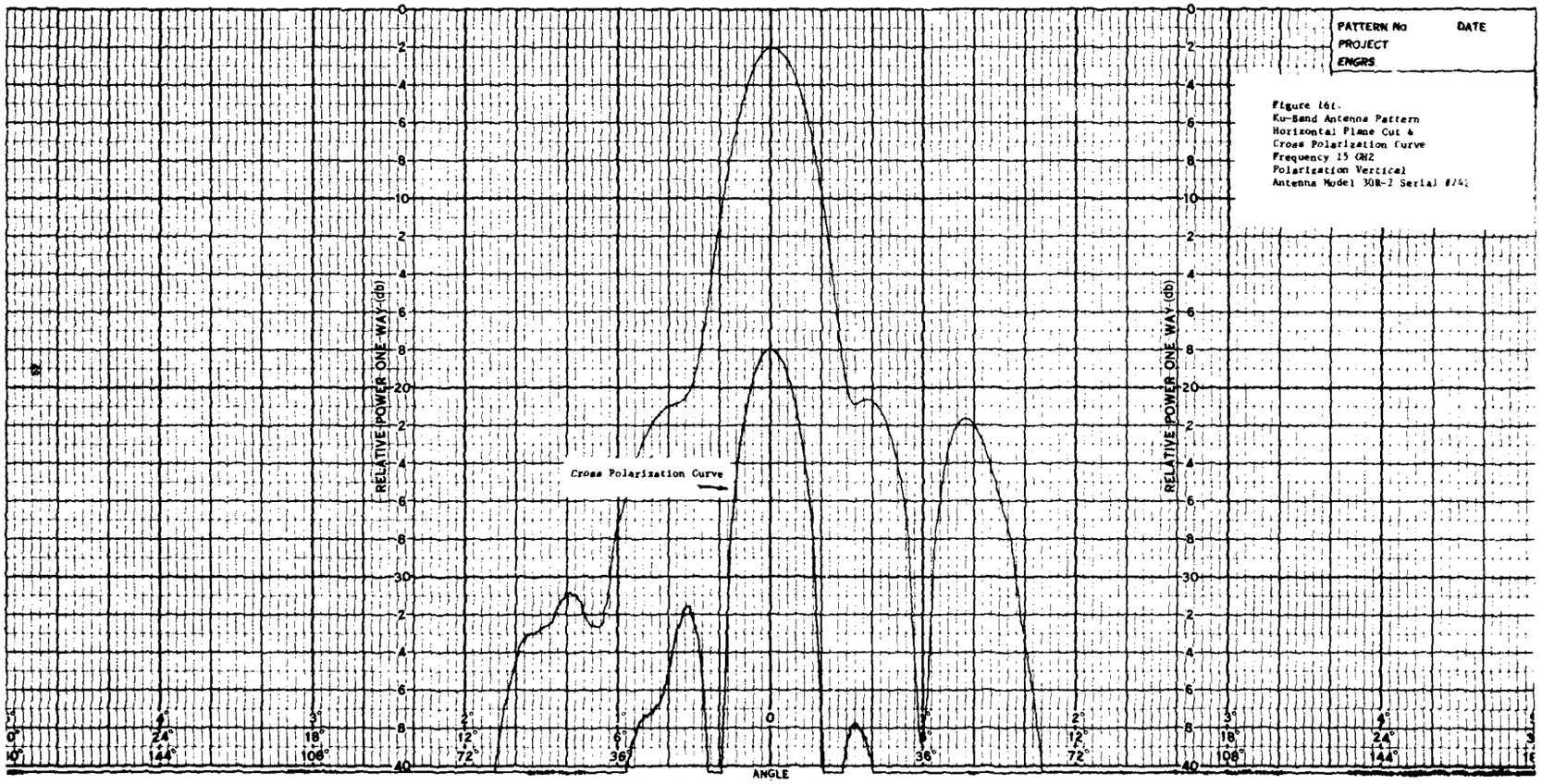
PATTERN No
DATE
PROJECT
ENGRS
Figure 16t.
Ku-Band Antenna Pattern
Horizontal Plane Cut &
Cross Polarization Curve
Frequency 15 GHZ
Polarization Vertical
Antenna Model 30R-2 Serial #24
Cross Polarization Curve
RELATIVE POWER ONE WAY (db)
ANGLE

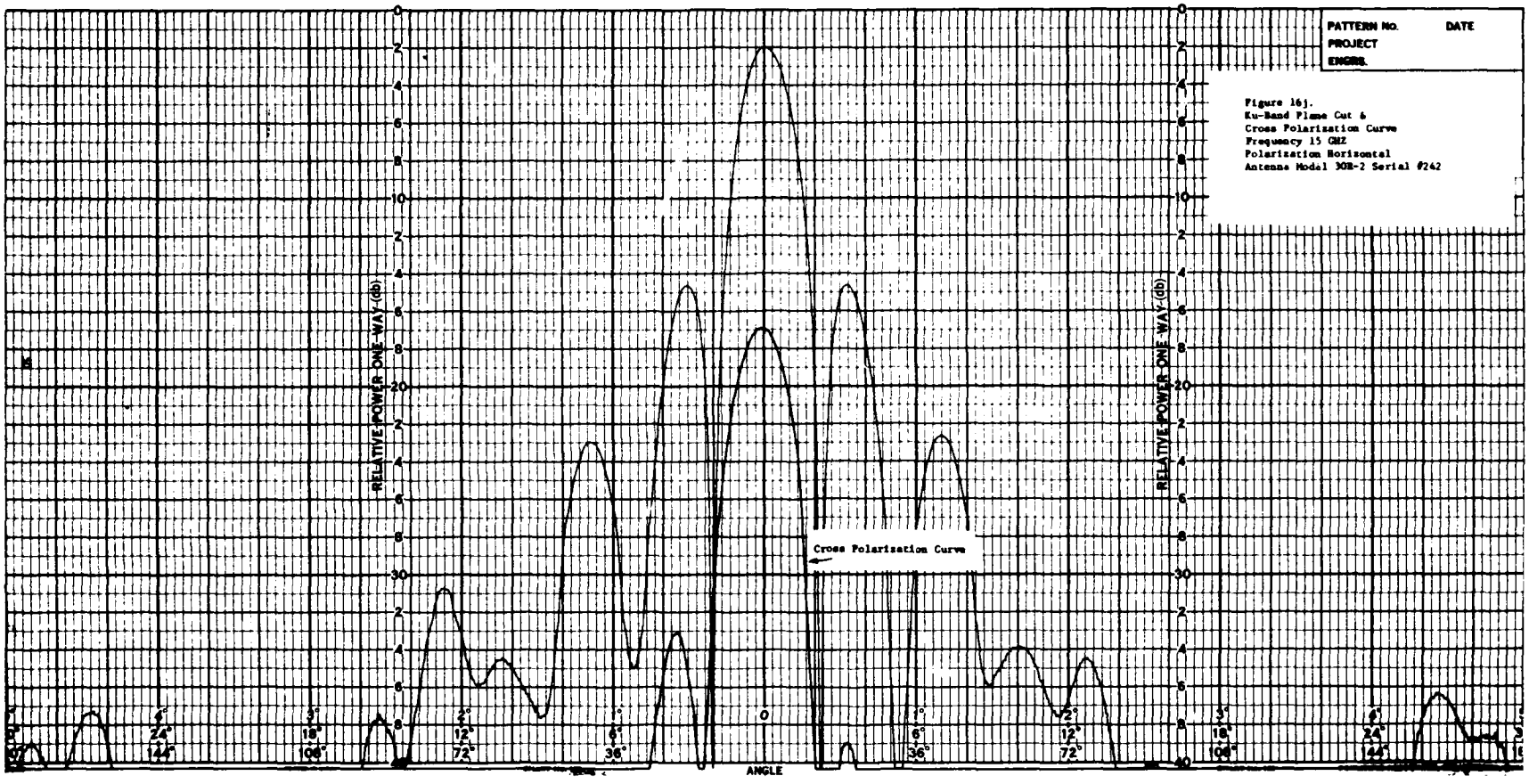
PATTERN No.
DATE
PROJECT
ENGRS.
Figure 16j.
Ku-Band Plane Cut &
Cross Polarization Curve
Frequency 15 GHZ
Polarization Horizontal
Antenna Model 30B-2 Serial #242
RELATIVE POWER ONE WAY-(db)
Cross Polarization Curve
ANGLE
0
2
4
6
8
10
20
30
40
24'
144'
18'
108'
12'
72'
6'
36'
1°
6'
12'
72'
18'
108'
24'
144'

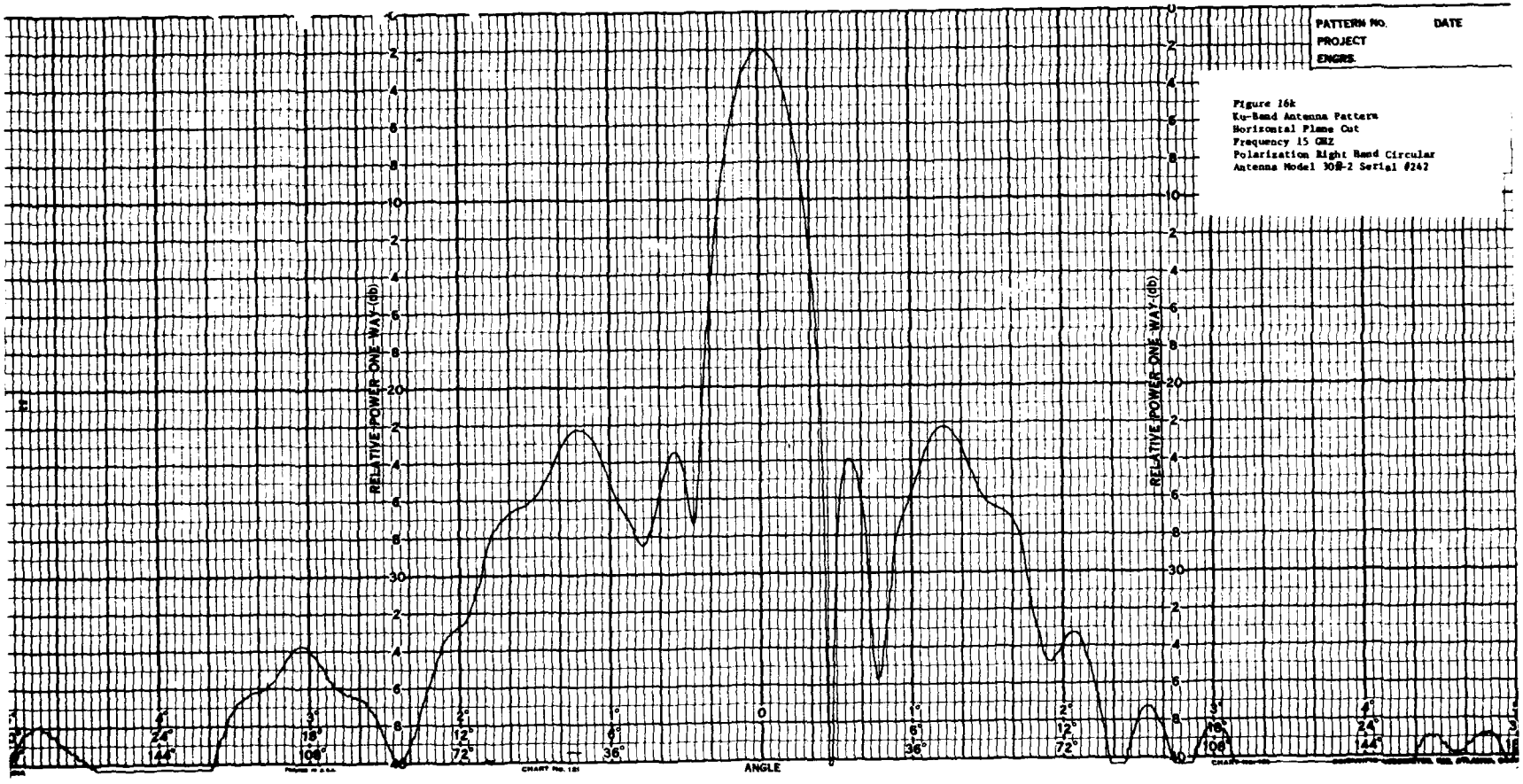
PATTERN NO.
DATE
PROJECT
ENGRS.
Figure 16k
Ku-Band Antenna Pattern
Horizontal Plane Cut
Frequency 15 GHZ
Polarization Right Hand Circular
Antenna Model 30@-2 Serial #242
RELATIVE POWER-ONE-WAY-(db)
ANGLE
0
1°
6'
36°
2°
12'
72°
3°
18'
108°
4°
24'
144°

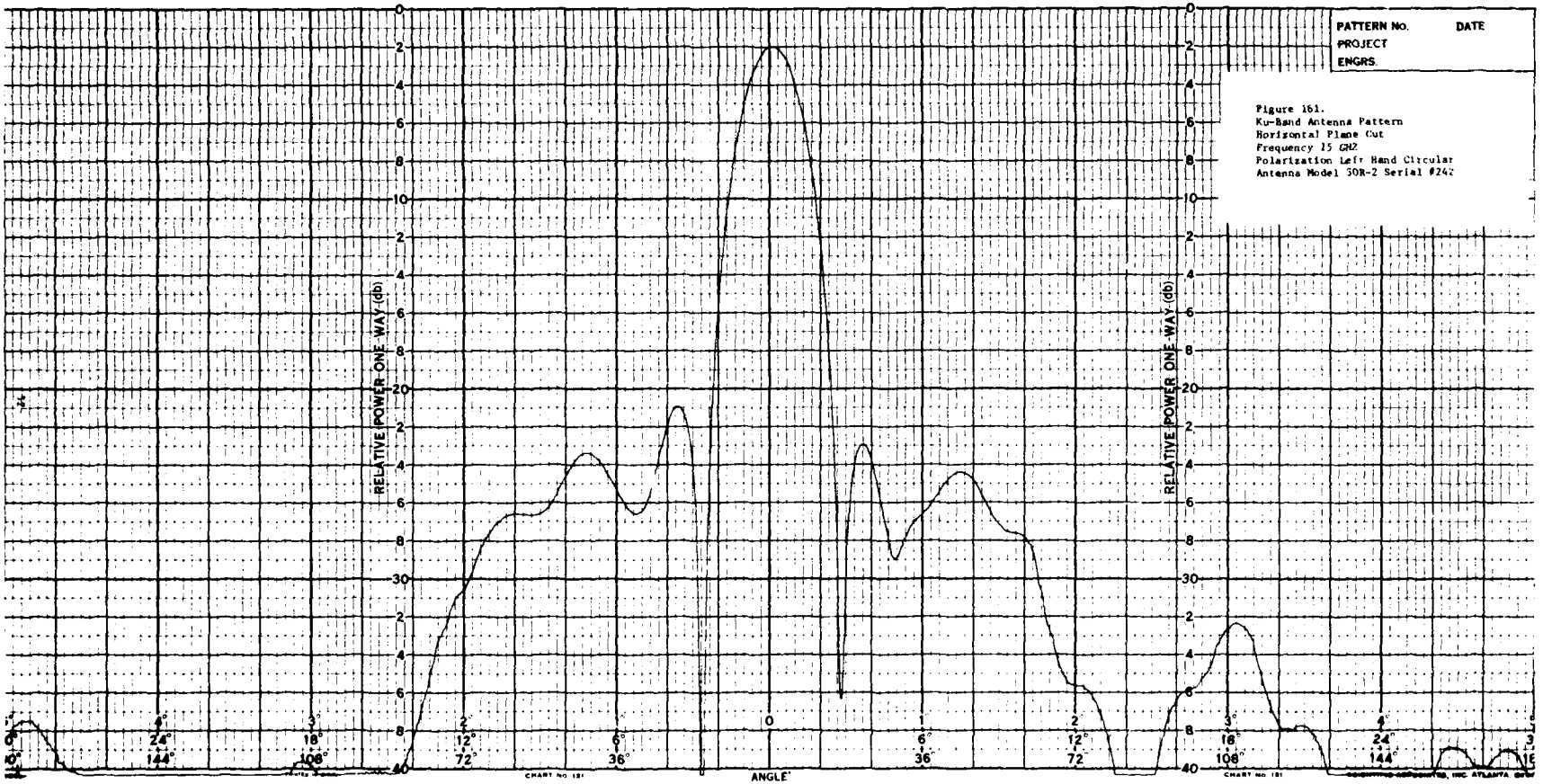
PATTERN No.
DATE
PROJECT
ENGRS.
Figure 161.
Ku-Band Antenna Pattern
Horizontal Plane Cut
Frequency 15 GHZ
Polarization Left Hand Circular
Antenna Model 30R-2 Serial #242
RELATIVE POWER ONE-WAY (db)
ANGLE
CHART NO 121

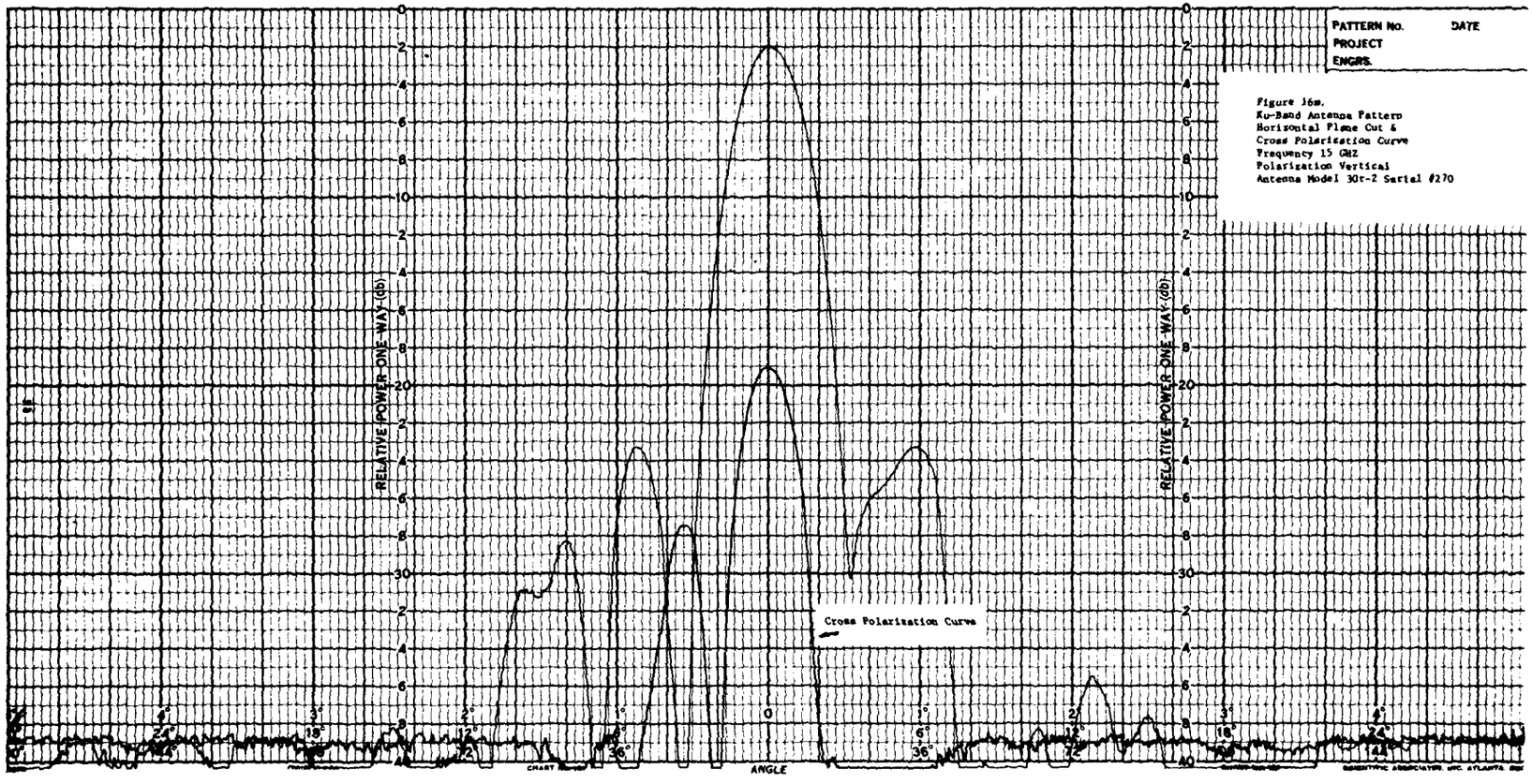
PATTERN No.
DATE
PROJECT
ENGRS.
Figure 16m.
Ku-Band Antenna Pattern
Horizontal Plane Cut &
Cross Polarization Curve
Frequency 15 GHZ
Polarization Vertical
Antenna Model 30t-2 Serial #270
RELATIVE POWER ONE WAY (db)
Cross Polarization Curve
ANGLE

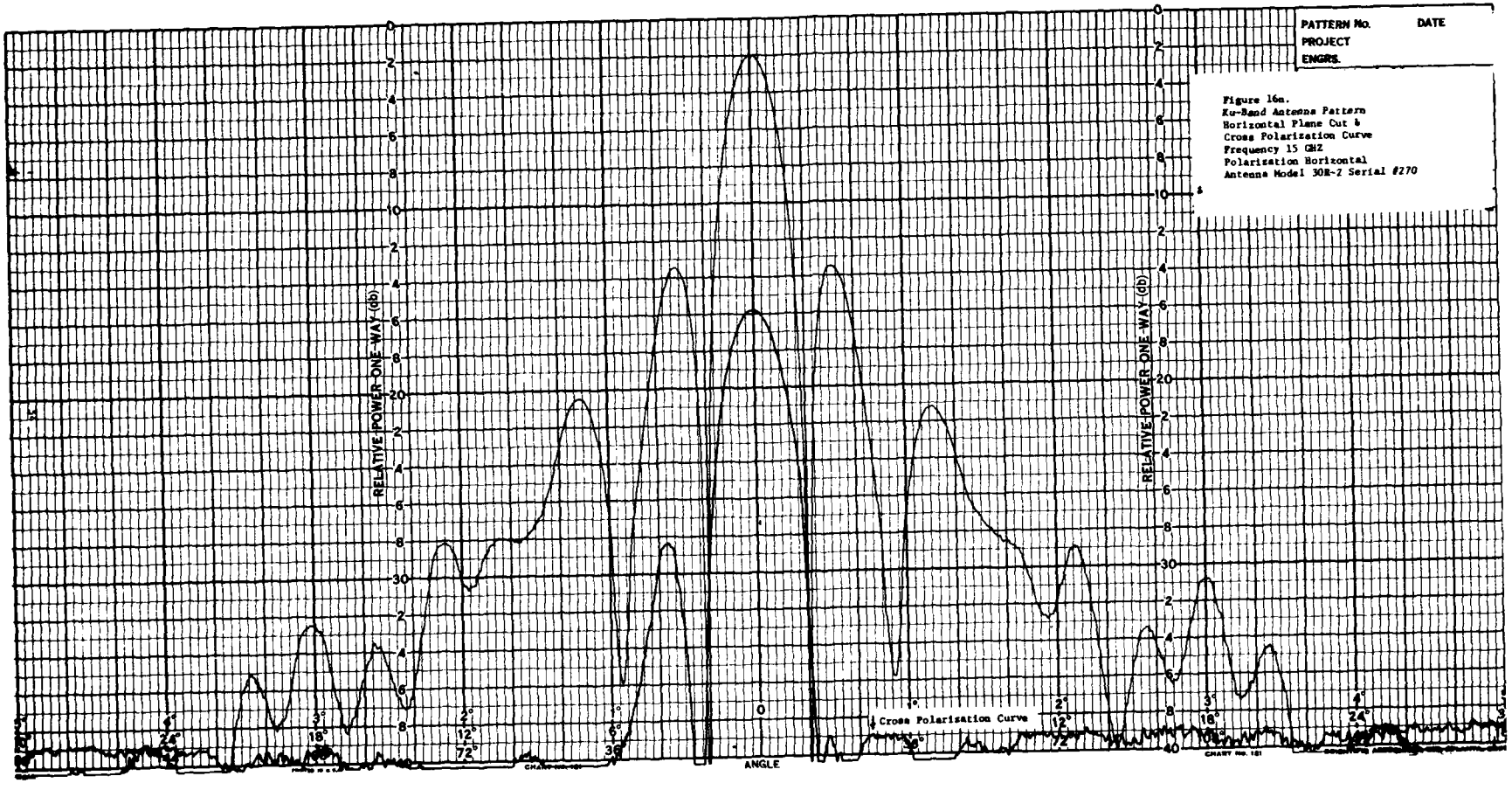
PATTERN No.
DATE
PROJECT
ENGRS.
Figure 16a.
Ku-Band Antenna Pattern
Horizontal Plane Cut &
Cross Polarization Curve
Frequency 15 GHZ
Polarization Horizontal
Antenna Model 30R-2 Serial #270
RELATIVE POWER ONE-WAY (db)
ANGLE
& Cross Polarization Curve

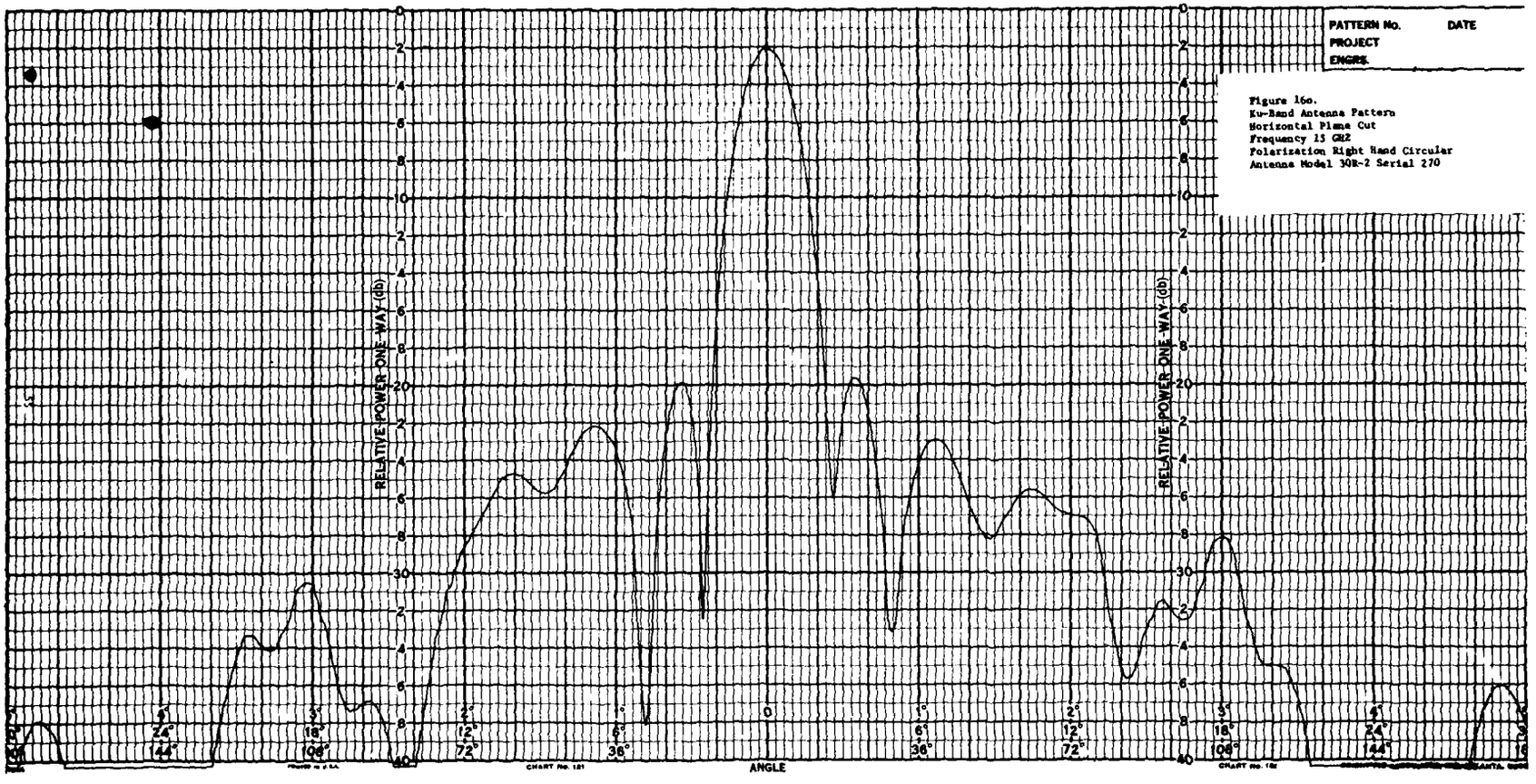

Figure 16o.
Ku-Band Antenna Pattern
Horizontal Plane Cut
Frequency 15 GHZ
Polarization Right Hand Circular
Antenna Model 30R-2 Serial 270

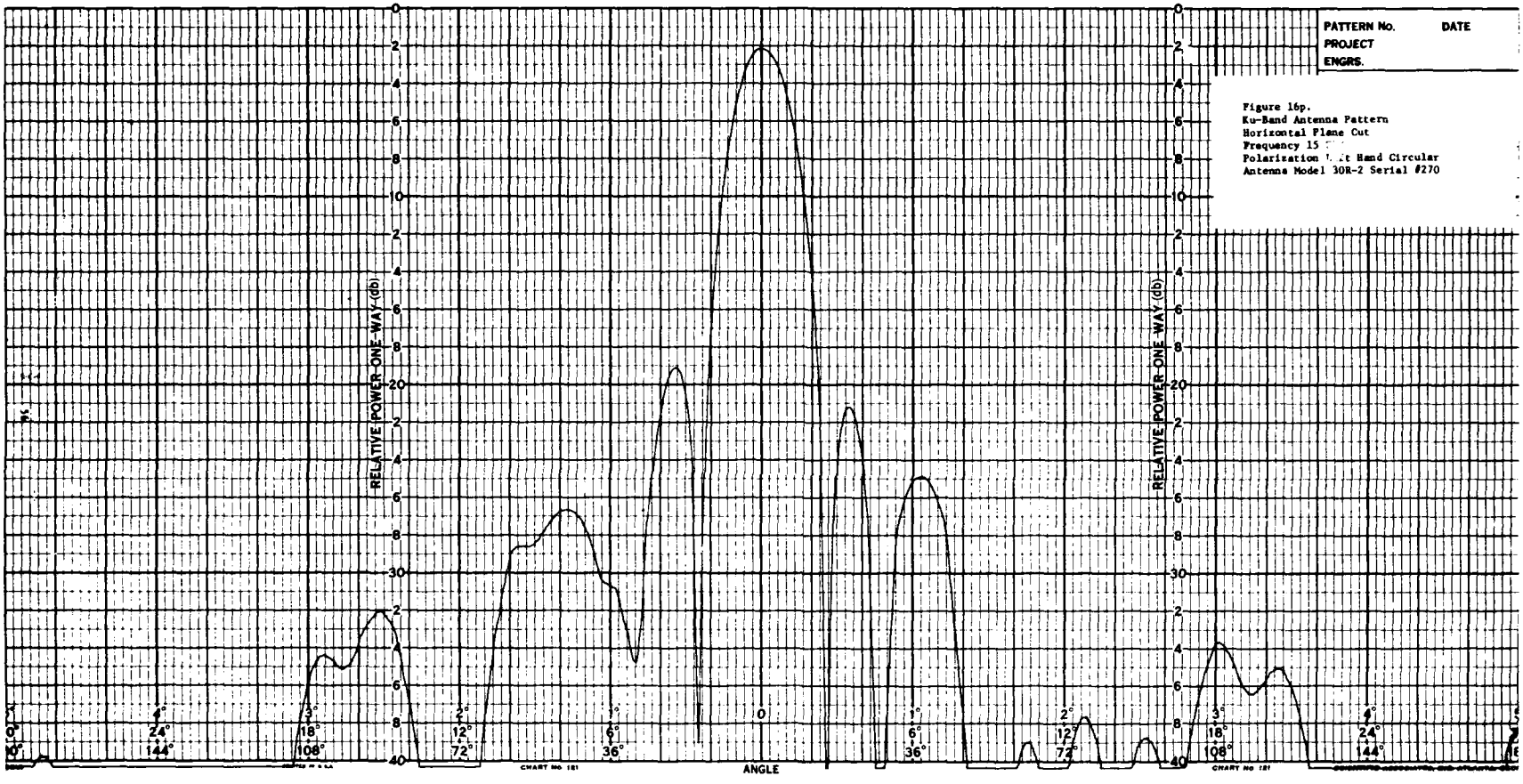
PATTERN No.
DATE
PROJECT
ENGRS.
Figure 16p.
Ku-Band Antenna Pattern
Horizontal Plane Cut
Frequency 15
Polarization
Antenna Model 30R-2 Serial #270
RELATIVE POWER-ONE WAY (db)
ANGLE
4° 24° 144°
3° 18° 108°
2° 12° 72°
1° 6° 36°
0
CHART No 181

studied. The data represent the basic reflection coefficient (referred to by the RAE investigators as "reflection loss"). The data has been corrected to remove differences in the path length losses on the reflected and direct signals. In the case of Bldg 206 the grazing angle is 35°. The precision indicated in the tables is higher than the experimental accuracy and could be rounded off.

Tables 4 through 17 show the actual data values collected and the various stages of manipulation required to arrive at the values summarized in Table 3. For the most part the same transmitter power was used on the direct and reflected path measurements, so the reflection coefficient computation merely involves a correction for the path differential. It should be noted that the actual phase center of the antennas is slightly offset from the ground position of the plumb bob used on the tripod mounts; these offsets amount to 1.698 ft at C Band and 1.875 ft at Ku. Practically these offsets make negligible difference in the computations but have been included for the sake of rigor.

3.3 Reflection Data for Corrugated Surfaces

3.3.1 Field Test Data

Tables 18 and 19 summarize the results obtained in the corrugated section of Bldg 22 for the specular and one space harmonic angle at C and Ku bands respectively. The values predicted by the Army's theoretical model are also shown for comparison purposes. The grazing angle of 40 degrees was selected because the theory predicted that a spatial harmonic at C Band should occur at 57° grazing on the same side of the normal as the

Building 1
Band C
Grazing Angle 20°

TABLE 4

RECORDED DATA

Polarization	DIRECT PATH				REFLECTED PATH				$\frac{P_{RR}}{P_{RD}}$	$\frac{P_{tD}}{P_{tR}}$	K_1+K_2	Range Crtn $\frac{R_R^2}{R_D^2}$	Refl Coeff $K_1+K_2+K_3$
	P_t* Measd	P_t** Actual P_{tD}	P_{Rcvd} P_{RD}	Corrected Range R_D	P_t* Measd	P_t** Actual P_{tR}	P_{Rcvd} P_{RR}	Corrected Range R_R	K_1	K_2		K_3	
V	-11.5	+22.8	-2.3	353.681			-6.1	376.608	-3.8	0	-3.8	.55	-3.25
H	-11.5	+22.8	-1.9	353.681			-15.1	376.608	-13.2	0	-13.2	.55	-12.65
LHC	-11.5	+22.8	-2.2	353.681			-15.45	376.608	-13.25	0	-13.25	.55	-12.7
RHC	-11.5	+22.8	-2.2	353.681			-15.1	376.608	-12.9	0	-12-9	.55	-12.35

Building 1
Band C
Grazing Angle 30°

TABLE 5

RECORDED DATA

Polarization	DIRECT PATH				REFLECTED PATH				$\frac{P_{RR}}{P_{RD}}$	$\frac{P_{tD}}{P_{tR}}$	K_1+K_2	Range Crtn $\frac{R_R^2}{R_D^2}$	Refl Coeff $K_1+K_2+K_3$
	P_t* Measd	P_t** Actual P_{tD}	P_{Rcvd} P_{RD}	Corrected Range R_D	P_t* Measd	P_t** Actual P_{tR}	P_{Rcvd} P_{RR}	Corrected Range R_R	K_1	K_2		K_3	
V	-11.5	22.8	-1.6	325.659			-7.7	376.58	-6.1	0	-6.1	1.26	-4.84
H	-11.5	22.8	-1.7	325.659			-12.4	376.58	-10.7	0	-10.7	1.26	-9.44
LHC	-11.5	22.8	-1.5	325.659			-20.6	376.58	-19.1	0	-19.1	1.26	-17.84

* Corrected Boonton Reading; ** Cal Factor 34.3 db

PRECEDING PAGE BLANK-NOT FILMED

Building 1
Band C
Grazing Angle 40°

TABLE 6

RECORDED DATA

Polarization	DIRECT PATH				REFLECTED PATH				$\frac{P_{RR}}{P_{RD}}$ K_1	$\frac{P_{tD}}{P_{tR}}$ K_2	K_1+K_2	Range Crtn $\frac{R_R^2}{R_D^2}$ K_3	Refl Coeff $K_1+K_2+K_3$
	P_t* Measd	P_t** Actual P_{tD}	P_{Rcvd} P_{RD}	Corrected Range R_D	P_t* Measd	P_t** Actual P_{tR}	P_{Rcvd} P_{RR}	Corrected Range R_R					
V	-11.5	22.8	-0.7	287.663			-18.5	376.611	-17.8	0	-17.8	2.34	-15.46
H	-11.5	22.8	-1.0	287.663			-19.1	376.611	-18.1	0	-18.1	2.34	-15.76
LHC	-11.5	22.8	-0.8	287.663			-27.3	376.611	-26.5	0	-26.5	2.34	-24.16

Building 1
Band Ku
Grazing Angle 20°

TABLE 7

RECORDED DATA

Polarization	DIRECT PATH				REFLECTED PATH				$\frac{P_{RR}}{P_{RD}}$ K_1	$\frac{P_{tD}}{P_{tR}}$ K_2	K_1+K_2	Range Crtn $\frac{R_R^2}{R_D^2}$ K_3	Refl Coeff $K_1+K_2+K_3$
	P_t* Measd	P_t** Actual P_{tD}	P_{Rcvd} P_{RD}	Corrected Range R_D	P_t* Measd	P_t** Actual P_{tR}	P_{Rcvd} P_{RR}	Corrected Range R_R					
V	-30.0	-30.0	-59.0	353.327	-30.0	-30.0	-70.5	376.254	-11.5	0	-11.5	.55	-10.95
H	-30.0	-30.0	-58.0	353.327	0.0	0.0	-57.0	376.254	+1.0	-30.0	-29.0	.55	-28.45
LHC	-30.0	-30.0	-60.0	353.327	-30.0	-30.0	-80.0	376.253	-20.0	0	-20.0	.55	-19.45
RHC	-30.0	-30.0	-60.5	353.327	-30.0	-30.0	-75.5	376.254	-15.0	0	-15.0	.55	-14.45

* Corrected Boonton Reading; ** Cal Factor 34.3 db

Building 206
Band C
Grazing Angle 35°

TABLE 8

RECORDED DATA

Polarization	DIRECT PATH				REFLECTED PATH				$\frac{P_{RR}}{P_{RD}}$	$\frac{P_{tD}}{P_{tR}}$	K_1+K_2	Range Crtn $\frac{R_R^2}{R_D^2}$	Refl Coeff $K_1+K_2+K_3$
	P_t* Measd	P_t** Actual P_{tD}	P_{Rcvd} P_{RD}	Corrected Range R_D	P_t* Measd	P_t** Actual P_{tR}	P_{Rcvd} P_{RR}	Corrected Range R_R	K_1	K_2		K_3	
V	-11.5	+22.8	-2.6	307.884	-11.5	+22.8	-11.9	376.603	-9.3	0	-9.3	1.75	-7.55
H	-11.5	+22.8	-2.9	307.884	-11.5	+22.8	-16.6	376.603	-13.7	0	-13.7	1.75	-11.95
LHC	-11.5	+22.8	-2.3	307.884	-11.5	+22.8	-20.7	376.603	-18.4	0	-18.4	1.75	-16.65
RHC	-11.5	+22.8	-2.3	307.884	-11.5	+22.8	-23.9	376.603	-21.6	0	-21.6	1.75	-19.85

Building 206
Band Ku
Grazing Angle 35°

TABLE 9

RECORDED DATA

Polarization	DIRECT PATH				REFLECTED PATH				$\frac{P_{RR}}{P_{RD}}$	$\frac{P_{tD}}{P_{tR}}$	K_1+K_2	Range Crtn $\frac{R_R^2}{R_D^2}$	Refl Coeff $K_1+K_2+K_3$
	P_t* Measd	P_t** Actual P_{tD}	P_{Rcvd} P_{RD}	Corrected Range R_D	P_t* Measd	P_t** Actual P_{tR}	P_{Rcvd} P_{RR}	Corrected Range R_R	K_1	K_2		K_3	
V	-30.0	-30.0	-57.7	307.53	-30.0	-30.0	-65.5	376.249	-7.8	0	-7.8	1.75	-6.05
H	-30.0	-30.0	-56.5	307.53	-30.0	-30.0	-72.5	376.249	-16.0	0	-16.0	1.75	-14.25
LHC	-30.0	-30.0	-59.3	307.53	-30.0	-30.0	-77.0	376.249	-17.7	0	-17.7	1.75	-15.95
RHC	-30.0	-30.0	-58.5	307.53	-30.0	-30.0	-72.5	376.249	-14.0	0	-14.0	1.75	-12.25

* Corrected Boonton Reading; ** Cal Factor 34.3 db

Building 485
Band C
Grazing Angle 10°

TABLE 10

RECORDED DATA

Polarization	DIRECT PATH				REFLECTED PATH				$\frac{P_{RR}}{P_{RD}}$	$\frac{P_{tD}}{P_{tR}}$	K_1+K_2	Range Crtn $\frac{R_R^2}{R_D^2}$	Refl Coeff $K_1+K_2+K_3$
	P_t* Measd	P_t** Actual P_{tD}	P_{Rcvd} P_{RD}	Corrected Range R_D	P_t* Measd	P_t** Actual P_{tR}	P_{Rcvd} P_{RR}	Corrected Range R_R	K_1	K_2		K_3	
V	-11.5	+22.8	-4.3	370.872	-11.5	+22.8	-7.2	376.578	-2.9	0	-2.9	0.13	-2.77
H	-11.5	+22.8	-4.5	370.872	-11.5	+22.8	-15.7	376.578	-11.2	0	-11.2	0.13	-11.07
LHC	-11.5	+22.8	-4.4	370.872	-11.5	+22.8	-9.7	376.578	-5.3	0	-5.3	0.13	-5.17
RHC	-11.5	+22.8	-4.4	370.872	-11.5	+22.8	-9.6	376.578	-5.2	0	-5.2	0.13	-5.07

Building 485
Band C
Grazing Angle 20°

TABLE 11

RECORDED DATA

Polarization	DIRECT PATH				REFLECTED PATH				$\frac{P_{RR}}{P_{RD}}$	$\frac{P_{tD}}{P_{tR}}$	K_1+K_2	Range Crtn $\frac{R_R^2}{R_D^2}$	Refl Coeff $K_1+K_2+K_3$
	P_t* Measd	P_t** Actual P_{tD}	P_{Rcvd} P_{RD}	Corrected Range R_D	P_t* Measd	P_t** Actual P_{tR}	P_{Rcvd} P_{RR}	Corrected Range R_R	K_1	K_2		K_3	
V	-11.5	+22.8	-4.7	353.672	-11.5	+22.8	-7.6	376.468	-2.9	0	-2.9	0.54	-2.36
H	-11.5	+22.8	-4.9	353.672	-11.5	+22.8	-25.3	376.468	-20.4	0	-20.4	0.54	-19.86
LHC	-11.5	+22.8	-4.5	353.672	-11.5	+22.8	-12.2	376.468	-7.7	0	-7.7	0.54	-7.16
RHC	-11.5	+22.8	-4.5	353.672	-11.5	+22.8	-11.9	376.468	-7.4	0	-7.4	0.54	-6.86

* Corrected Boonton Reading; ** Cal Factor 34.3 db

Building 485
Band C
Grazing Angle 30°

TABLE 12

RECORDED DATA

Polarization	DIRECT PATH				REFLECTED PATH				$\frac{P_{RR}}{P_{RD}}$	$\frac{P_{tD}}{P_{tR}}$	K_1+K_2	Range Crtn $\frac{R_R^2}{R_D^2}$	Refl Coeff $K_1+K_2+K_3$
	P_t* Measd	P_t** Actual P_{tD}	P_{Rcvd} P_{RD}	Corrected Range R_D	P_t* Measd	P_t** Actual P_{tR}	P_{Rcvd} P_{RR}	Corrected Range R_R	K_1	K_2		K_3	
V	-11.5	+22.8	-4.2	325.754	-11.5	+22.8	-10.9	376.492	-6.7	0	-6.7	1.26	-5.44
H	-11.5	+22.8	-2.9	325.754	-11.5	+22.8	-25.3	376.492	-22.4	0	-22.4	1.26	-21.14
LHC	-11.5	+22.8	-4.0	325.754	-11.5	+22.8	-18.1	376.492	-14.1	0	-14.1	1.26	-12.84
RHC	-11.5	+22.8	-4.0	325.754	-11.5	+22.8	-17.5	376.492	-13.5	0	-13.5	1.26	-12.24

Building 485
Band C
Grazing Angle 40°

TABLE 13

RECORDED DATA

Polarization	DIRECT PATH				REFLECTED PATH				$\frac{P_{RR}}{P_{RD}}$	$\frac{P_{tD}}{P_{tR}}$	K_1+K_2	Range Crtn $\frac{R_R^2}{R_D^2}$	Refl Coeff $K_1+K_2+K_3$
	P_t* Measd	P_t** Actual P_{tD}	P_{Rcvd} P_{RD}	Corrected Range R_D	P_t* Measd	P_t** Actual P_{tR}	P_{Rcvd} P_{RR}	Corrected Range R_R	K_1	K_2		K_3	
V	-11.5	+22.8	-4.3 (EST)*	287.851	-11.5	+22.8	-13.1	376.663	-8.8	0	-8.8	2.34	-6.46
H	-11.5	+22.8	-4.3	287.851	-11.5	+22.8	-20.9	376.663	-16.6	0	-16.6	2.34	-14.26
LHC	-11.5	+22.8	-4.3	287.851	-11.5	+22.8	-23.6	376.663	-19.3	0	-19.3	2.34	-16.96
RHC	-11.5	+22.8	-4.3	287.851	-11.5	+22.8	-21.8	376.663	-17.5	0	-17.5	2.34	-15.16

* Corrected Boonton Reading; ** Cal Factor 34.3 db (EST)* Direct Path Obstructed by Traffic Sign

Building 485
Band KU
Grazing Angle 10°

TABLE 14

RECORDED DATA

Polarization	DIRECT PATH				REFLECTED PATH				$\frac{P_{RR}}{P_{RD}}$	$\frac{P_{tD}}{P_{tR}}$	K_1+K_2	Range Crtn $\frac{R_R^2}{R_D^2}$	Refl Coeff $K_1+K_2+K_3$
	P_t* Measd	P_t** Actual P_{tD}	P_{Rcvd} P_{RD}	Corrected Range R_D	P_t* Measd	P_t** Actual P_{tR}	P_{Rcvd} P_{RR}	Corrected Range R_R	K_1	K_2		K_3	
V	+10.0	+10.0	-19.1	370.518	+10.0	+10.0	-22.7	376.224	-3.6	0	-3.6	0.13	-3.47
H	+10.0	+10.0	-17.8	370.518	+10.0	+10.0	-27.0	376.224	-9.2	0	-9.2	0.13	-9.07
LHC	+10.0	+10.0	-20.8	370.518	+10.0	+10.0	-26.3	376.224	-5.5	0	-5.5	0.13	-5.37
RHC	+10.0	+10.0	-20.6	370.518	+10.0	+10.0	-26.2	376.224	-5.6	0	-5.6	0.13	-5.47

Building 485
Band Ku
Grazing Angle 20°

TABLE 15

RECORDED DATA

Polarization	DIRECT PATH				REFLECTED PATH				$\frac{P_{RR}}{P_{RD}}$	$\frac{P_{tD}}{P_{tR}}$	K_1+K_2	Range Crtn $\frac{R_R^2}{R_D^2}$	Refl Coeff $K_1+K_2+K_3$
	P_t* Measd	P_t** Actual P_{tD}	P_{Rcvd} P_{RD}	Corrected Range R_D	P_t* Measd	P_t** Actual P_{tR}	P_{Rcvd} P_{RR}	Corrected Range R_R	K_1	K_2		K_3	
V	-30.0	-30.0	-58.0	353.318	-30.0	-30.0	-67.0	376.114	-9.0	0	-9.0	.54	-8.46
H	-30.0	-30.0	-57.5	353.318	0	0	-52.0	376.114	+5.5	-30.0	-24.5	.54	-23.96
LHC	-30.0	-30.0	-59.0	353.318	-30.0	-30.0	-72.0	376.114	-13.0	0	-13.0	.54	-12.46
RHC	-30.0	-30.0	-59.5	353.318	-30.0	-30.0	-73.0	376.114	-13.5	0	-13.5	.54	-12.96

* Corrected Boonton Reading; ** Cal Factor 34.3 db

Building 485
Band Ku
Grazing Angle 30°

TABLE 16

RECORDED DATA

Polarization	DIRECT PATH				REFLECTED PATH								
	P_t* Measd	P_t** Actual P_{tD}	P_{Rcvd} P_{RD}	Corrected Range R_D	P_t* Measd	P_t** Actual P_{tR}	P_{Rcvd} P_{RR}	Corrected Range R_R	$\frac{P_{RR}}{P_{RD}}$ K_1	$\frac{P_{tD}}{P_{tR}}$ K_2	K_1+K_2	Range Crtn $\frac{R_R^2}{R_D^2}$ K_3	Refl Coeff $K_1+K_2+K_3$
V	-30.0	-30.0	-61.0	325.431	0.0	0.0	-43.5	376.138	+17.5	-30.0	-12.5	1.26	-11.24
H	-30.0	-30.0	-58.0	325.431	0.0	0.0	-65.5	376.138	-7.5	-30.0	-37.5	1.26	-36.24
LHC	-30.0	-30.0	-62.0	325.431	0.0	0.0	-51.0	376.138	+11.0	-30.0	-19.0	1.26	-17.74
RHC	-30.0	-30.0	-62.5	325.431	0.0	0.0	-50.0	376.138	+12.5	-30.0	-17.5	1.26	-16.24

Building 485
Band Ku
Grazing Angle 40°

TABLE 17

RECORDED DATA

NOTE: Direct path obstructed. Signal level estimated from other grazing angles. Possible error in refl coeff +2 1/2 db

Polarization	DIRECT PATH				REFLECTED PATH								
	P_t* Measd	P_t** Actual P_{tD}	P_{Rcvd} P_{RD}	Corrected Range R_D	P_t* Measd	P_t** Actual P_{tR}	P_{Rcvd} P_{RR}	Corrected Range R_R	$\frac{P_{RR}}{P_{RD}}$ K_1	$\frac{P_{tD}}{P_{tR}}$ K_2	K_1+K_2	Range Crtn $\frac{R_R^2}{R_D^2}$ K_3	Refl Coeff $K_1+K_2+K_3$
V	-30.0	-30.0	-60.0 (EST)	287.497	-30.0	-30.0	-67.5	376.309	-7.5	0	-7.5	2.34	-5.16
H	0.0	0.0	(EST) -30.0	287.497	0.0	0	-50.5	376.309	-20.5	0	-20.5	2.34	-18.16
LHC	0.0	0.0	(EST) -30.0	287.497	0.0	0	-45.5	376.309	-15.5	0	-15.5	2.34	-13.16
RHC	0.0	0.0	-30.0 (EST)	287.497	0.0	0	-41.0	376.309	-11.0	0	-11.0	2.34	-8.66

* Corrected Boonton Reading; ** Cal Factor 34.3 db

Table 18 BLDG 22 DATA SUMMARY

Band C

Grazing Angle 40°

Space Harmonic at 57° grazing on transmitter side. P -3 mode.

Pol	Specular		Space Harmonic	
	Predicted	Actual	Predicted	Actual
V	-8.0	-8.3	-2.6	-5.8
H	-14.0	-10.2	-2.4	-6.1
LHC	NA	-14.6	NA	-21
RHC	NA	-15.6	NA	-22

Table 19 BLDG 22 DATA SUMMARY

Band Ku

Grazing Angle 40°

Space Harmonic at 52° - Opposite side to Transmitter P - 1 mode

Pol	Specular		Space Harmonic	
	Predicted	Actual	Predicted	Actual
V	-5.4	-15.2	-14.0	-22.7
H	-4.3	-16-2	-15.2	-15.2
LHC	NA	-23.7	NA	-27.2
RHC	NA	-24.2	NA	-27.7

transmitter. The theory also predicted that the level of this space harmonic should be greater than the level of the specular reflection itself. The spatial harmonics for a grazing angle of 20° were also of interest, but presented some experimental problems. The perimeter of the parking area in front of Bldg 22 is denoted by a line of fixed concrete blocks which passed within a foot or two of the 20° survey points, thus any movement of the vehicles upon which the antennas were mounted would be virtually impossible due to the obstruction.

The experimental procedure for this test was fundamentally the same as for the basic tests described in 2.2.1, except that the antenna tripods were mounted on the back of trucks to provide the additional height required to illuminate the corrugated surface. Following the measurements at specular geometry the receiving antenna/truck were moved to the position predicted by the Army theory for the location of a space harmonic. A strong signal peak was noted at C Band, considerably stronger than the specular signal, and within six inches of the predicted position. A probe was made to determine the width of this lobe. The -3 db point was observed to occur at about 5 1/2 feet along the semicircular arc from the peak, thus eliminating any suspicions that the "lobe" may have been due to scalloping of a sidelobe leakage signal. The experiment was repeated at Ku Band, in this case the P_{-1} mode space harmonic was measured at 52° grazing near the specular ray.

Tables 20 through 23 show the details of the actual measured data and computations.

Building 22 (Corrugated)
Band C
Grazing Angle 40° (Specular)

TABLE 20

RECORDED DATA

Polarization	DIRECT PATH				REFLECTED PATH				$\frac{P_{RR}}{P_{RD}}$	$\frac{P_{tD}}{P_{tR}}$	K_1+K_2	Range Crtn $\frac{R_R^2}{R_D^2}$	Refl Coeff $K_1+K_2+K_3$
	P_t* Measd	P_t** Actual P_{tD}	P_{Rcvd} P_{RD}	Corrected Range R_D	P_t* Measd	P_t** Actual P_{tR}	P_{Rcvd} P_{RR}	Corrected Range R_R	K_1	K_2		K_3	
V	-11.5	+22.8	-4.7	287.74	-11.5	+22.8	-15.3	376.568	-10.6	0	-10.6	2.34	-8.3
H	-11.5	+22.8	-3.6	287.74	-11.5	+22.8	-16.1	376.568	-12.5	0	-12.5	2.34	-10.2
LHC	-11.5	+22.8	-3.7	287.74	-11.5	+22.8	-20.6	376.568	-16.9	0	-16.9	2.34	-14.6
RHC	-11.5	+22.8	-3.7	287.74	-11.5	+22.8	-21.6	376.568	-17.9	0	-17.9	2.34	-15.6

Building 22 (Corrugated)
Band C
Grazing Angle 40° (Space Harmonic at 57°)

TABLE 21

RECORDED DATA

Polarization	DIRECT PATH ≠				REFLECTED PATH				$\frac{P_{RR}}{P_{RD}}$	$\frac{P_{tD}}{P_{tR}}$	K_1+K_2	Range Crtn $\frac{R_R^2}{R_D^2}$	Refl Coeff $K_1+K_2+K_3$
	P_t* Measd	P_t** Actual P_{tD}	P_{Rcvd} P_{RD}	Corrected Range R_D	P_t* Measd	P_t** Actual P_{tR}	P_{Rcvd} P_{RR}	Corrected Range R_R	K_1	K_2		K_3	
V	-11.5	+22.8	-4.7	≠	-11.5	+22.8	-12.8	≠	-8.1	0	-8.1	2.3	-5.8
H	-11.5	+22.8	-3.6	≠	-11.5	+22.8	-12.0	≠	-8.4	0	-8.4	2.3	-6.1
LHC	-11.5	+22.8	-3.7	≠	-11.5	+22.8	-27	≠	-23.3	0	-23.3	2.3	-21
RHC	-11.5	+22.8	-3.7	≠	-11.5	+22.8	-28	≠	-24.3	0	-24.3	2.3	-22

* Corrected Boonton Reading; ** Cal Factor 34.3 db ≠ Use Specular Geometry Range Correction

Building 22 (Corrugated)
Band Ku
Grazing Angle 40° (Specular)

TABLE 22

RECORDED DATA

Polarization	DIRECT PATH				REFLECTED PATH				$\frac{P_{RR}}{P_{RD}}$	$\frac{P_{tD}}{P_{tR}}$	K_1+K_2	Range Crtn $\frac{R_R^2}{R_D^2}$	Refl Coeff $K_1+K_2+K_3$
	P_t* Measd	P_t** Actual P_{tD}	P_{Rcvd} P_{RD}	Corrected Range R_D	P_t* Measd	P_t** Actual P_{tR}	P_{Rcvd} P_{RR}	Corrected Range R_R	K_1	K_2		K_3	
V	Odbm	0	-27	287.386	0	0	-44.5	376.214	-17.5	0	-17.5	2.3	-15.2
H	Odbm	0	-26.5	287.386	0	0	-45	376.214	-18.5	0	-18.5	2.3	-16.2
LHC	Odbm	0	-27	287.386	0	0	-53	376.214	-26	0	-26	2.3	-23.7
RHC	Odbm	0	-27	287.386	0	0	-53.5	376.214	-26.5	0	-26.5	2.3	-24.2

Building 22 (Corrugated)
Band Ku
Grazing Angle 40° (Spatial Harmonic at 52°)

TABLE 23

RECORDED DATA

Polarization	DIRECT PATH				REFLECTED PATH				$\frac{P_{RR}}{P_{RD}}$	$\frac{P_{tD}}{P_{tR}}$	K_1+K_2	Range Crtn $\frac{R_R^2}{R_D^2}$	Refl Coeff $K_1+K_2+K_3$
	P_t* Measd	P_t** Actual P_{tD}	P_{Rcvd} P_{RD}	Corrected Range R_D	P_t* Measd	P_t** Actual P_{tR}	P_{Rcvd} P_{RR}	Corrected Range R_R	K_1	K_2		K_3	
V	Odbm	0	-27	≠	Odbm	0	-52	≠	-25	0	-25	2.3	-22.7
H	Odbm	0	-26.5	≠	Odbm	0	-44	≠	-17.5	0	-17.5	2.3	-15.2
LHC	Odbm	0	-27	≠	Odbm	0	-56.5	≠	-29.5	0	-29.5	2.3	-27.2
RHC	Odbm	0	-27	≠	Odbm	0	-57	≠	-30	0	-30	2.3	-27.7

* Corrected Boonton Reading; ** Cal Factor 34.3 db ≠ Use Specular Geometry Range Correction

3.3.2 Comparison with Scale-Model Measurements

Measurements have been made at USAECOM on scale-model surfaces. Metal surfaces were machined for illumination on the Army's 70 GHz laboratory set-up to model the Building 22 corrugations at 15.5 GHz. The results of these scaled measurements were becoming available as the draft of this report was being completed and the preliminary results are shown below.

Specular Reflections at 40° Grazing

Polarization	IITRI Field Test Data	USAECOM Scaled Measurements
Vertical	-15.2 db	-14.5
Horizontal	-16.2	-18.5
Left Hand Circular	-23.7	-23.0
Right Hand Circular	-24.2	-23.0

For the non-specular case the space harmonic at 52° (opposite side of normal to transmitter) grazing was measured as follows:

Space Harmonic

Polarization	IITRI Field Test Data	USAECOM Scaled Measurements
Vertical	-22.7 db	-23.0
Horizontal	-15.2	-15.0
Left Hand Circular	-27.2	-25.0
Right Hand Circular	-27.7	-25.0

It can be seen that excellent agreement was achieved between the scale model measurements and the field test results for Ku Band. This tends

to support the hypothesis that the software model is the source of the disagreement between the predicted and field measured values for the particular values of L/λ and h/λ corrugations on Bldg 22 at Ku Band (Ref Fig 13).

3.4 Results of Long Range Test on Building 206

For this test the C-Band transmitting antenna was set at its lowest position on the tripod mount (approximately 5 1/2 feet from the feed to ground level), on the overrun of runway 23 at Patterson Field. Standard gain horns were used at the mobile receiving site, the measurement device being a calibrated Scientific-Atlanta wide coverage receiver. The transmitting dish was aimed towards Bldg 206 and the received signal was probed at a point on the active runway where the specular ray crossed the centerline (Position A). A second probe was made on taxiway 17 where the reflected ray crossed the taxiway (Position B). Finally the transmit and receive antennas were aimed towards each other down the runway centerline and the direct path signal measured (c). No attempt was made to reduce ground bounce signals, other than illumination reduction due to the fall-off of elevation sidelobes of the transmitting dish. The experiment was repeated for horizontal polarization and then the entire procedure was repeated for Ku Band.

The signal levels encountered at each point are noted in the following table.

Band	Polarization	Reflected Signal A	B	Direct Path C
C	Vertical	-43	-44	-57
C	Horizontal	-44	-47	-58
Ku	Vertical	-70.5	-70	-71
Ku	Horizontal	-72.5	-73.5	-72.5

The reported data are dbm values. The transmit power for C Band was about +30 dbm, while the transmit power for Ku Band was +10 dbm. It will be noted that the direct path signal at C Band is considerably lower than that received on the reflected path. This is entirely consistent with the observations made during the flight testing of the doppler MLS at this site on an earlier program (Reference 9). The loss in direct path signal strength has been conjectured as due to shadowing by the humped runway. It should also be noted that there is no significant difference in direct path signal strength between vertical and horizontal polarization because the propagation of microwave energy over a hump seems to be relatively independent of polarization. Whatever the reason, it is obvious that the multipath ratios observed on the long range tests cannot be rigorously compared to reflection coeeficients obtained in short range tests, except through computation or simulation tools which take into account the effects of ground reflections, shadowing by runway humps, etc. In a long range type of experiment there are many unknowns and it is a difficult matter to infer the value of any one parameter. On the other hand; if fundamental data such as terrain profile details, reflection coefficients, structural geometry and antenna patterns are known, it is conceptually easier matter to synthesize a model

and predict the multipath situation for a given test. It is hoped that the fundamental data from Table 3 can be input to a multipath model and the predicted and actual results compared.

However, some corrulations between short and long range data might be inferred.

One can see consulting the following table, that for C Band there is

Building 206 - 35° Grazing Angle

	C-Band		Ku Band	
	Short Range	Long Range	Short Range	Long Range
VP	-7.55db	-43 to -44db	-6.05db	-70.5 to -70db
HP	-11.95db	-44 to -47db	-14.25db	-72.5 to -73.5db
Δ	4.4db	0 to 4db	8.4db	2 to 3.5db

Δ = Difference between HP and VP multipath
(+Δ indicates HP less multipath than VP)

reasonable agreement in the differences between the short range and long range data for the differences between HP and VP multipath levels. For Ku Band, while the agreement between short and long range data is not as good, the differences between HP and VP mulitpath data are at least of the same order of magnitude.

If the airfield geometry for Building 206 would have been such that the grazing angle had been 20° instead of 35°, one might expect that the direct to mulitpath ratios would have shown a more pronounced difference between Horizontal and Vertical polarization.

IV. EFFECT OF GROUND ILLUMINATION ON SPATIAL CHARACTERISTICS OF MULTIPATH

4.1 Purpose

This addendum is intended to describe the results of an experiment aimed at investigating the effects of ground reflections on mulitpath signal characteristics. During earlier experimental work at Wright-Patterson AFB by the Air Force Flight Dynamics Laboratory and IITRI it was shown that certain structures exhibited multipath characteristics in which the reflected signal was broken up into narrow azimuth lobes in the specular region. This was in contrast to the reflections from a flat plat structure such as a wire mesh screen in which the reflected signal exhibited a smooth pattern in the vicinity of the specular reflection region. Several hypotheses were advanced at the time to explain these fine grain spatial variations, which typically showed lobes of peak-to-peak variation in the neighborhood of 1.5 feet on the runway (some 1200 ft from the reflecting surface). A suggestion was made by Lincoln Laboratory that the fine grain structure was due to the effects of ground reflections on the transmitted signal, brought about by the use of antennas having substantial elevation sidelobe gain in the direction of the ground bounce point. The experiment described here duplicates the geometric conditions of one of the earlier tests, but with substantial control of the ground illuminated by the transmitter.

4.2 Experimental Technique

In order to explore this possibility an experiment was run in Area B of Wright-Patterson AFB, Ohio, using CW signals, and a narrow beam transmitting antenna with vertical polarization. The transmitter was set-up at location

T-69 as shown in Figures 15 and 17, essentially on the "overrun" of the loop road runway, the signal being beamed at the south pier of Building 22. The specular region of the reflection on the runway was readily located using survey marks from the previous work and then the actual signal peak was located with standard gain horn and a Scientific-Atlanta receiver. The transmitting antenna (height five feet) was boresighted on a point approximately five ft up on the reflecting surface i.e., with the aperture plane of the dish vertical and the RF boresight horizontal. A probe was then made over a distance of ten feet in the specular region, the signal strength being measured every six inches along a line parallel to the runway centerline. At each point the receiving antenna (approximately 5 feet off the ground) was aimed towards the reflecting surface and the attenuators on the receiver were set to bring the signal level meter to a null reading. The required attenuator setting for each position was then recorded as the measure of signal strength (0 db attenuation represents a signal level of approximately -81 dbm). The readings were then spot checked at two foot intervals to determine measurement repeatability. Following this set of measurements the transmitting dish was then tilted in its elevation plane by 3.3 degrees upwards . The gain of the dish in the direction of the pier is down by approximately 14 db at this angle, but the sidelobe shoulder illuminating the ground is falling at a rate of about 10 db per degree, approximately the rate of sidelobe fall-off which has been widely discussed as that required for an MLS antenna. The set of measurements was then repeated with the reduced ground reflected signal. The results are shown in Table 24 and Figure 18.

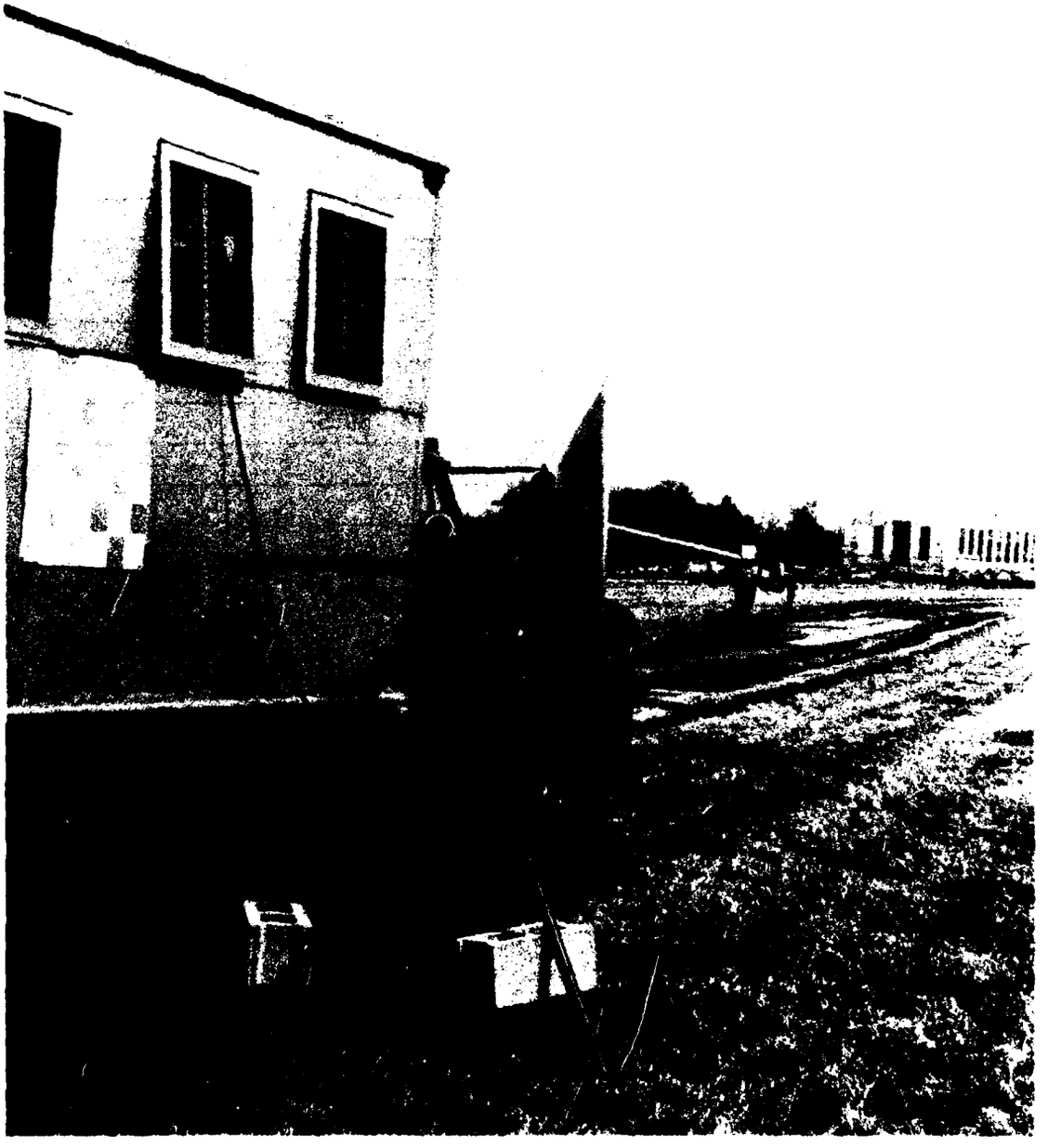

Figure 17
Photo of C-Band Transmitting
Antenna

TABLE 24 RECORDED DATA BLDG 22
GROUND ILLUMINATION TEST

Distance Feet	Attenuator Setting	Attenuator Setting	Spot Check Values	
	Dish Level	Dish Tilted	Level	Tilted
0	38.5	37	37.5	36.5
1/2	39	37		
1	38	35.5		
1 1/2	35	33.5		
1 3/4	33.5	32		
2	34.5	32.5	33.5	32
2 1/2	37	35.5		
3	39	37.5		
3 1/2	39.5	38		
4	40.5	37	39.5	37
4 1/2	40	36.5		
5	41.5	36.5		
5 1/2	42.5	38		
6	42	37.5	41.5	38.5
6 1/2	40.5	37		
7	40	37.5		
7 1/2	39.5	37.5		
8	38	37	38	36.5
8 1/2	39.5	37.5		
9	40.5	39		
9 1/2	40	38.5		
10	38.5	37		

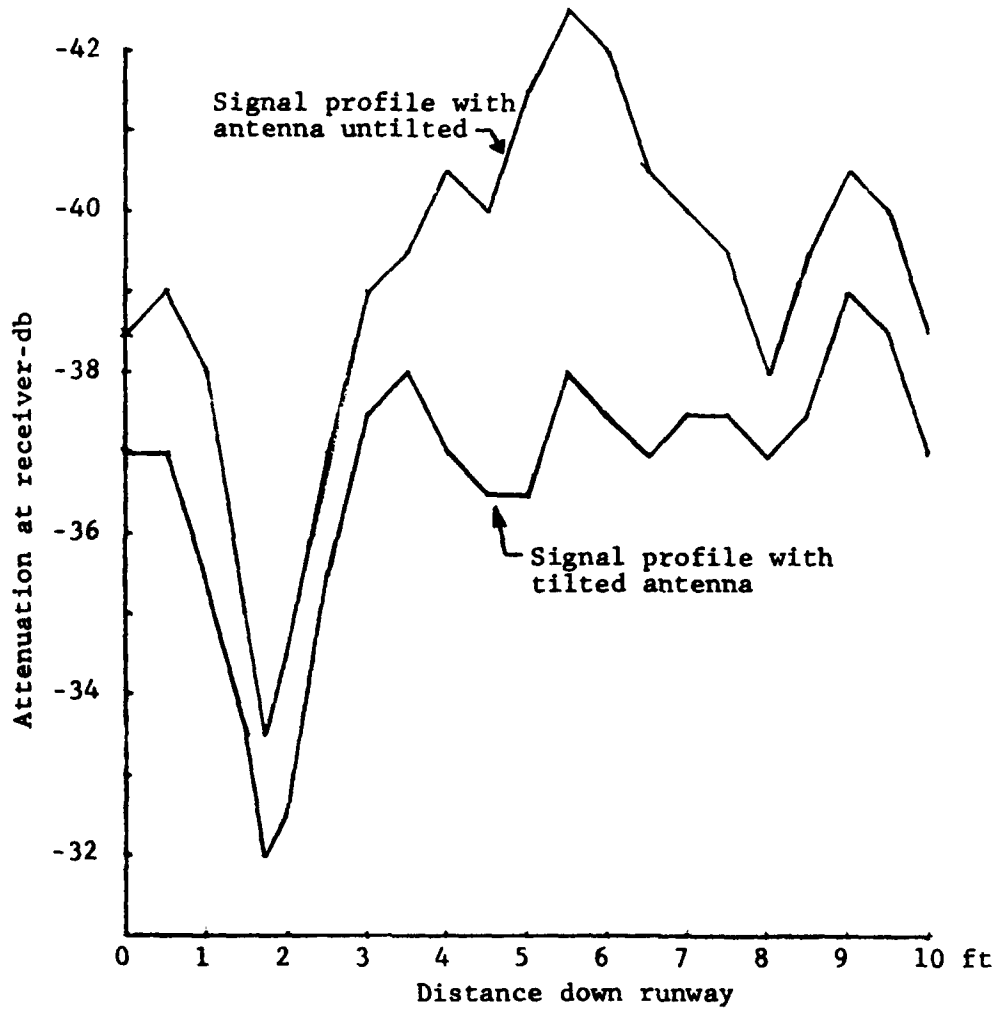

Figure 18
Signal Profile with and without Ground Illumination on Transmit Path

4.3 Observations

4.3.1 The results show extremely good repeatability. The measurement resolution of the Scientific-Atlanta receiver is 1/2 db, determined by the built-in attenuators. The spot-check readings are at most 1 db different from the initial set at the corresponding spatial position.

4.3.2 The observed signal level is approximately -40 dbm. This agrees very closely with the value which would be expected over a free space path of 4200 feet for the transmitter power and antennas used.

4.3.3 The high frequency spatial lobe structure which was observed on previous programs was not observed in either of the two sets of measurements, with or without the antenna tilted. The peak-to-null spacing observed in the data is about 3 feet 9 inches.

4.4 Conclusions

It had previously been suggested by Calspan and IITRI that the fine grain spatial variability of the reflected signal in the expected specular region was due to interference between the reflections from the two piers of Building 22. These piers are spaced almost 300 feet apart and would give rise to interferometer type lobes of one or two foot extent on the runway. The use of the narrow beam dish aimed at the South pier reduces the illumination of the North pier by some 15 db, so the possibility of an interferometer effect is eliminated.

The virtual elimination of ground bounce on the transmission path produces no change in the shape of the spatial pattern on the runway, it merely changes the signal level, all other factors being the same. The

measurements strongly suggests that it is the interference effect and not the ground bounce which gives rise to the fine grain variation that was observed in earlier measurements.

This finding tends to strengthen the arguments for performing reflection coefficient measurements by short range measurements under tight environment control.

The existence of interference phenomena would affect various types of MLS systems differently, depending on airport geometry. A doppler MLS might experience difficulties due to interference effects on the reference signal. The effects on a scanning beam would depend on system beamwidth and the exact geometry of the sources of reflection. The pier geometry situation described here might not affect a narrow beam Scanning Beam Guidance System (SBGS), however if the piers were closer together, the hangar further away, or the illumination angle slightly shorter, interference would be observed. If, for example, Building 22 were situated at the location of Building 206 at Patterson Field, the piers would be equally illuminated by a 1° wide TRSB operating on Runway 23 and fading of the multipath signal could occur. Its net effect on a TRSB receiver would be highly dependent on the condition of the direct path guidance signal and the type of processor logic which will eventually be implemented in MLS.

The existence of this type of phenomenon is important in simulation work if the results are to be credible. It is clearly inadequate to model the hypothetical case (alluded to above) by a single flat plate reflector, since the manifestation of the multipath signal would not be accurately

modelled. The use of multiple facets to simulate the reflecting surface would more realistically produce the modulation imposed on the multipath observed by an aircraft in the final stage of a landing on Runway 23.

V. CONCLUSIONS AND RECOMMENDATIONS

5.1 Comments on Data

Good experimental practice would dictate that an error model be constructed to permit an estimate to be made of the inherent accuracy in the data. The derivation of such a model was unfortunately beyond the limited resources available for the effort. It is encouraging to note however, that a good deal of consistency was obtained in the experimental results, even allowing for the fact that four or five different operators were involved in the data collection. The fact that polarization changes were readily made by means of switches means that relative accuracy between VP and CP data should be very good, since no other parameters were varied between these two sets of measurements. Furthermore, it is possible to predict the levels of CP reflections expected, if one has previously measured the reflection coefficients on VP and HP, and if certain assumptions can be made about phase changes occuring at the reflecting surface. By resolving a circularly polarized wave into vertical and horizontal components and applying the measured reflection coefficients for these polarizations it is a simple matter to predict the levels of right and left hand circularly polarized reflected energy to be expected. The actual components can be measured by using the capability of the antenna polarizers to be switched back and forth readily from linear to either sense of circular polarization.

As an example consider the case of Building 1 data for 20° grazing at C Band. The measured coefficients are -3.25 db on VP and -12.65 on HP. The VP component corresponds to a voltage reflection coefficient of 0.68786 and the HP to a value of 0.23308. If we solve the equations

$$A + B = .68786$$

and

$$A - B = .23308$$

we have A = .46047 and B = .22739

as the components of circularly polarized waves resulting from the reflection. The value of B corresponds to the voltage reflection coefficient of the circular component which would be measured if the transmitter and receiver were polarized in the same sense. This value is equivalent to -12.86 db, which corresponds very well with the observed value of -12.7 db. The value corresponding to A would have been observed if the sense of the receive and transmit circular polarizations were opposite each other.

The basic ellipticity of the antennas was field checked on direct path measurements and found to be excellent. The cross-polarization rejection on CP was also measured and found to be better than 20 db for both sets of antennas.

Intuitively one would expect that a case in which the HP and VP reflection coefficients are close in value would lead to a very low value for the associated CP measurement. A case in point is the data for Bldg 1 at C Band and 40° grazing. The levels measured for HP and VP are very close to each other and so the associated CP measurement would be expected to produce

reflected wave components in which almost all of the energy is concentrated in the sense of circularity opposite to that of the incident wave. This is borne out by a CP measured reflection coefficient of only -24 db. On the other hand, if the measurements of HP and VP show that either one is substantially lower than the other, the reflected signal would appear to be linearly polarized at whichever polarization exhibits the stronger reflection. The reflection coefficient measured on CP should then appear to be lower by 3 db than that measured on a system using linear polarization of this type. For example Table 3 shows that for Building 1 at Ku Band and 20° grazing the VP reflection coefficient is -11 db and the HP coefficient is very low (-28.5 db). The expected CP reflection coefficient would be -14 db. Note that the measured coefficient for right hand circularly polarized energy was -14.5 db, once more tending to strengthen the credibility of the data. Since the VP and HP data were obtained by making physical changes in the antenna configuration (the entire dish along with its associated feed assembly was rotated 90° about the boresight axis) the VP and HP measurements were essentially independent of each other. Therefore, it is reassuring that the VP, HP and CP can be related to each other in this manner.

The data summarized in Tables 3, 18 and 19 represent the result of sixteen independent comparisons of specular reflection coefficients as a function of polarization. In every one of these measurements the vertically polarized transmission yielded a stronger reflection than the horizontally polarized transmission for the same conditions of grazing angle, frequency band and reflecting surface. The relative difference varies from almost

zero (e.g. the 40° specular case at Ku Band for Bldg 1) to as much as 25 db (the 30° specular case for Bldg 485 at Ku Band).

If we examine the relative differences between VP and HP we see that over 60% of the cases show an advantage of more than 6 db to using HP rather than VP in a guidance system; more than 80% of the cases indicate an advantage of 3 db or more. The data summary is shown in the following table.

Margin by which HP is better than VP	C Band Cases	Ku Band Cases	Total Cases
0 - 3 db	2	1	3
3 - 6 db	2	1	3
6 - 10 db	3	1	4
> 10 db	2	4	6

A comparison between VP and CP is also interesting

Margin by which CP is better than VP	C Band Cases	Ku Band Cases	Total Cases
0 - 3 db	1	1	2
3 - 6 db	1	4	5
6 - 10 db	6	2	8
> 10 db	1	0	1

It can be readily seen that almost 88% of the cases show that CP has an advantage of at least 3 db over VP and over 50% of the test cases showed an advantage in excess of 6 db for CP over VP.

A statistical comparison of HP vs CP is also interesting as follows:

	Margin by which HP differs from CP	C Band Cases	Ku Band Cases	Total Cases
(a) HP better by:	> 10 db	1	3	4
	6 - 10 db	1	1	2
	3 - 6 db	1	1	2
	0 - 3 db	1	1	2
(b) CP better by:	0 - 3 db	1	0	1
	3 - 6 db	2	0	2
	6 - 10 db	2	1	3
	> 10 db	0	0	0

If the data is pooled (C and Ku) the net effect is that differences between HP and CP are fairly equally distributed around zero db (approximately 60/40 percent), showing that neither of these alternatives has a clear superiority over the other for the range of grazing angles considered in this experiment. It is notable however that the Ku Band results alone tend to indicate a superiority for HP, with fairly large differences (> 10 db).

The statistical breakout of C Band is almost a flat distribution for the CP/HP differences, 55% of the results showing CP to be better and 45% showing HP to be better. Considering the small sample sizes one would be tempted to claim no significant difference between CP and HP at C Band.

The Army's theoretical results for corrugated surfaces are worthy of comment vis-a-vis the results for Bldg 22.

a) The predicted and measured values for the specular case at C Band are in remarkable agreement (within 1 db on VP; 3.8 db on HP).

b) The location for the P_{-3} mode space harmonic was predicted within ten arc minutes of its measured location.

c) The space harmonic was predicted to be stronger than the specular reflection and to have horizontally and vertically polarized components of almost identical amplitude. The measured HP and VP components were in fact within 1/2 db of the each other and stronger than the specular ray. The predicted and measured levels in the space harmonic agreed within a few decibels.

The agreement at Ku Band is not quite as good. The relative levels of specular energy on VP and HP is closely predicted, but their absolute levels are off by 10 db. However, measurements made by the Army on a metalic scale model surface machined to model dimensions of Building 22 corrugations for illumination in a laboratory setup at 70 GHz agree absolutely to within better than 1 to 3 db with the Ku Band measurements. This would indicate that the Army's theoretical model is not precise for the Building 22 corrugations at Ku Band as the corrugation period and height to RF wavelength ratios become to large to be accommodated by the present software routines. This would also indicate that both the full scale and the 70 GHz physical modeling measurement are reliable. Some computer runs are presently under way using the Army's software to see if the predictions appear to trend towards the measured values as the critical ratios are approached.

The model certainly appears to be an excellent and reliable tool for C Band predictions without much qualification. The results of the additional tests may further endorse its use at Ku Band.

It was hoped at the outset that the results of the Area C tests on Bldg 206 could be spot-checked by applying the short-range test data to a computer model of the full scale geometry. Unfortunately it was not possible for the Army to carry out this exercise and no comparison was possible within the scope of IITRI's efforts. It should be noted however that the long range tests include the effects of ground reflections on the signal, and these may dominate the test results. It is interesting to note, however, that there is reasonable agreement especially at C Band, between the short range and long range data for the difference between HP and VP multipath levels. It would be of great interest and value if the test parameters could be input to a simulation such as the Lincoln Lab multipath model to correlate the short and long-range results. The results of the long range tests in Area B at Wright-Patterson (Section IV) illustrated some effects of ground illumination on multipath signal characteristics. Perhaps even more important the long range Area B tests demonstrated the necessity of accurately modeling multipath reflecting surfaces.

5.2 Summary Conclusions

Based on the data collected in this program one may readily conclude that solely from a propagational viewpoint either horizontal or circular polarization would be significantly better choice than vertical for MLS. For sixteen essentially independent specular reflection measurements, each on three polarizations, every case was found to show that vertically polarized radiation exhibited stronger reflections than either horizontally or circularly polarized signals under the same conditions.

The tests also showed that the Army's model for predicting reflections from corrugated surfaces is a reliable tool for C Band.

The comparison of field measurements with scale model measurements in the laboratory was remarkably good for the corrugated surface at Ku Band.

The field tests verify theoretical predictions that non-specular space harmonics can be produced by corrugated surfaces and that the signal level of space harmonics can be substantially higher than that in the direction of the specular reflection, but usually in a direction that is not likely to be operationally offensive.

Although all of the sixteen specular measurements conducted during this effort showed VP to result in stronger reflections than the corresponding HP cases, the presence of corrugations can result in space harmonics in which the reverse is true. (Noting again that the space harmonics usually occur in directions that are not operationally offensive.).

5.3 Recommendations

It is recommended that the simple but highly effective test procedure and hardware assembled under this effort be utilized for future exploration of other structures for deepening the data base. This limited effort has provided multi-frequency, multipolarization data not available elsewhere.

It is urged that Department of Defense (DOD) representatives conduct a survey of military airfields to determine the relative frequency with which various types of structures occur in practice. This will permit the results of this and future measurement effort to be placed in the context of its applicability to multipath situations peculiar to DOD airport environments.

The propagational data can be incorporated into simulations to predict the multipath environment at typical and/or specific airports. These predictions should be spot-checked using available hardware. The availability of a reliable and inexpensive multipath-prediction tool would be invaluable for projecting the performance of MLS at a wide variety of sites.

REFERENCES

1. Murphy, E.J., NA-522, "Miscellaneous Tests on AILS and MODILS," Technical Note No. 5, N.A.F.E.C., covering tests of December 1971.

2. Demko, Capt Paul S., "Polarization/Multipath Study," VL-5-72, U.S. Army Electronics Command, Fort Monmouth, New Jersey, June 1972.

3. Benjamin, J. and Peake, G.E.J. (ed), Intramual Contribution to the Microwave Landing System Study (Phase I), Technical Memo RAD 1021, Royal Aircraft Establishment, May 1973.

4. Walker, D. and Bennett, G.J., "Building Surface Reflection Measurements at C-Band", Technical Memo RAD 1048, Royal Aircraft Establishment February 1974.

5. Litchford, G.B., Study and Analysis of SC-117, National and USAF Plans for a New Landing System, Technical Report AFFDL-TR-72-76, Air Force Flight Dynamics Laboratory, WPAFB, July 1972.

6. Brindley, A. E., et al, Multipath Environment Evaluation, IIT Research Institute, November 1974.

7. Calhoun, L. C., and Herro, J.J., Documentation of the Test Geometry Set, IIT Research Institute, October 1974.

8. Calhoun, L. C., et al, Data Handler Documentation, IIT Research Institute, September 1974

9. Brindley, A.E., et al, Analysis, Test and Evaluation Support to the USAF Advanced Landing System Program, IIT Research Institute (Technical Report AFFDL-TR-74-62), May 1974.

10. Shnidman, E.A., The Logan MLS Multipath Experiment, Lincoln Laboratory, M.I.T. Project Report ATC-55, September 1975.

11. Mink, J.W., Energy Considerations of Beams Reflected from Periodic Surfaces, Technical Memorandum, Communications/Automatic Data Processing Laboratory, U.S. Army Electronics Command, Ft Monmouth, N.J., August 1975.

12. Schwering, F.K. and Whitman G., Scattering by Sinusoidal Surfaces, A Theoretical Approach, Technical Memorandum, Communications Research Technical Area, U.S. Army Electronics Command, Ft Monmouth, N.J.

13. Private Communications with Mr. Demko and Dr. Mink, December 1975/ January 1976.

APPENDIX A

Site Surveys

A.1 GENERAL

A.1.1 PURPOSE OF SURVEYS

These surveys were undertaken to provide premeasured sites for location of the receiver and transmitter used for close in reflection coefficient measurements. The C-band reflectors were fitted with boresighted peep sights, and the edge of the feed waveguides on the K band dishes provided boresighted sights. The tripods mounting the reflectors were equipped with gravity levels and were adjustable in height. If the desired target location was marked, and the tripods adjusted for height and level; the antennas could be pointed at the desired target (either a reflecting surface, or the other antenna) by the sights without the time consuming and error prone process of determining antenna pointing by RF probing. The previous measurement program, described in "AFFDL-TR-74-150 MULTIPATH ENVIRONMENT EVALUATION IIT Research Institute, Chicago Illinois November 1974" showed clearly that specular reflections were quite strong on the buildings in areas B and C. The positions of specular reflection could be accurately predicted, provided the following were known:

1) Tilt of the reflecting surface (only vertical surfaces studied)
2) Incidence angle for reflection and transmission of energy (measured relative to the normal to the reflection surface plane)
3) Height of the ground, relative to the center of reflection spot at the various transmitter/receiver sites
4) Location of the center of the reflection spot
5) Location of the ground bounce point for placement of absorbers
6) Deviations of the earth from a plane around and close to the reflection site.

The survey provided all of the above data, and allowed rapid and sufficiently accurate antenna positioning.

In addition to surveys of the candidate sites for close in reflection coefficient measurement, "ghost sites" were surveyed. These consisted of a set out of points around an imaginary reflecting surface. These sites were especially useful for testing antenna sidelobe leakage without reflections from vertical surfaces present.

A.1.2 INTRODUCTION

All of the sites at which close in reflection coefficient measurements might be taken were carefully surveyed. These surveys were mostly done prior to completion of the equipment needed for the measurements, and were relatively easy to perform because the accuracy of the GFE survey tools was high enough that single measurements provided the requisite accuracy.

The surveys allowed the measurement antennas to be located directly at the proper points to measure specular reflection and greatly aided in locating the proper place for the radiation absorbers used to minimize ground effects. The surveys also provided a description of the surface to be tested, and the terrain around the surface.

Major GFE equipment used for surveying were:

1) A Wild T 2 theodolite, S/N 30575
2) A Hewlett-Packard distance measuring equipment (dme) S/N 1118A81958
3) Assorted auxiliary equipment, tripods, retroreflectors, etc.

The theodolite showed reproducability of about 15 - 20 arc seconds (σ) and leveling accuracies of 20 to 30 arc seconds/mm bubble. The dme was used with a constant environmental correction, and was good to 0.01 $\pm$ 1 ppm ft.

This appendix is organized as follows:

a) A glossary of terms used in the surveying
b) Description of method to obtain a perpendicular to the reflecting surface using tools at hand
c) Description of the surveying methods and data reduction.
d) Surveying results, in packages grouped by site.
e) Observations on the results of the surveys.

A.2 DEFINITIONS OF TERMS USED IN SITE SURVEYS

$\varkappa$ = incidence angle (measured from normal to surface) ⟨COMP - in. ang.⟩

$\varkappa_n$ = nominal incidence angle used to identify a survey data file ⟨NOM.⟩

φ = grazing angle = $90^\circ - \varkappa$

ξ = transit azimuth angle measured from offset point to transmitter/receiver site, reflecting surface or reference points; + to right from behind transit.

υ = transit elevation angle, measured from offset point to transmitter/receiver site, reflecting surface or reference points; + down, zero at zenith. ⟨MEAS - el⟩

$\Delta\xi$ = correction for azimuth scale zeroing on transit = $\xi - \xi_m$ ⟨er⟩

ξ_m = transit azimuth reading ⟨MEAS - az⟩

h_t = height of transit and dme gimbal axis during reading ⟨MEAS - tr ht⟩

h_{t180} = height of transit and dme* gimbal axis during initial auto-colimation ⟨h_t⟩

h_r = height of retroreflectors used as targets during angle setout and measurement ⟨MEAS - tgt ht⟩

h_{r180} = height of mark placed on reflecting surface representing intersection of autocolimation axis and surface ⟨h_r⟩

a = measured offset distance - distance of offset transit point, in the zero plane, from the reflecting surface ⟨a⟩

ξ_{180} = transit azimuth reading at autocolimation ⟨az⟩

υ_{180} = transit elevation reading at autocolimation ⟨el⟩

x_o = location in x axis of transit offset point ⟨x_o⟩

y_o = location in y axis of transit offset point ⟨y_o⟩

z_o = location in z axis of transit offset point ⟨z_o⟩

R_d = range, measured with dme* from transit offset point to transmitter/receiver point ⟨MEAS - dist⟩

R_f = range from reference point to transmitter/receiver site ⟨COMP - rng⟩

ζ = tilt of reflection surface from perpendicular to earth gravity plane, positive implies top of surface leans away from reflection test sites. Measured, if possible, from autocolimation data.

x = x coordinate of transmitter/receiver site ⟨x⟩ **

y = y coordinate of transmitter/receiver site ⟨y⟩ **

z = z coordinate of transmitter/receiver site ⟨z⟩ **

h_a = height of transmit/receive antenna above local ground

Δh_ζ = correction added to h_a for receive antenna for reflecting surface tilt

NOTES: * dme = distance measuring equipment
names given in angle brackets ⟨ ⟩ used in printout of survey data
** points lie on surface of earth

A.3 INITIAL SET UP (AUTOCOLIMATION) GEOMETRY

A mirror was mounted on a steel square to bridge small scale unevenness in the surfaces (example, corrugations). The mirror was held against the reflecting surface to be measured, and the reflected image of the transit' objective centered in the cross hairs. This established a line perpendicular to the surface. Elevation measures of the perpendicular line indicated the degree of surface lean, and the perpendicular line was used to establish the zero incidence angle reference.

The initial set up proceedure was:

1) The transit site was located approximately perpendicular to the desired center of the reflecting surface, and distance "a" away from the surface.
2) The mirror fixture was held against the surface, and the transit adjusted to center the reflected image of the objective - thereby autocolimating and setting up a perpendicular line.
3) The transit azimuth was set to read 180° as closely as possible, and the transit elevation read.
4) A mark was placed on the reflecting surface at the position indicated by the transit cross-hairs after mirror removal.
5) Alternatively, the transit was tilted down to locate a mark at the intersection of the ground and the reflecting surface - the reference point.
6) The transit was used to take readings on three distant objects to provide a reference for future replacement of the transit over its offset site.
7) Optionally, a point at 0° incidence angle lying roughly on the circle of transmit/receive sites was established.

Equations used in initial set up:

Location of offset transit site coordinates;

$$x_o = 0$$
$$y_o = a$$
$$z_o = h_{r180} - h_{t180} - a\cot\left(v_{180}\right)$$

Building tilt (only measured for relatively smooth or regular surfaces);

$$\ell = v_{180} - 90^{\circ}$$ + implies top of building away from transit site.

See Figure A1 for details of initial set up.

A.4 SITE SURVEY GEOMETRY

The proceedure for setting out the points was as follows:

1) A table of values for transit azimuth and distance to site from the transit offset position was computed for the value of offset "a" for the site.
2) If the initial set up had just been completed, the transit was left as set. If the initial set up had been done at an earlier time, the transit was set up over the offset site, and azimuth reference adjusted to the values recorded at original initial set up.
3) Temporary point setouts were made at the proper transit angles for the desired incidence angles around the circle of transmit/receive sites.
4) The transit was replaced by the dme. The retroreflectors target was set up over the temporary points of 3), and the dme crosshairs centered over the target. Distance was measured, and the targets moved in or out over a radial from the dme to obtain the precomputed correct distance. The crosshairs of the dme were used to acertain that the target was moved on a true radial. The distance to the corrected position was recorded, and a permanent point set out.
5) The dme was replaced by the transit, and the transit readings on the three distant reference objects recorded. The target was set up directly over each of the premanently set out points of 4). The transit angles, transit gymbal height, and target height above the permanently set out point on the ground measured.
6) The survey data were reduced, and the data and derived results stored on digital tape cassette. The data were used to compute transmitter/receiver reflector heights for desired reflecting point height above the reference, and contours of site elevation were mapped by linear interpolation along lines connecting the transit offset site and the various transmit/receive sites, and along lines connecting adjacent transmit/receive sites.

The transmit/receive sites were identified by their nominal angle of incidence, κ_n. Each area surveyed was identifed by a site number in the form "n n n . d a m o y r x", where:

n n n. was the building number, or 99_ for a lost site

.d a m o y r was date of completion of survey

x was the number of survey on the building, with 0 as a start

SITE SURVEY GEOMETRY

Figure A 2 shows the relations of the various parameters of the site surveys. The following equations were used to reduce the survey data:

$$R_f = \sqrt{(R_d \sin \upsilon)^2 + a^2 + 2a(R_d \sin \upsilon) \cos \Phi}$$

$$\Phi = \Phi_m + \Delta\Phi$$

$$\varkappa = \arcsin\left[\frac{R_d \sin \upsilon \sin \Phi}{R_f}\right]$$

$$\varpi = 90^\circ - \varkappa$$

$$x = R_f \sin \varkappa$$

$$y = R_f \cos \varkappa$$

$$z = z_o + h_t - h_r + R_d \cos \upsilon$$

Added height correction for receive site when reflecting surface tilt is known, and is significant:

$$\Delta h_\zeta = y \tan(2\zeta)$$

The sites in Area B had already been included in a large scale survey as shown in the report "Multipath Environment Evaluation" IIT Research Institute, Chicago Illinois, Technical Report AFFDL-TR-74-150, November 1974. Figure A 3 is a reproduction of the overall site map for the referenced report. Building descriptions from the referenced survey are included in the package for each surveyed site, where applicable.

A.5 INDIVIDUAL SITE SURVEYS

A.5.1 GENERAL

Seven sites were surveyed in area B, and one site was spot surveyed in area C. Five of the sites in area B were on buildings 1, 6, 22 (2 sites), and 485. Two sites were "ghost sites" surveyed on the e dge of a hard stand overlooking an open area. In addition to the sidelobe tests described in A.1.1, these sites may be used for other supportive tests. The site in area C, building 206 was surveyed only for a 35° grazing angle for direct comparison with the long range data taken in area C.

The details of each site are reported in a package for each site on tne following pages. Each site package begins with a brief explanatory paragraph, followed by a self explanatory table containing the survey data input, ad the computed survey results. This table is self explaining, except for the term "BLK" which identifies the data's location on a digital magnetic tape. Following is a table giving the transmit/receive antenna heights for each nominal incidence angle, and ranges from the nominal angle to other transmit/receive sites identified by their nominal angles. The range data are useful in reducing the data from the direct looks. Following the height and range data, a contour map is presented for the terrain facing the desired reflecting surface. At the end, an overview of the building or reflecting surface is presented. These overviews were largely taken from the report "AFFDL-TR-74-150 MULTIPATH ENVIRONMENT EVALUATION", IIT Research Institute, Chicago Illinois; November 1974. Drawings taken from this report are identified by an asterix following their title.

INDIVIDUAL SITE SURVEYS

A.5.2 SITE 1.1610750 BUILDING 1, STEEL AND WIRE REINFORCED GLASS DOORS

Table A 1 lists the basic data, and Table A 2 the height and range data for this site. Figures A 5 and A 6 show the general arrangements of Building 1, and location of the reflection point. The reflection spot appears as an ellipse in this and subsequent figures because of differing vertical and horizontal scales. Figure A4 shows contours of the ground near the site.

A.5.3 SITE 6.1310750 BUILDING 6, STEEL AND WIRE REINFORCED GLASS DOORS

Tables A 3 and A 4 show the data for this site, and Figure A 7 the contours. Note that the site slopes away from the building assymetrically, with the plane of the earth being tipped down to the right. Figures A 8 and A 9 show general layout of the front side of Building 6.

A.5.4 SITE 22.1510750 BUILDING 22, POURED CONCRETE SECTION

The tabulated data for this site are found in Tables A 5 and A 6. The site contours are shown in Figure A 10. Although the contours of this site are among the best observed, it falls in a parking lot used heavily during the working day. Figures A 11 and A 12 show the approximate locations of this and the next reflection site. This site is the right hand one.

A.5.5 SITE 22.2710751 BUILDING 22, CORRUGATED SIDING

Tabulated data are found in Tables A 7 and A 8. The site contour is found in Figure A 13. This site is in the same parking lot as Site 22.1510750; and even though surveyed during a holiday, one sight had to be made trough a truck's windows (see notes, Table A 7). The corrugated siding begins above a five foot high apron wall, see section of the wall in Figure A 14. This will require an additional five feet transmitting and receiver antenna might, as shown in Table A 8 to measure reflection coeficients for corrugated siding. Table A 8 has a 12 foot rather than the usual 7 foot spot center height.

A.5.6 SITE 485.2210750 BUILDING 485, CONCRETE - STUCCO

An additional set of medium and short range sites were surveyed at incidence angles of 20° and 70° on Building 485, as can be seen from the range values for entries with the same nominal incidence angles in Table A 9. The values are identified only by nominal incidence angle in Table A 10, the height and range table, but they are in the same order as in Table A 9. The desired site may be located from joint examination of Tables A 10 and A 9.

INDIVIDUAL SITE SURVEYS

The shorter range sites were intended to make possible tests exploring the effects of varying illumination on the reflection spot. Building 485 was chosen for these survey points because it has the largest uniform areas of any building surveyed. The test site is quite uneven, as shown in the contours of Figure A15. It is also the only grass covered test site. The reflection spot centre height, see Table A10, was reduced to $5\frac{1}{2}$ feet, to allow compensation of site irregularity with the five to eight foot tripod range. The successful elimination of ground effects with the absorber, and the lower reflection from a grassy surface allowed this compromise on spot height. Figure A16 shows details of Building 485 in the area chosen for reflection coefficient measurment. The rough, stucco surface of this building is typical of many contemporary airport buildings.

A.5.7 SITE 999.0711750 GHOST SITE AT END OF AREA B RUNWAY

Tables A11 and A12 contain numerical descriptions of this site. Although the tip of the ground was not apparent to the naked eye, the contours of Figure A17 showed the site was too tipped to be used. Another ghost site was required.

A.5.8 SITE 991.1311750 GHOST SITE BETWEEN BUILDINGS 1 AND 485

Tables A13 and A14 list the data on this ghost site, which was found quite usable as shown by the contours of Figure A18. This site is located on the paved apron between Buildings 1 and 485, looking out over the grass to Loop Road. The point with nominal $+24^{\circ}$ incidence angle is the 0° point for site 1.1610750, see Tables A1 and A13. The two surveys could be tied together if desired.

A.5.9 SITE 206.1711750 LIMITED, BUILDING 206, AREA C. STEEL AND WIRE REINFORCED GLASS DOORS

A limited survey, and one set of tests were run on this site at a grazing angle of 35°, which corresponded to the grazing angle of energy from the azimuth transmitter site from the Doppler MLS tests. A long range probe was made in area C, transmitting energy from the azimuth MLS site, and checking for reflected and direct energy on the runway. The Building 206 site contour is shown in Figure A19.

Table A1 BUILDING 1 SURVEY DATA

SITE 1.1610750 TAPE 101175002.0

	ft	in		ft	in		ft	in		deg	mn	sc		deg	mn	sc
a	68	7.250	h_r	5	.687	h_t	5	3.375	az	179	59	39	el	89	51	30
	ft			ft			ft		er	0	0-15		blk	2		
x_o	-.006		y_o	68.603		z_o	-.393									

NOTE: Survey centered just to right of center of doors on building 1. Building lean about .31° top toward sites (out).

BLK	NOM.	MEAS											COMP				
		tgt ht		tr ht		az			el			dist	in. ang.	rng	x	y	z
	deg	ft	in	ft	in	deg	mn	sc	deg	mn	sc	ft	deg	ft	ft	ft	ft
3	0	4	11.000	5	3.375	0	0	0	90	34	24	121.937	-.002	190.535	-.008	190.535	-1.249
4	10	5	.750	5	3.375	15	32	34	90	23	17	123.064	9.994	190.046	32.983	187.162	-1.017
5	-10	4	11.875	5	3.375	344	27	43	90	28	55	123.009	-9.984	189.993	-32.941	187.115	-1.145
6	20	5	.500	5	3.375	30	35	45	90	25	10	127.537	19.998	189.824	64.919	178.377	-1.096
7	-20	4	11.875	5	3.375	329	25	36	90	24	40	127.699	-19.987	189.996	-64.943	178.552	-1.027
8	30	5	.750	5	3.375	44	43	34	90	20	0	134.992	30.006	189.966	95.001	164.504	-.969
9	-30	4	11.625	5	3.375	315	17	4	90	19	48	134.977	-29.992	189.962	-94.959	164.525	-.867
10	40	5	.250	5	3.375	57	48	0	90	13	24	144.389	40.015	190.026	122.185	145.536	-.704
11	-40	5	.125	5	3.375	302	13	0	90	14	29	144.396	-39.997	190.052	-122.157	145.593	-.740
12	50	5	.750	5	3.375	69	47	34	90	8	38	155.076	49.990	190.008	145.534	122.159	-.573
13	-50	5	.750	5	3.375	290	11	57	90	13	59	155.067	-49.989	189.999	-145.524	122.156	-.814
14	60	5	1.750	5	3.375	80	53	47	90	4	26	166.649	60.011	189.985	164.551	94.959	-.482
15	-60	5	.000	5	3.375	279	7	48	90	12	45	166.618	-59.979	189.991	-164.504	95.054	-.739
16	70	5	1.750	5	3.375	91	9	38	90	1	31	178.555	70.000	189.974	178.518	64.974	-.345
17	-70	4	11.500	5	3.375	268	50	51	90	4	47	178.595	-69.990	190.030	-178.558	65.024	-.328
18	80	5	2.000	5	3.375	100	46	40	89	57	0	190.506	80.009	190.024	187.142	32.965	-.121
19	-80	4	11.750	5	3.375	259	13	57	90	0	0	190.464	-79.987	190.006	-187.113	33.034	-.100
20		EOF															

TABLE A2 BUILDING 1

HEIGHT & RANGE

SITE 1.1610750 TAPE 131175001.0

	ft	in
SPOT CENTRE HEIGHT	7	0.000

NOM HEIGHT ANG REQUIRED			RANGES TO					
			ANG	RANGE	ANG	RANGE	ANG	RANGE
deg	ft	in	deg	ft	deg	ft	deg	ft
0	8	2.989	10	33.164	-10	33.109	20	66.057
10	8	.207	-10	65.925	20	33.122	-20	98.304
-10	6	1.746	20	98.250	-20	33.127	30	129.926
20	8	1.159	-20	129.863	30	33.126	-30	160.478
-20	8	.325	30	160.560	-30	33.132	40	190.019
30	7	11.629	-30	189.961	40	33.147	-40	217.981
-30	7	10.409	40	217.973	-40	33.138	50	244.197
40	7	8.459	-40	244.343	50	33.040	-50	268.729
-40	7	8.880	50	268.716	-50	33.095	60	291.146
50	7	6.878	-50	291.059	60	33.188	-60	311.221
-50	7	9.774	60	311.267	-60	33.086	70	329.049
60	7	5.784	-60	329.055	70	33.077	-70	344.413
-60	7	8.670	70	344.338	-70	33.155	80	357.086
70	7	4.150	-70	357.077	80	33.150	-80	367.023
-70	7	3.937	80	367.104	-80	33.114		
80	7	1.460	-80	374.255				
-80	7	1.205						

Table A 3 BUILDING 6 SURVEY DATA

SITE 6.1310750 TAPE 101175002.0

a	ft	in	h_r	ft	in	h_t	ft	in	az	deg	mn	sc	el	deg	mn	sc
	8	.750		4	8.750		4	7.750		180	0	0		89	42	32

x_o	ft	y_o	ft	z_o	ft	er				blk	
	0.000		8.062		.042		0	2	0		85

NOTES: First survey done, just to left of center of door area on building 6. Some of data on left (-) improperly recorded, and values to which distances were set entered to nearest foot. Building verticality about 0.29° top toward sites (out).

BLK	NOM.	MEAS										COMP				
		tgt ht		tr ht		az			el			dist	in. ang.	rng	x	y	z
	deg	ft	in	ft	in	deg	mn	sc	deg	mn	sc	ft	deg	ft	ft	ft	ft
86	0	3	10.750	4	7.750	0	1	25	90	38	20	190.004	.054	198.054	.188	198.054	-1.326
87	10	4	6.125	4	9.625	10	27	21	90	29	46	182.130	10.046	190.056	33.155	187.142	-1.242
88	-10	3	10.500	4	7.750	349	31	46	90	34	1	182.000	-9.996	189.925	-32.969	187.042	-.987
89	20	4	6.375	4	9.625	20	52	28	90	30	37	182.510	20.040	190.056	65.128	178.548	-1.312
90	-20	3	9.250	4	7.750	339	6	27	90	31	2	183.000	-19.995	190.548	-65.158	179.061	-.734
91	30	4	6.500	4	9.625	31	15	45	90	31	59	182.960	30.032	189.887	95.035	164.394	-1.399
92	-30	3	9.250	4	7.750	328	42	53	90	27	13	183.000	-29.990	189.932	-94.937	164.503	-.531
93	40	4	6.250	4	9.625	41	36	30	90	31	26	183.960	40.026	190.053	122.230	145.532	-1.358
94	-40	4	5.750	4	7.750	318	21	52	90	7	24	184.000	-39.988	190.103	-122.167	145.652	-.187
95	50	4	6.375	4	9.625	51	55	4	90	30	57	184.920	50.036	189.987	145.615	122.030	-1.351
96	-50	4	2.500	4	7.750	308	5	19	90	5	25	185.000	-49.965	190.082	-145.539	122.269	.188
97	60	4	6.750	4	9.625	62	8	40	90	37	2	186.160	60.027	190.046	164.630	94.943	-1.723
98	-60	4	2.625	4	7.750	297	51	58	90	8	23	186.000	-59.950	189.905	-164.380	95.095	.015
99	70	4	6.375	4	9.625	72	18	29	90	38	13	187.350	70.023	189.939	178.511	64.890	-1.769
100	-70	4	2.750	4	7.750	287	41	39	90	0	32	187.000	-69.951	189.610	-178.120	65.002	.430
101	80	4	6.125	4	9.625	82	24	16	90	38	48	188.730	80.026	189.947	187.076	32.898	-1.796
102	-80	4	2.500	4	7.750	277	37	16	89	53	41	189.000	-79.938	190.241	-187.315	33.236	.827
103		EOF															

TABLE A4 BUILDING 6

HEIGHT & RANGE

SITE 6.1310750 TAPE 131175001.0

	ft	in
SPOT CENTRE HEIGHT	7	0.000

NOM HEIGHT			RANGES TO							
ANG	REQUIRED		ANG	RANGE	ANG	RANGE	ANG	RANGE		
deg	ft	in	deg	ft	deg	ft	deg	ft		
0	8	3.915	10	34.725	-10	34.938	20	67.806		
10	8	2.915	-10	66.124	20	33.108	-20	98.645		
-10	7	11.852	20	98.465	-20	33.164	30	129.993		
20	8	3.746	-20	130.288	30	33.087	-30	160.681		
-20	7	8.815	30	160.864	-30	33.147	40	190.365		
30	8	4.792	-30	189.973	40	33.095	-40	218.010		
-30	7	6.377	40	217.995	-40	33.118	50	244.274		
40	8	4.300	-40	244.398	50	33.154	-50	268.778		
-40	7	2.244	50	268.823	-50	33.060	60	291.246		
50	8	4.219	-50	291.155	60	33.094	-60	311.164		
-50	6	9.739	60	311.370	-60	33.067	70	329.091		
60	8	8.681	-60	329.011	70	33.103	-70	344.056		
-60	6	11.809	70	344.219	-70	33.081	80	356.918		
70	8	9.233	-70	356.631	80	33.119	-80	367.193		
-70	6	6.839	80	366.605	-80	33.069				
80	8	9.552	-80	374.392						
-80	6	2.074								

Table A 5 BUILDING 22 (CONCRETE) SURVEY DATA

SITE 22.1510750 TAPE 101175002.0

	ft	in		ft	in		ft	in		deg	mn	sc		deg	mn	sc
a	63	3.000	h_r	5	4.500	h_t	5	2.000	az	180	1	32	el	89	34	15
	ft			ft			ft		er	0	0-32		blk	21		
x_o	.028		y_o	63.248		z_o	-.265									

NOTE: Survey on concrete portion of building 22, center marked by nail in wall. Lean unmeasurable.

BLK	NOM.	MEAS											COMP				
		tgt ht		tr ht		az			el			dist	in. ang.	rng	x	y	z
	deg	ft	in	ft	in	deg	mn	sc	deg	mn	sc	ft	deg	ft	ft	ft	ft
22	10	4	1.250	5	2.000	14	53	14	90	50	53	128.508	9.983	190.317	32.993	187.435	-1.104
23	-10	4	.000	5	2.000	345	7	16	90	49	10	128.477	-9.988	190.285	-33.005	187.401	-.936
24	20	4	.500	5	2.000	29	23	0	90	49	4	132.537	19.985	190.189	65.004	178.735	-1.032
25	-20	4	.375	5	2.000	330	39	33	90	39	54	132.530	-19.968	190.196	-64.953	178.761	-.668
26	30	4	1.000	5	2.000	43	6	48	90	43	51	139.084	29.971	190.227	95.032	164.788	-.956
27	-30	3	10.375	5	2.000	316	56	31	90	33	14	139.067	-29.944	190.235	-94.957	164.841	-.307
28	40	4	2.500	5	2.000	55	57	45	90	32	34	147.473	39.962	190.238	122.188	145.811	-.704
29	-40	3	10.750	5	2.000	304	4	55	90	24	46	147.437	-39.940	190.225	-122.122	145.849	-.056
30	50	4	2.125	5	2.000	67	54	30	90	28	17	157.097	49.948	190.144	145.549	122.353	-.568
31	-50	3	11.250	5	2.000	292	7	56	90	18	55	157.224	-49.942	190.287	-145.646	122.459	.098
32	60	4	1.625	5	2.000	79	1	31	90	25	19	167.652	59.954	190.123	164.576	95.191	-.468
33	-60	4	.375	5	2.000	281	3	30	90	18	20	167.661	-59.901	190.196	-164.550	95.382	-.024
34	70	4	1.250	5	2.000	89	21	52	90	20	18	178.559	69.922	190.096	178.544	65.258	-.257
35	-70	4	.500	5	2.000	270	40	36	90	17	1	178.492	-69.895	190.058	-178.477	65.330	-.023
36	80	4	2.000	5	2.000	99	7	44	90	14	52	189.608	79.944	190.129	187.209	33.196	-.085
37	-80	4	2.875	5	2.000	260	55	23	90	12	42	189.507	-79.902	190.072	-187.127	33.324	-.038
38		EOF															

TABLE A6 BUILDING 22

HEIGHT & RANGE

SITE 22.1510750 TAPE 131175001.0

SPOT CENTRE HEIGHT	ft	in
	7	0.000

NOM HEIGHT ANG REQUIRED			RANGES TO							
			ANG	RANGE	ANG	RANGE	ANG	RANGE		
deg	ft	in	deg	ft	deg	ft	deg	ft		
10	8	1.259	-10	65.998	20	33.173	-20	98.330		
-10	7	11.234	20	98.392	-20	33.096	30	130.019		
20	8	.384	-20	129.958	30	33.108	-30	160.564		
-20	7	8.018	30	160.595	-30	33.075	40	190.020		
30	7	11.473	-30	189.990	40	33.129	-40	217.979		
-30	7	3.692	40	217.978	-40	33.145	50	244.231		
40	7	8.449	-40	244.310	50	33.106	-50	268.850		
-40	7	.681	50	268.701	-50	33.172	60	291.139		
50	7	6.819	-50	291.195	60	33.162	-60	311.270		
-50	6	10.816	60	311.418	-60	33.023	70	329.198		
60	7	5.625	-60	329.127	70	33.031	-70	344.351		
-60	7	.289	70	344.415	-70	33.122	80	357.214		
70	7	3.087	-70	357.022	80	33.211	-80	367.064		
-70	7	.287	80	367.096	-80	33.154				
80	7	1.024	-80	374.337						
-80	7	.461								

Table A7 BUILDING 22 (CORRUGATED) SURVEY DATA

SITE 22.2710751 TAPE 101175002.0

	ft	in		ft	in		ft	in		deg	mn	sc		deg	mn	sc
a	62	11.375	h_r	4	1.062	h_t	5	3.375	az	180	0	1	el	90	48	54
	ft			ft			ft		er	0	0-18		blk	66		
x_o	.000		y_o	62.941		z_o	-.297									

notes: Survey in corrugated area to right of center door in building 22, centered in the largest low area of the siding. Extra height required to illuminate corrugated siding as it is above five foot high concrete base. Data for 60° left (-60°) taken through truck windshield.

BLK	NOM.	MEAS											COMP				
		tgt ht		tr ht		az			el			dist	in. ang.	rng	x	y	z
	deg	ft	in	ft	in	deg	mn	sc	deg	mn	sc	ft	deg	ft	ft	ft	ft
67	0	5	5.375	5	3.375	359	59	26	90	19	34	124.690	-.009	187.635	-.031	187.635	-1.173
68	10	4	9.875	5	3.375	14	53	40	90	31	43	128.499	10.006	190.017	33.017	187.127	-1.024
69	-10	4	11.250	5	3.375	345	6	19	90	33	28	128.458	-10.012	189.974	-33.028	187.080	-1.204
70	20	4	10.000	5	3.375	29	21	23	90	28	2	132.564	20.003	189.949	64.975	178.490	-.930
71	-20	4	11.125	5	3.375	330	38	19	90	26	46	132.584	-20.014	189.964	-65.016	178.491	-.975
72	30	4	9.375	5	3.375	43	5	38	90	29	5	139.086	30.006	189.982	95.010	164.518	-.973
73	-30	4	11.375	5	3.375	316	55	10	90	23	36	139.066	-30.003	189.966	-94.992	164.510	-.918
74	40	4	8.625	5	3.375	55	56	58	90	24	17	147.430	40.011	189.975	122.141	145.506	-.776
75	-40	4	11.375	5	3.375	304	3	52	90	20	8	147.437	-40.008	189.986	-122.143	145.518	-.827
76	50	4	8.125	5	3.375	67	53	30	90	19	4	157.127	50.011	189.992	145.566	122.095	-.564
77	-50	4	11.000	5	3.375	292	6	22	90	16	12	157.116	-50.019	189.972	-145.569	122.060	-.673
78	60	4	8.500	5	3.375	78	59	14	90	12	44	167.640	60.004	189.996	164.548	94.985	-.345
79	-60	4	5.875	5	3.375	280	59	33	90	20	55	167.650	-60.030	189.975	-164.573	94.900	-.525
80	70	4	8.375	5	3.375	89	20	26	90	9	47	178.567	69.991	190.023	178.554	65.018	-.222
81	-70	4	7.375	5	3.375	270	39	21	90	11	57	178.637	-70.010	190.075	-178.624	64.977	-.251
82	80	4	7.500	5	3.375	99	7	2	90	8	32	189.512	80.017	189.996	187.119	32.935	-.111
83	-80	4	8.500	5	3.375	260	54	31	90	5	12	189.494	-80.000	189.996	-187.110	32.989	-.011
84		EOF															

TABLE A8 BUILDING 22

HEIGHT & RANGE

SITE 22.2710751 TAPE 131175001.0

	ft	in
SPOT CENTRE HEIGHT	12	0.000

NOM HEIGHT ANG	REQUIRED		RANGES TO ANG	RANGE	ANG	RANGE	ANG	RANGE
deg	ft	in	deg	ft	deg	ft	deg	ft
0	13	2.084	10	33.052	-10	33.001	20	65.647
10	13	.294	-10	66.045	20	33.105	-20	98.412
-10	13	2.449	20	98.380	-20	33.120	30	130.012
20	12	11.164	-20	129.992	30	33.125	-30	160.578
-20	12	11.705	30	160.635	-30	33.076	40	190.042
30	12	11.687	-30	190.003	40	33.129	-40	217.983
-30	12	11.024	40	217.964	-40	33.133	50	244.269
40	12	9.314	-40	244.285	50	33.117	-50	268.736
-40	12	9.929	50	268.732	-50	33.152	60	291.111
50	12	6.775	-50	291.136	60	33.094	-60	311.330
-50	12	8.077	60	311.298	-60	33.148	70	329.105
60	12	4.144	-60	329.122	70	33.078	-70	344.482
-60	12	6.308	70	344.426	-70	33.058	80	357.110
70	12	2.666	-70	357.178	80	33.207	-80	367.064
-70	12	3.019	80	367.145	-80	33.093		
80	12	1.338	-80	374.230				
-80	12	.132						

Table A9 BUILDING 485 SURVEY DATA

SITE 485.2210750 TAPE 101175002.0

a	h_r	h_t	az	el
7 ft 10.625 in	4 ft 7.125 in	4 ft 7.125 in	180 deg 0 mn 4 sc	90 deg 0 mn 0 sc

x_o	y_o	z_o	er	blk
.000 ft	7.885 ft	0.000 ft	0 deg 8 mn 40 sc	39

NOTES ON SECOND SHEET!

BLK	NOM.	MEAS tgt ht		tr ht		az			el			dist	COMP in. ang.	rng	x	y	z
	deg	ft	in	ft	in	deg	mn	sc	deg	mn	sc	ft	deg	ft	ft	ft	ft
40	0	5	2.250	5	1.500	0	0	10	90	37	27	181.343	.141	189.217	.465	189.217	-2.037
41	10	5	2.625	5	1.500	10	19	42	90	36	52	182.119	10.040	189.867	33.101	186.960	-2.046
42	-10	5	.875	5	.375	349	24	27	90	39	37	182.149	-10.016	189.896	-33.029	187.002	-2.140
43	20	5	2.750	5	1.500	20	44	11	90	37	56	182.533	20.032	189.910	65.055	178.419	-2.118
44	20	4	11.875	5	1.500	20	53	24	90	53	14	156.502	20.044	163.867	56.166	153.941	-2.287
45	20	4	10.500	5	1.500	21	7	6	91	6	31	130.456	20.073	137.809	47.300	129.438	-2.274
46	-20	5	1.375	5	.375	338	58	59	90	41	31	182.525	-20.024	189.900	-65.027	178.419	-2.287
47	-20	4	10.875	5	.375	338	50	36	90	59	3	156.448	-20.023	163.810	-56.088	153.908	-2.562
48	-20	4	11.750	5	.375	338	38	5	91	6	34	130.591	-20.035	137.946	-47.260	129.598	-2.476
49	30	4	11.750	5	1.500	31	8	55	90	44	54	183.100	30.056	189.866	95.096	164.335	-2.245
50	-30	5	1.875	5	.375	328	35	15	90	43	9	183.144	-30.033	189.913	-95.052	164.415	-2.423
51	40	4	10.500	5	1.500	41	29	10	90	50	9	183.975	40.050	189.921	122.206	145.381	-2.433
52	-40	5	2.500	5	.375	318	14	37	90	45	23	183.994	-40.032	189.945	-122.176	145.438	-2.606
53	50	4	11.250	5	1.500	51	45	43	90	48	52	185.034	50.034	189.981	145.607	122.030	-2.442
54	-50	5	2.250	5	.375	307	58	13	90	48	30	185.128	-50.014	190.078	-145.639	122.142	-2.767
55	60	4	11.750	5	1.500	62	0	7	90	49	11	186.163	60.043	189.956	164.578	94.854	-2.517
56	-60	5	1.500	5	.375	297	41	58	90	21	54	186.125	-60.052	189.932	-164.572	94.815	-1.279
57	70	4	11.625	5	1.500	72	9	16	90	50	30	187.412	70.032	189.937	178.519	64.862	-2.596
58	70	5	.500	5	1.500	72	32	50	90	32	33	161.500	70.060	164.011	154.179	55.931	-1.445
59	70	4	9.500	5	1.500	73	4	22	90	26	21	135.524	70.081	138.003	129.747	47.016	-.705
60	-70	4	11.875	5	.375	287	31	18	90	13	58	187.387	-70.066	189.927	-178.548	64.751	-.719
61	-70	4	11.125	5	.375	287	10	7	90	9	17	161.545	-70.056	164.063	-154.225	55.960	-.332
62	-70	5	.625	5	.375	286	42	22	90	4	50	135.392	-70.011	137.884	-129.578	47.132	-.211
63	80	5	.375	5	1.500	82	16	44	90	32	33	188.778	80.065	189.970	187.121	32.775	-1.693
64	-80	5	1.750	5	.375	277	26	49	90	6	14	188.802	-80.050	190.004	-187.146	32.827	-.456
65		EOF															

Table A9 continued

SITE 485.2210750 TAPE 101175002

SECOND SHEET WITH NOTES:

NOTES: Survey of building 485, centered on window with nail arb. set in base of building at same height as ground around transit. Phoney elevation angle used for offset measurement, as window not marked for elevation measure after autocolimation. Value of elevation forced nail to represent zero height and height of transit. Window (and probably wall) leans about 0.06° top toward sites (out). Distance of offset "a" measured to concrete wall surrounding window. Distance on 50° Left (-50°) not checked after short incremental correction. Two shorter range values set out at 20° and 70° incidence angles for "range uniformity" tests.

TABLE A10 BUILDING 485

HEIGHT & RANGE

SITE 485.2210750 TAPE 201175002.0

	ft	in
SPOT CENTRE HEIGHT	5	6.000

NOM HEIGHT			RANGES TO					
ANG	REQUIRED		ANG	RANGE	ANG	RANGE	ANG	RANGE
deg	ft	in	deg	ft	deg	ft	deg	ft
0	7	6.455	10	32.713	-10	33.568	20	65.485
10	7	6.561	-10	66.131	20	33.075	20	40.276
-10	7	7.688	20	98.459	20	95.125	20	98.825
20	7	7.419	20	26.042	20	52.100	-20	130.082
20	7	9.454	20	26.057	-20	123.640	-20	112.255
20	7	9.288	-20	122.542	-20	106.245	-20	94.560
-20	7	9.450	-20	26.090	-20	51.953	30	160.742
-20	8	.746	-20	25.863	30	151.544	-30	40.354
-20	7	11.717	30	146.533	-30	59.129	40	170.199
30	7	8.946	-30	190.148	40	33.077	-40	218.093
-30	7	11.084	40	218.090	-40	33.103	50	244.363
40	7	11.204	-40	244.382	50	33.059	-50	268.852
-40	8	1.272	50	268.805	-50	33.064	60	291.181
50	7	11.311	-50	291.247	60	33.142	-60	311.372
-50	8	3.215	60	311.415	-60	33.244	70	329.181
60	8	.209	-60	329.150	70	33.074	70	40.287
-60	6	9.353	70	344.397	70	321.115	70	298.176
70	8	1.160	70	25.926	70	51.934	-70	357.068
70	6	11.349	70	26.008	-70	332.845	-70	308.405
70	6	2.465	-70	308.805	-70	284.113	-70	259.326
-70	6	2.635	-70	25.863	-70	52.042	80	367.065
-70	5	9.984	-70	26.179	80	342.133	-80	40.236
-70	5	8.534	80	317.025	-80	59.319		
80	7	2.323	-80	374.268				
-80	5	11.483						

Table A11 FIRST GHOST SITE SURVEY DATA

SITE 999.0711750 TAPE 101175002.0

a	h_r	h_t	az	el
0 ft .000 in	5 ft 2.750 in	5 ft 2.750 in	180 deg 0 mn 0 sc	90 deg 0 mn 0 sc

x_o	y_o	z_o		
0.000 ft	0.000 ft	0.000 ft	er-281-54-33	blk 104

NOTE: This is "no building" site for study of antenna fields over the ground. It is located at the end of the Area B "active runway".

BLK	NOM.	MEAS tgt ht		tr ht		az			el			dist	COMP in. ang.	rng	x	y	z
	deg	ft	in	ft	in	deg	mn	sc	deg	mn	sc	ft	deg	ft	ft	ft	ft
105	0	5	2.625	5	2.750	281	54	15	89	46	17	190.000	-.005	189.998	-.016	189.998	.768
106	10	5	1.750	5	2.750	291	54	31	89	35	16	189.976	9.999	189.971	32.986	187.085	1.450
107	-10	5	3.000	5	2.750	271	54	53	89	58	1	189.978	-9.994	189.977	-32.971	187.094	.088
108	20	5	2.500	5	2.750	301	54	31	89	22	21	190.006	19.999	189.994	64.980	178.537	2.101
109	-20	5	3.500	5	2.750	261	54	31	90	14	3	189.986	-20.000	189.984	-64.980	178.526	-.838
110	30	5	3.000	5	2.750	311	54	20	89	13	8	189.994	29.996	189.976	94.977	164.530	2.569
111	-30	5	3.500	5	2.750	251	54	47	90	23	3	189.945	-29.996	189.940	-94.959	164.499	-1.336
112	40	5	2.500	5	2.750	321	51	13	89	8	50	190.004	39.944	189.982	121.977	145.653	2.848
113	-40	5	3.625	5	2.750	241	54	7	90	35	15	189.962	-40.007	189.952	-122.117	145.496	-2.020
114	50	5	2.000	5	2.750	331	54	40	89	6	14	190.036	50.001	190.012	145.562	122.132	3.034
115	-50	5	2.375	5	2.750	231	54	27	90	40	26	189.990	-50.001	189.976	-145.534	122.110	-2.203
116	60	5	1.750	5	2.750	341	55	7	89	6	34	189.976	60.009	189.953	164.519	94.949	3.036
117	-60	5	2.625	5	2.750	221	53	25	90	41	54	189.994	-60.018	189.979	-164.558	94.935	-2.305
118	70	5	1.375	5	2.750	351	54	44	89	6	58	189.970	70.003	189.947	178.495	64.956	3.045
119	-70	5	3.500	5	2.750	211	54	31	90	40	20	189.984	-70.000	189.970	-178.514	64.972	-2.291
120	80	5	3.750	5	2.750	361	55	20	89	5	43	189.990	80.013	189.966	187.087	32.944	2.916
121	-80	5	2.625	5	2.750	201	54	49	90	48	59	190.011	-79.995	189.991	-187.102	33.006	-2.696
122		EOF															
123		EOF	EOT														

TABLE A12 FIRST "GHOST" SITE

HEIGHT & RANGE

SITE 999.0711750 TAPE 131175001.0

	ft	in
SPOT CENTRE HEIGHT	7	0.000

NOM HEIGHT REQUIRED			RANGES TO					
ANG			ANG	RANGE	ANG	RANGE	ANG	RANGE
deg	ft	in	deg	ft	deg	ft	deg	ft
0	6	2.777	10	33.131	-10	33.082	20	65.999
10	5	6.598	-10	65.957	20	33.116	-20	98.339
-10	6	10.934	20	98.324	-20	33.136	30	129.923
20	4	10.779	-20	129.960	30	33.106	-30	160.554
-20	7	10.067	30	160.569	-30	33.098	40	189.825
30	4	5.168	-30	189.937	40	32.944	-40	217.927
-30	8	4.032	40	217.753	-40	33.146	50	244.224
40	4	1.815	-40	244.094	50	33.308	-50	268.545
-40	9	.248	50	268.697	-50	33.094	60	291.059
50	3	11.585	-50	291.096	60	33.141	-60	311.311
-50	9	2.439	60	311.241	-60	33.172	70	329.031
60	3	11.567	-60	329.078	70	33.089	-70	344.342
-60	9	3.662	70	344.361	-70	33.054	80	357.068
70	3	11.458	-70	357.010	80	33.144	-80	366.991
-70	9	3.497	80	367.002	-80	33.099		
80	4	1.001	-80	374.190				
-80	9	8.362						

Table A13 SECOND GHOST SITE SURVEY DATA

SITE 991.1311750 TAPE 131175002.0

	ft	in		ft	in		ft	in		deg	mn	sc		deg	mn	sc
a	0	.000	h_r	5	.312	h_t	5	.312	az	180	0	0	el	90	0	0
	ft			ft			ft		er	-45	-8	-33	blk	123		
x_o	0.000		y_o	0.000		z_o	0.000									

NOTES: This is "ghost site" on edge of pavement in front of building 1. The +24° datum is the 0° point of the survey in front of building 1 (Location 1.1610750), so the two surveys can be related if desired.

BLK	NOM.	MEAS											COMP				
		tgt ht		tr ht		az			el			dist	in. ang.	rng	x	y	z
	deg	ft	in	ft	in	deg	mn	sc	deg	mn	sc	ft	deg	ft	ft	ft	ft
124	0	4	6.125	5	.312	45	8	33	89	49	41	189.976	0.000	189.975	0.000	189.975	1.085
125	10	4	6.875	5	.312	55	9	20	89	44	20	189.982	10.013	189.980	33.032	187.086	1.318
126	-10	4	6.938	5	.312	35	9	25	89	50	44	190.023	-9.985	190.022	-32.949	187.143	.960
127	20	4	8.500	5	.312	65	7	47	89	38	26	190.016	19.987	190.012	64.948	178.567	1.509
128	-20	4	7.625	5	.312	25	9	17	89	52	45	190.020	-19.987	190.019	-64.952	178.573	.791
129	24	4	6.250	5	.312	69	34	6	89	44	12	133.932	24.425	133.930	55.382	121.943	1.120
130	30	4	8.125	5	.312	75	8	7	89	38	50	189.926	29.992	189.922	94.940	164.489	1.518
131	-30	4	7.250	5	.312	15	8	14	89	56	41	190.002	-30.005	190.001	-95.016	164.537	.605
132	40	4	7.625	5	.312	85	9	18	89	41	16	190.067	40.012	190.064	122.202	145.570	1.426
133	-40	4	6.938	5	.312	5	8	59	90	1	51	190.054	-39.992	190.053	-122.145	145.605	.345
134	50	4	7.250	5	.312	95	8	16	89	41	17	189.992	49.995	189.989	145.530	122.134	1.456
135	-50	4	7.500	5	.312	355	9	2	90	4	53	190.003	-49.991	190.002	-145.533	122.151	.131
136	60	4	6.750	5	.312	105	8	25	89	40	5	190.024	59.997	190.020	164.559	95.016	1.564
137	-60	4	8.063	5	.312	345	8	26	90	8	47	190.000	-60.001	189.999	-164.547	94.994	-.131
138	70	4	7.437	5	.312	115	8	46	89	41	7	189.926	70.003	189.923	178.473	64.946	1.449
139	-70	4	7.500	5	.312	335	8	22	90	13	33	190.026	-70.003	190.024	-178.568	64.982	-.347
140	80	4	5.625	5	.312	125	9	25	89	50	13	189.955	80.014	189.954	187.076	32.938	1.097
141	-80	4	7.688	5	.312	325	9	22	90	17	14	190.033	-79.986	190.030	-187.135	33.042	-.567
142		EOF															
143		EOF	EOT														

TABLE A14 SECOND "GHOST" SITE

HEIGHT & RANGE

SITE 991.1311750 TAPE 131175002.0

	ft	in
SPOT CENTRE HEIGHT	7	0.000

NOM ANG deg	HEIGHT REQUIRED ft	in	RANGES TO ANG deg	RANGE ft	ANG deg	RANGE ft	ANG deg	RANGE ft
0	5	10.971	10	33.156	-10	33.071	20	65.942
10	5	8.172	-10	65.982	20	33.033	-20	98.353
-10	6	.478	20	98.272	-20	33.130	24	109.789
20	5	5.682	-20	129.900	24	57.426	30	33.131
-20	6	2.303	24	132.994	30	160.512	-30	33.178
24	5	10.550	30	58.094	-30	156.313	40	70.874
30	5	5.779	-30	189.956	40	33.183	-40	217.906
-30	6	4.737	40	218.045	-40	33.082	50	244.254
40	5	6.883	-40	244.348	50	33.067	-50	268.758
-40	6	7.852	50	268.703	-50	33.121	60	291.134
50	5	6.524	-50	291.063	60	33.128	-60	311.263
-50	6	10.426	60	311.277	-60	33.152	70	329.018
60	5	5.226	-60	329.106	70	33.133	-70	344.439
-60	7	1.575	70	344.334	-70	33.124	80	357.058
70	5	6.606	-70	357.041	80	33.144	-80	366.998
-70	7	4.175	80	367.046	-80	33.068		
80	5	10.825	-80	374.212				
-80	7	6.806						

Table A15 BUILDING 206 (AREA C) SURVEY DATA

SITE 206.1711750 TAPE 201175002.0

	ft	in		ft	in		ft	in		deg	mn	sc		deg	mn	sc
a	8	.000	h_r	4	8.000	h_t	4	9.062	az	179	59	48	el	90	24	47
	ft			ft			ft		er	-1	-6	-56	blk	143		
x_o	-.000		y_o	7.999		z_o	-.030									

NOTE: Single angle (plus zero) on building 206, area C.

BLK	NOM.	MEAS											COMP				
		tgt ht		tr ht		az			el			dist	in. ang.	rng	x	y	z
	deg	ft	in	ft	in	deg	mn	sc	deg	mn	sc	ft	deg	ft	ft	ft	ft
144	0	4	5.375	4	9.062	1	6	47	90	12	41	189.966	-.002	197.964	-.008	197.964	-.424
145	55	4	6.250	4	9.062	58	8	50	90	4	43	185.504	55.007	189.975	155.632	108.946	-.051
146	-55	4	5.500	4	9.062	304	5	50	90	7	39	185.551	-54.994	190.024	-155.648	109.008	-.146
147		EOF															
148		EOF	EOT														

TABLE A16 BUILDING 206

HEIGHT & RANGE

SITE 206.1711750 TAPE 201175002.0

	ft	in
SPOT CENTRE HEIGHT	6	0.000

NOM HEIGHT			RANGES TO					
ANG	REQUIRED		ANG	RANGE	ANG	RANGE	ANG	RANGE
deg	ft	in	deg	ft	deg	ft	deg	ft
0	6	5.093	55	179.299	-55	179.267		
55	6	.612	-55	311.280				
-55	6	1.762						

A.6 OBSERVATIONS ON THE SURVEYS' DATA

A.6.1 BUILDING TILT

Tilt of the building could only be measured for fairly smooth surfaces, as the mirror holding fixture could not be made large enough to "average" over rougher surfaces, such as poured concrete. When measured, the tilt value is noted on the survey data tables. None of the measured tilts were large, but even a half degree tilt requires some correction in transmitter/receiver antenna heights.

A.6.2 BUILDING SURFACES

Buildings 1, 6 and 206 were all used as sites for steel doors with wire reinforced glass in steel frames above a belt line. These were quite smooth surfaces. Building 22 provided the only practical example of a corrugated surface, that is a surface with periodic sizeable surface undulations. Building 485 provided the only sample of a surface with fairly large random roughness over a large flat area, the concrete stucco surface above the building foundation level.

A.6.3 SURVEYING TECHNIQUE, ACCURACY, FUTURE USES

An accuracy analysis was not run on the survey data, but examination of the survey tables show that angles fell within $\pm$ 0.1° of nominal and ranges within 0.08 foot (less than 1 inch) of nominal. The offset value was remeasured after initial set up, and corrected for offsets in the surface of interest (see Figure A14 for an example, the corrugated surface of interest is set in from the concrete apron wall), and the correct value used in computing the survey data tables.

These survey data can be used for future measurement programs, as angles can be quite accurately interpolated between the existing set out 10° points. The technique can be used for measuring other sites, and the actual measurement uses two men for less than one day for each site. The reduction and storage of the survey data was computerized, and the data reduction for each site presented here required less than one hour of elapsed time.

The speed and accuracy of the surveying can be attributed to two factors:

1) Using highly accuracte instruments to allow single readings to be used

2) Computerization of data reduction and storage.

A.6.4 LOCATION OF REFLECTION SPOT CENTRE

Reference of the entire survey system to the intersection of the reflecting surface with the ground simplified computation of transmitter/receiver heights and setting up a target for various reflection spot center heights. It only required measuring up the desired center height above the reference mark, and fastening the 2 foot square mylar bulls eye target to the building surface.

A.6.5 AUXILIARY USES

The ranges computed between transmitter/receiver sites were useful when correcting the direct antenna looks for space attenuation. Also, the ghost sites could be used for auxiliary measurements, such as vertical probes, as the ranges between and heights of the various receiver/transmitter sites are accuratly known.

INITIAL SET UP (AUTOCOLIMATION) GEOMETRY

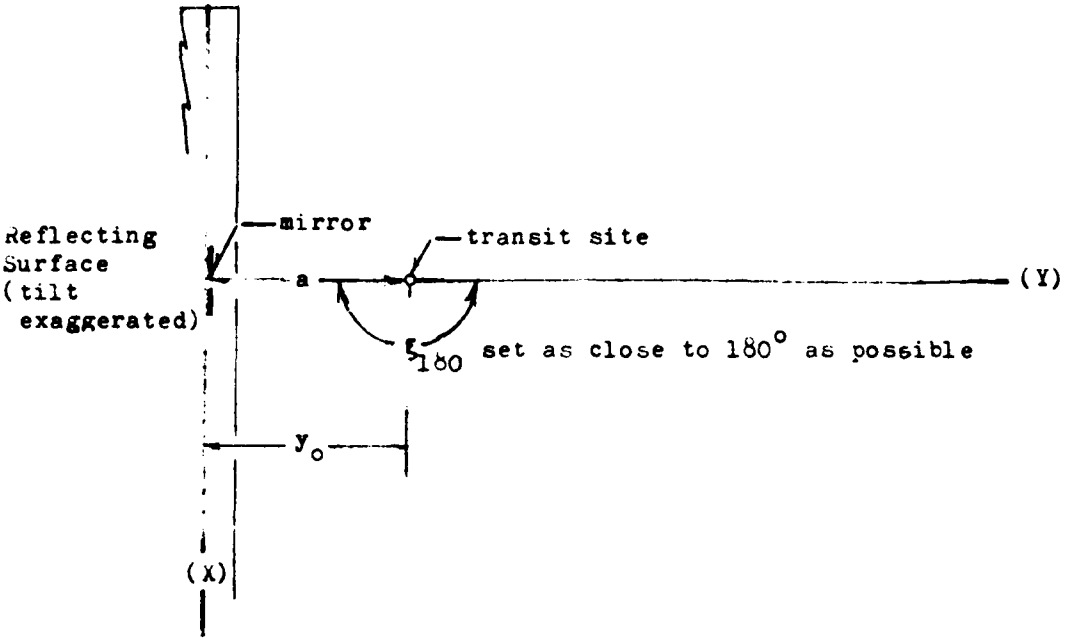

PLAN VIEW

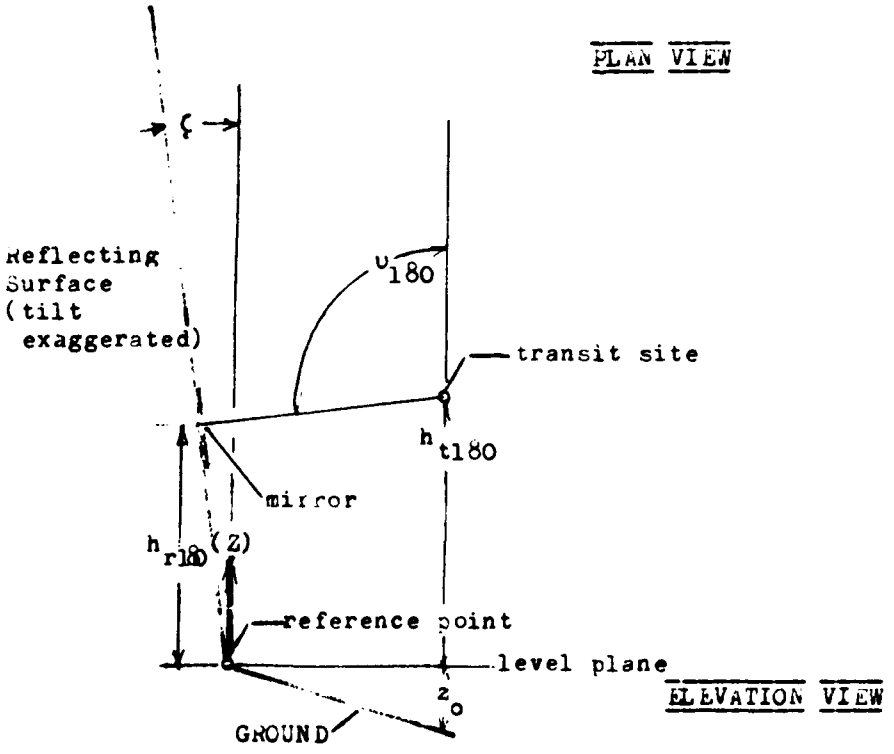

ELEVATION VIEW

Figure A1 INITIAL SET UP GEOMETRY

SITE SURVEY GEOMETRY

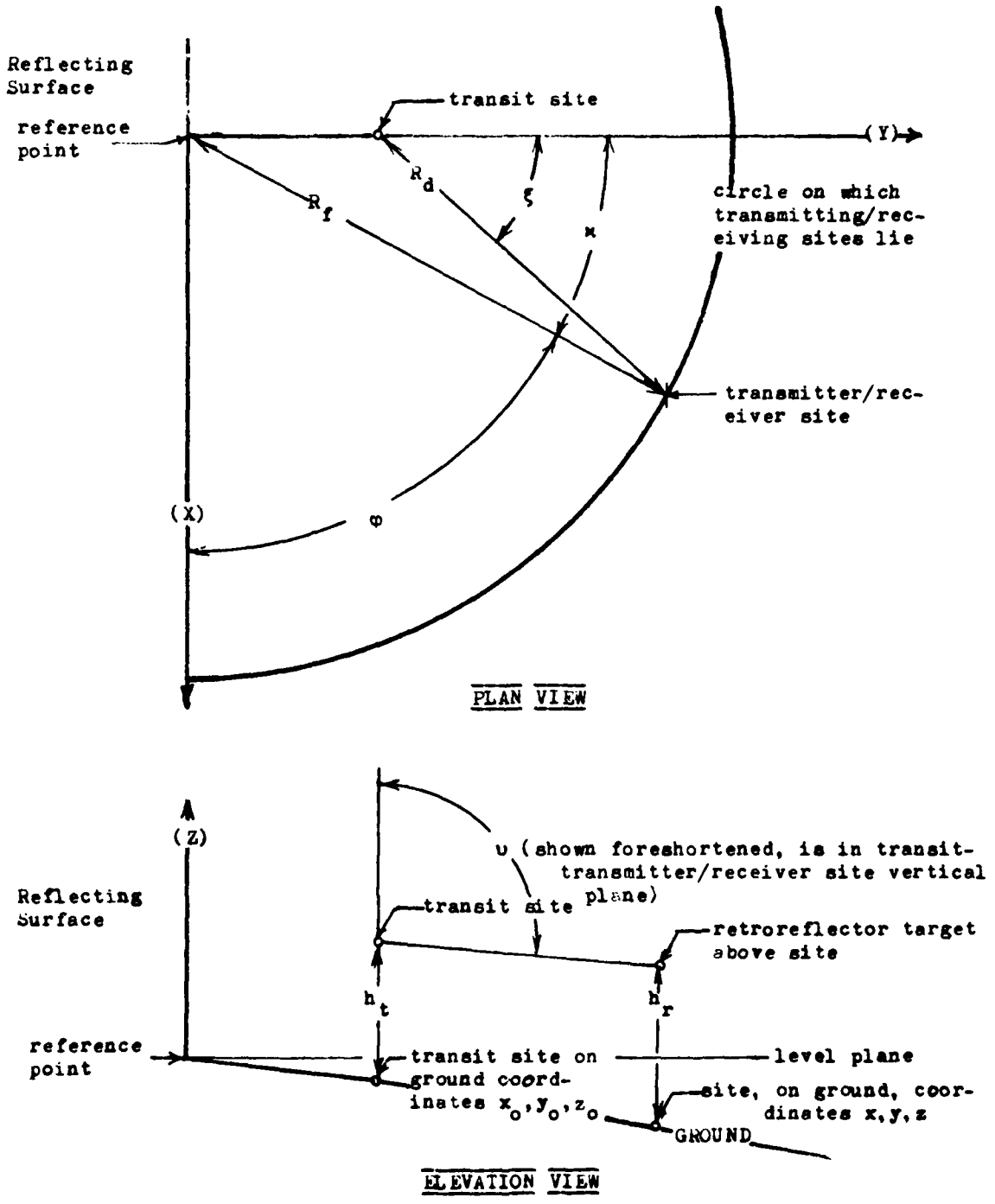

Figure A 2 SITE SURVEY GEOMETRY

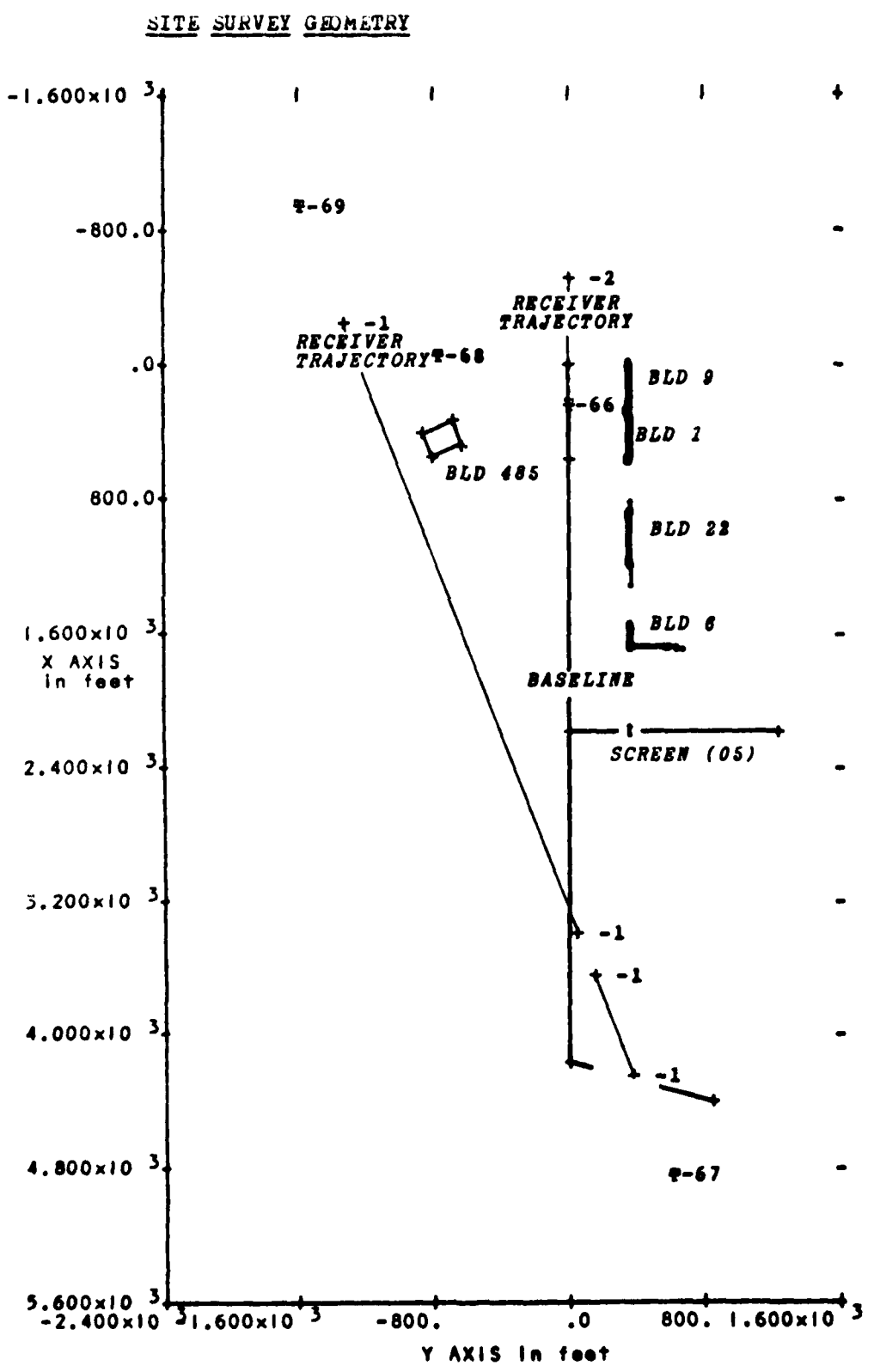

Figure A3 Area B Site Map

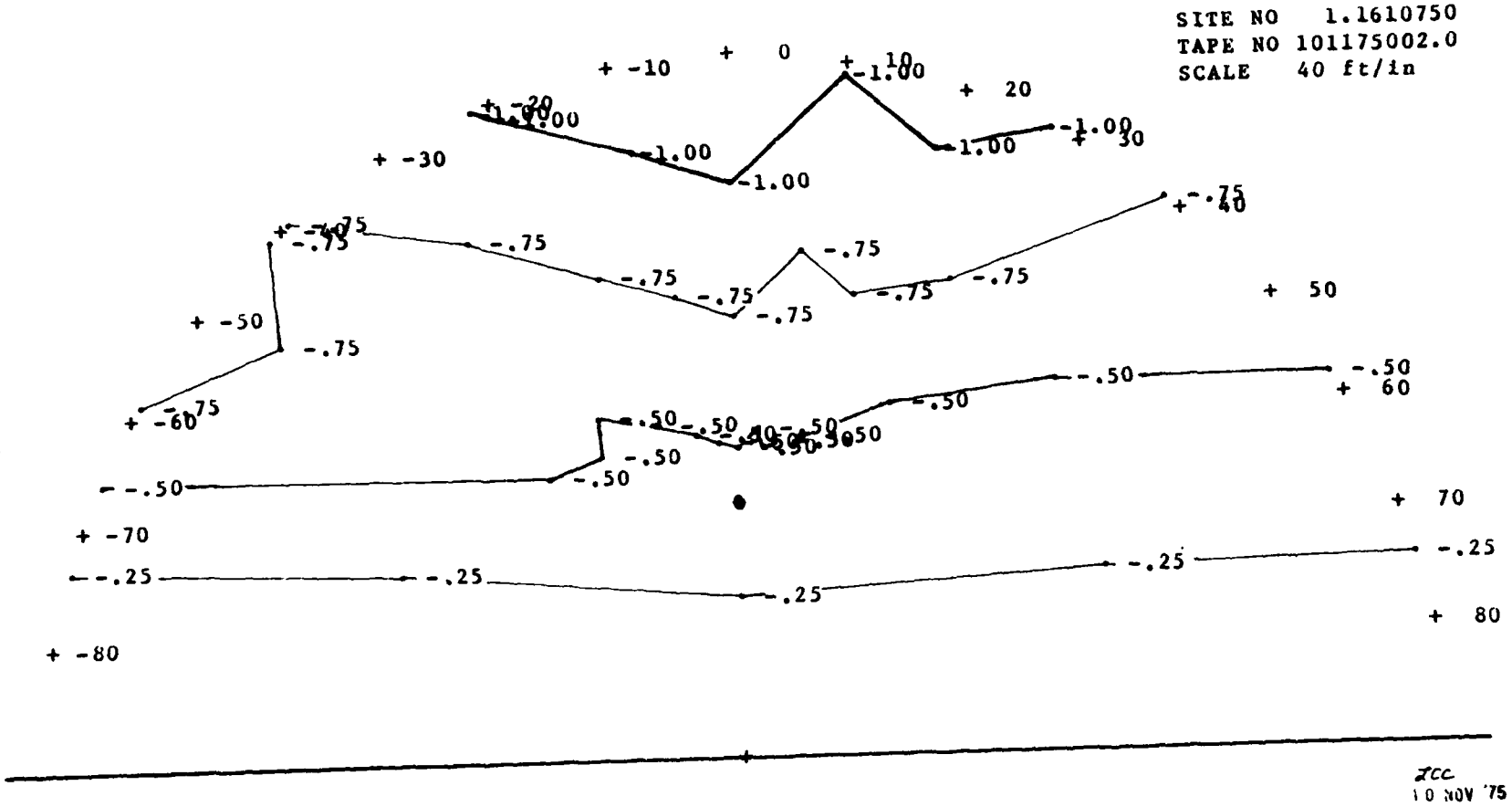

Figure A4 Building 1 Site Contour

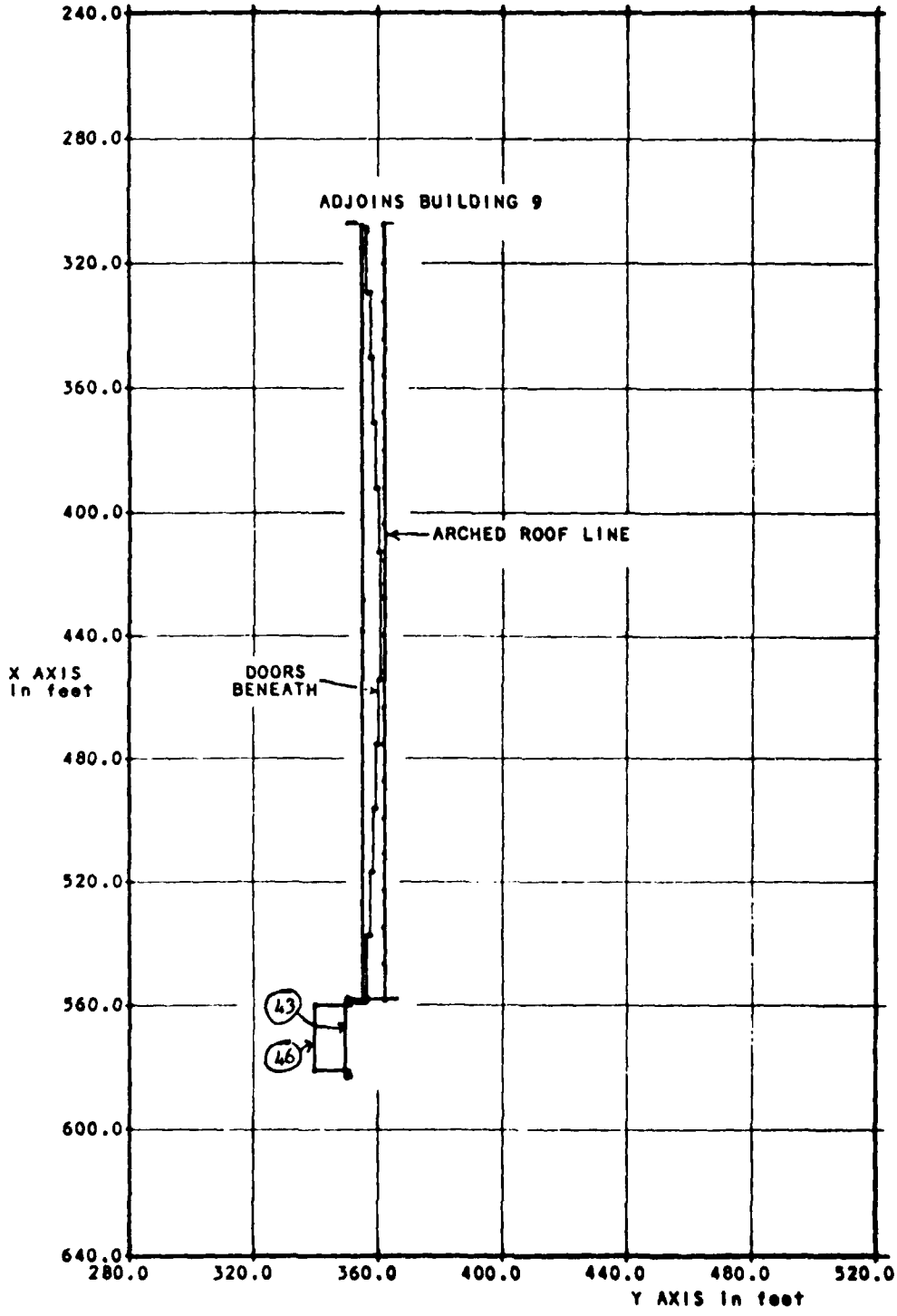

Figure A5 Building 1 Plan

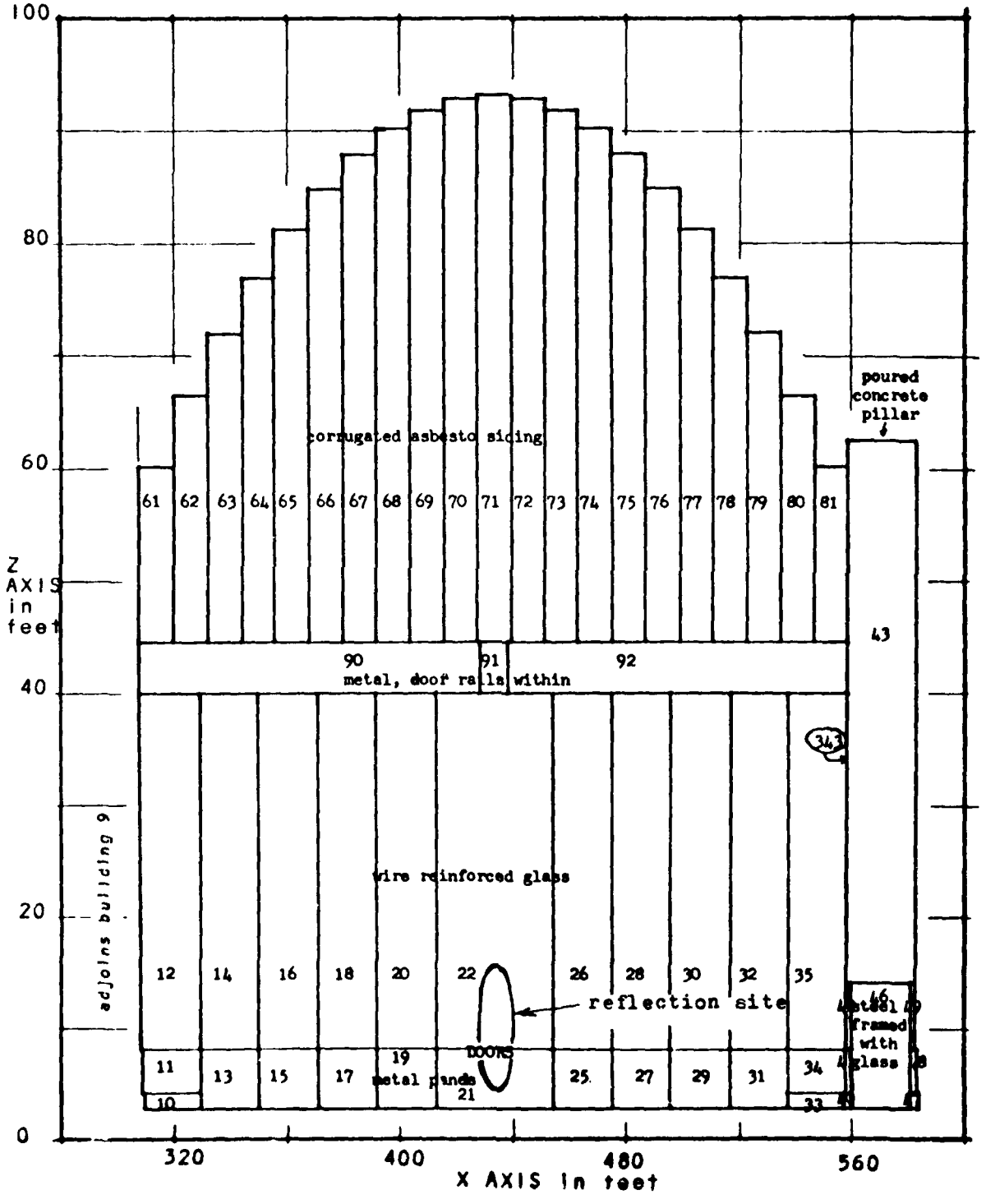

Figure A6 Building 1 Front Elevation

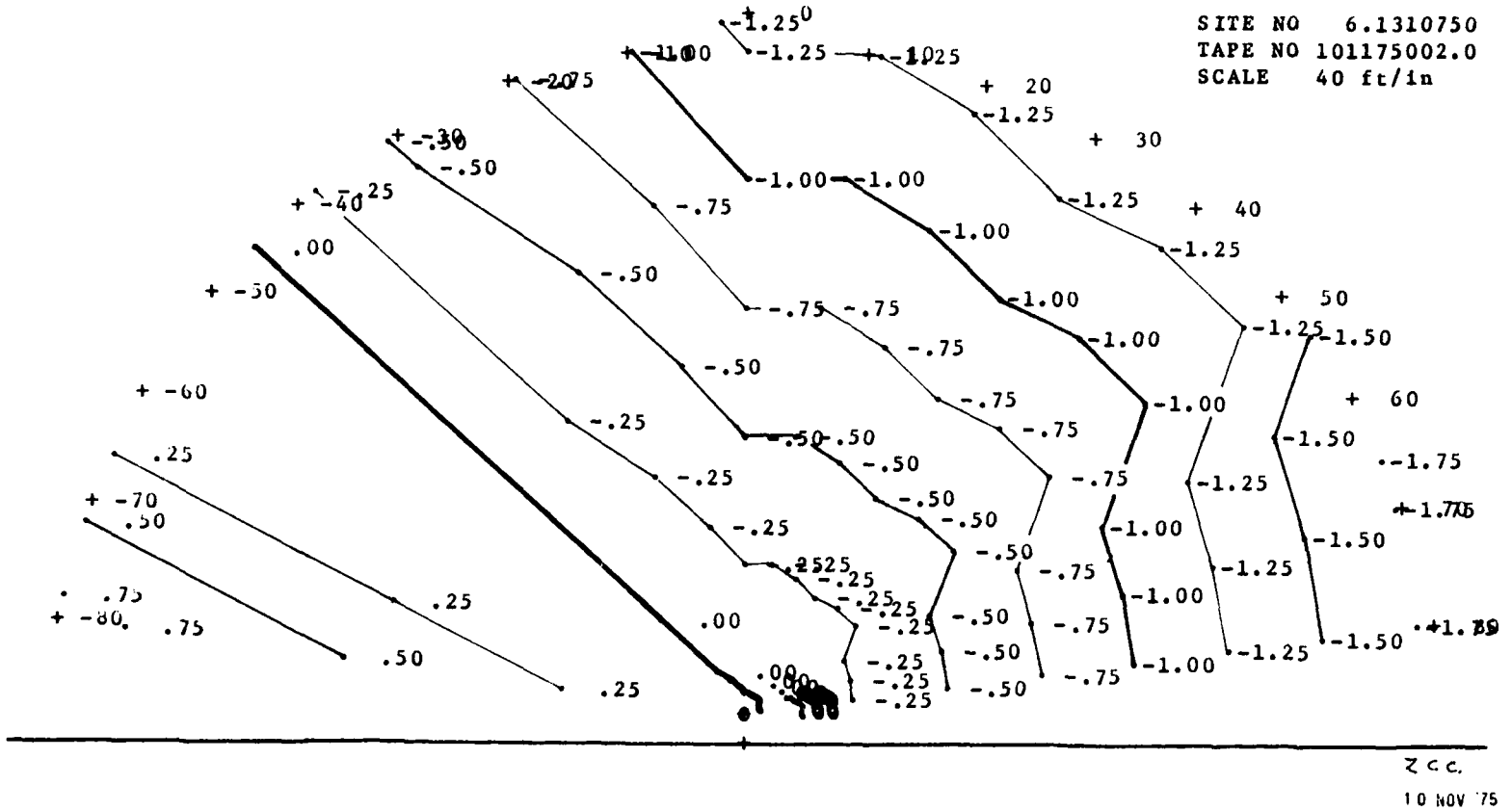

Figure A7 Building 6 Site Contour

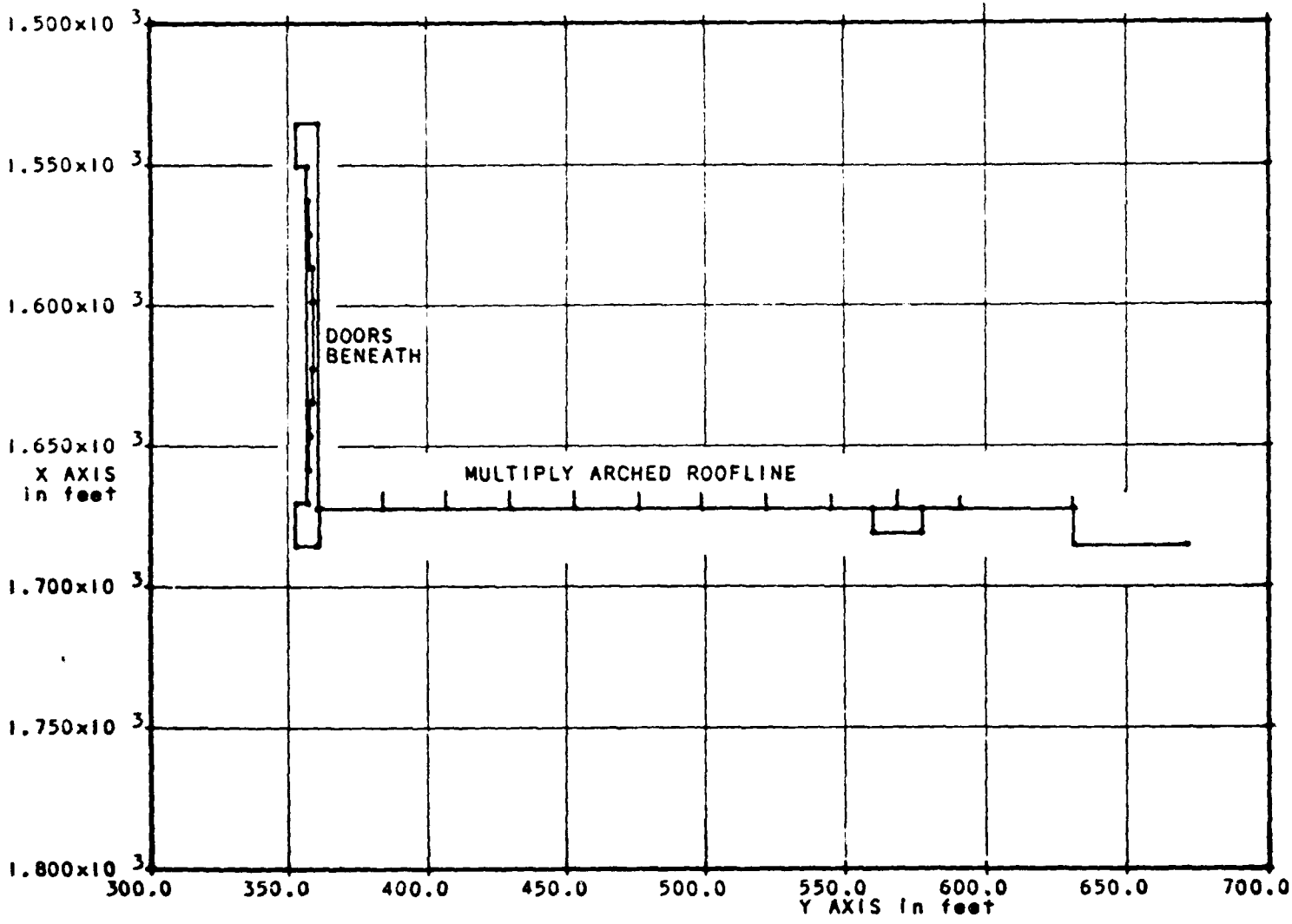

Figure A8 Building 6 Plan

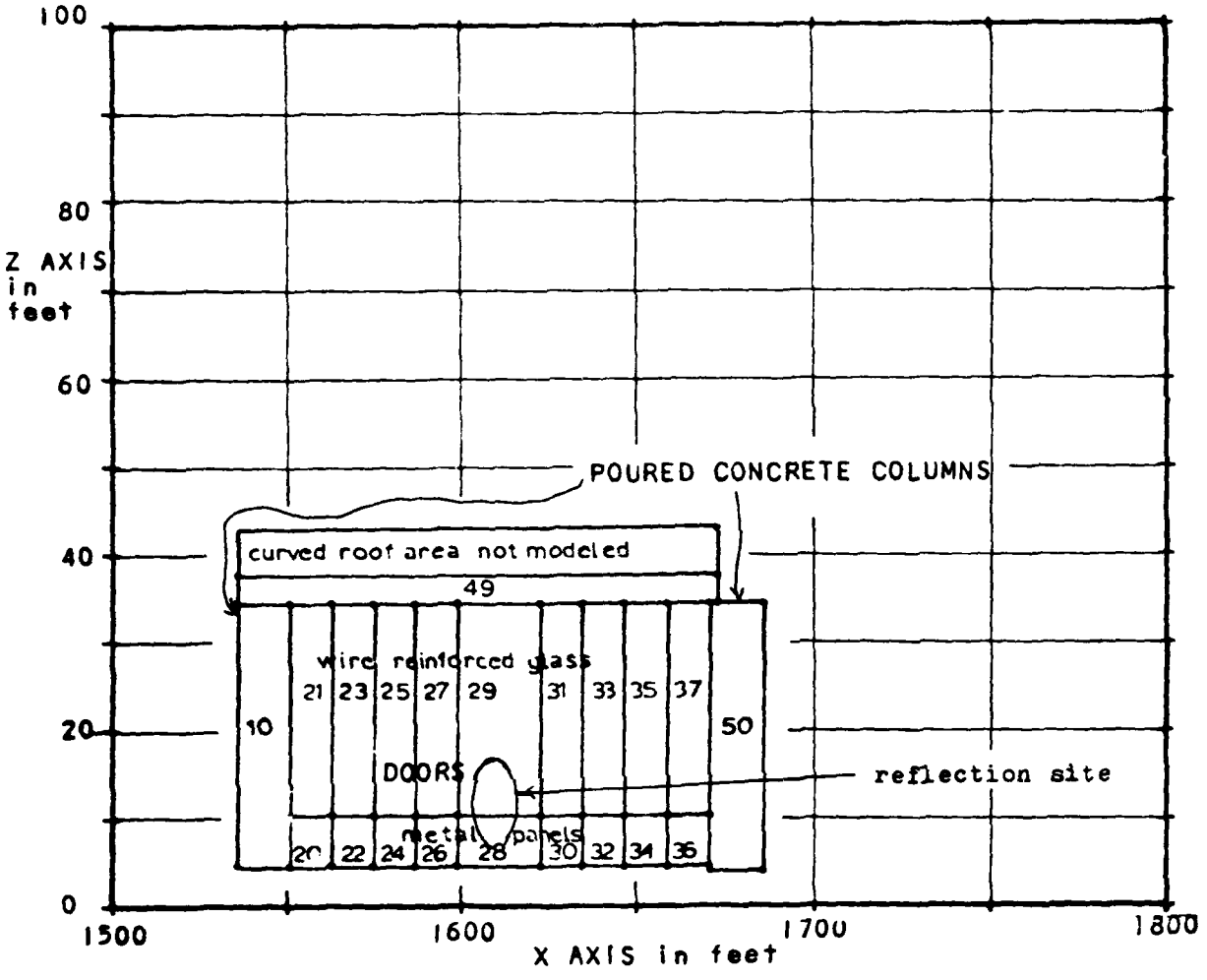

Figure A9 Building 6 Front Elevation

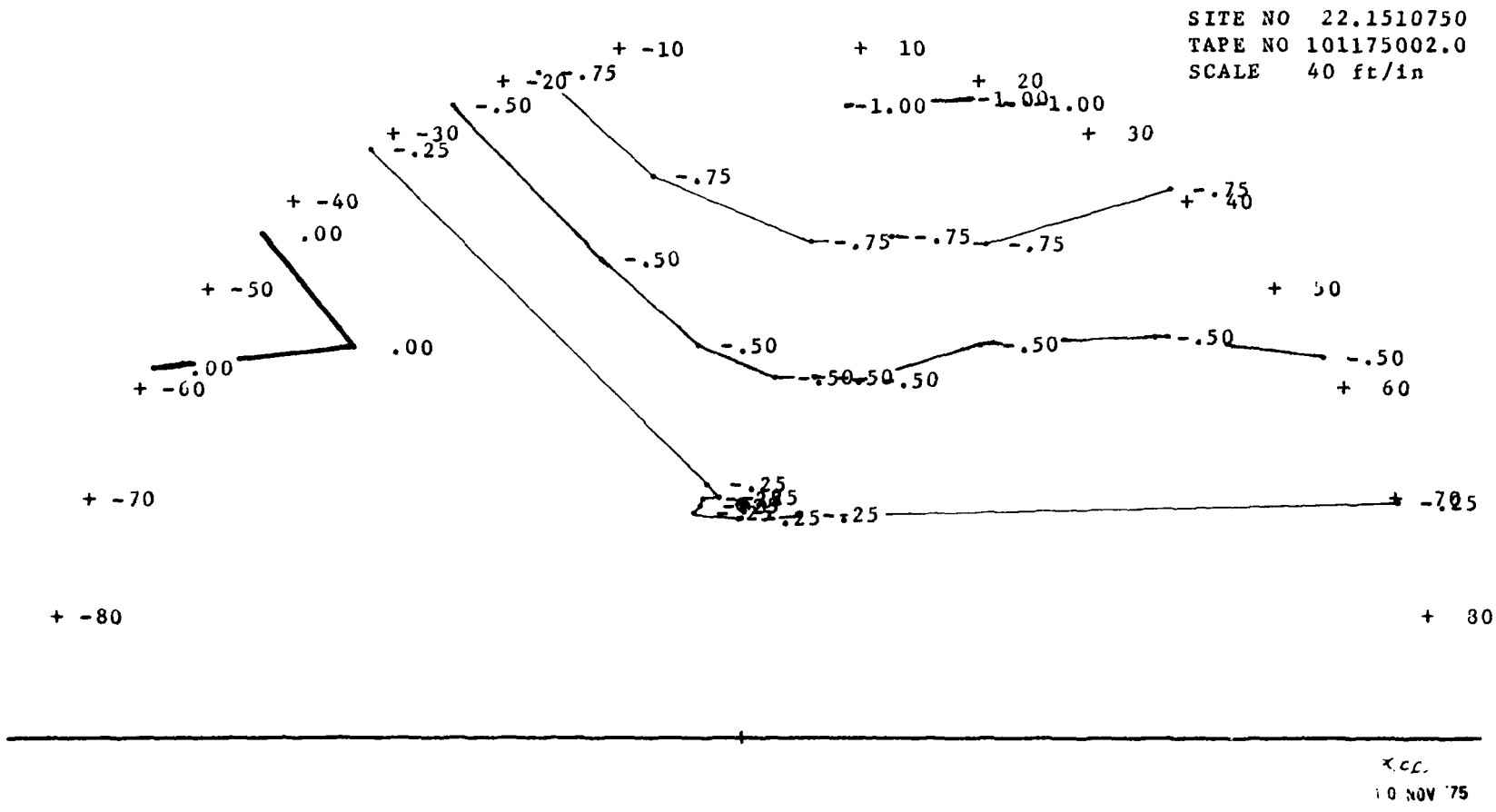

Figure A10 Building 22 Site Contour
Poured Concrete Section

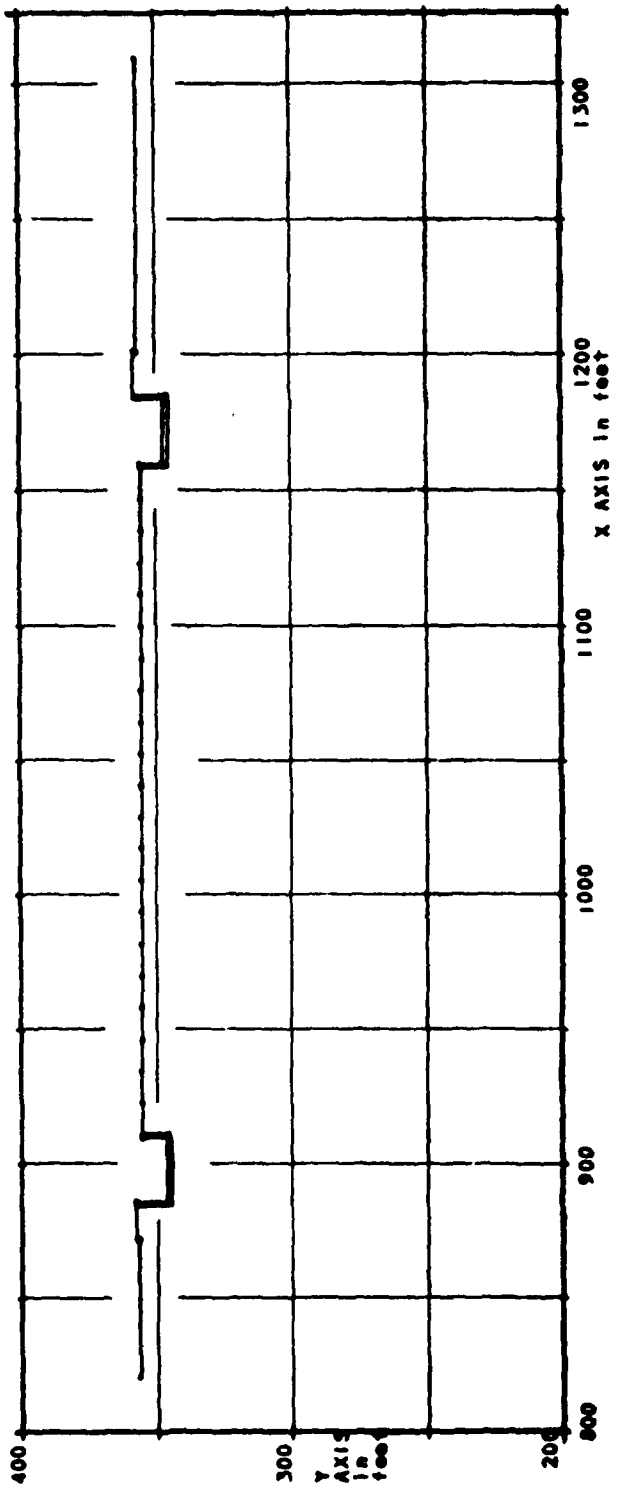

Figure A11 Building 22 Plan

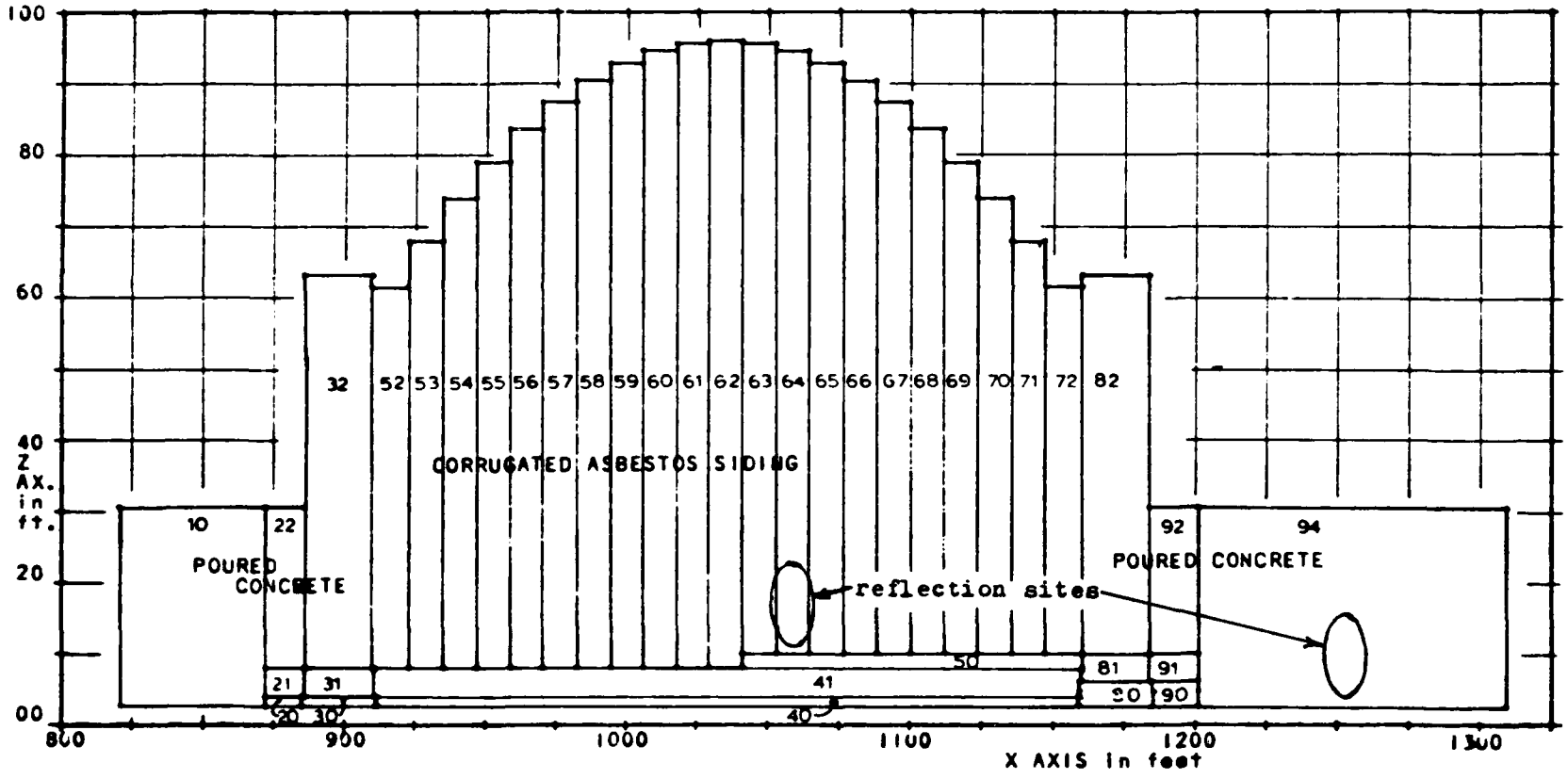

Figure A12 Building 22 Front Elevation

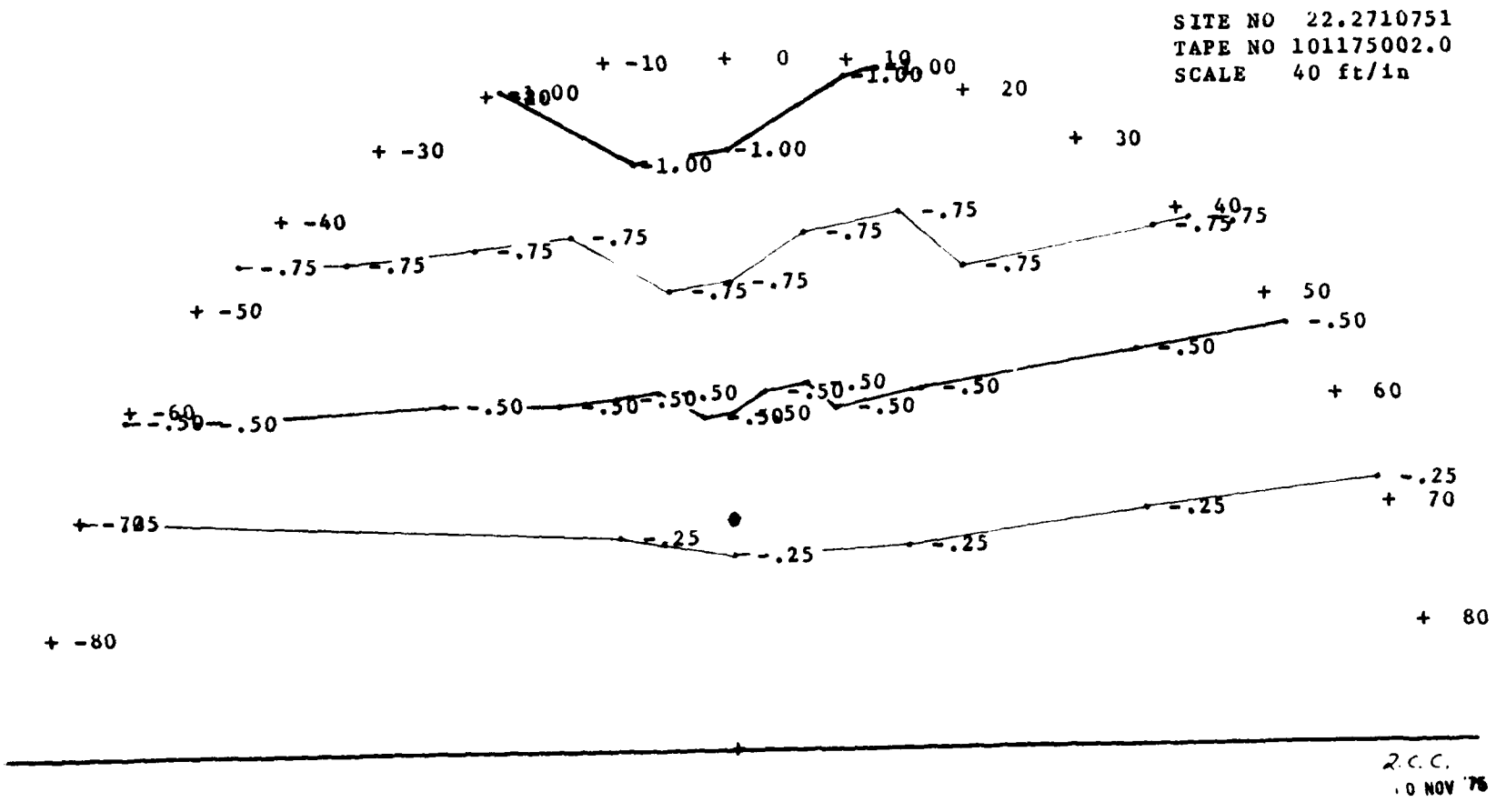

Figure A13 Building 22 Site Contour

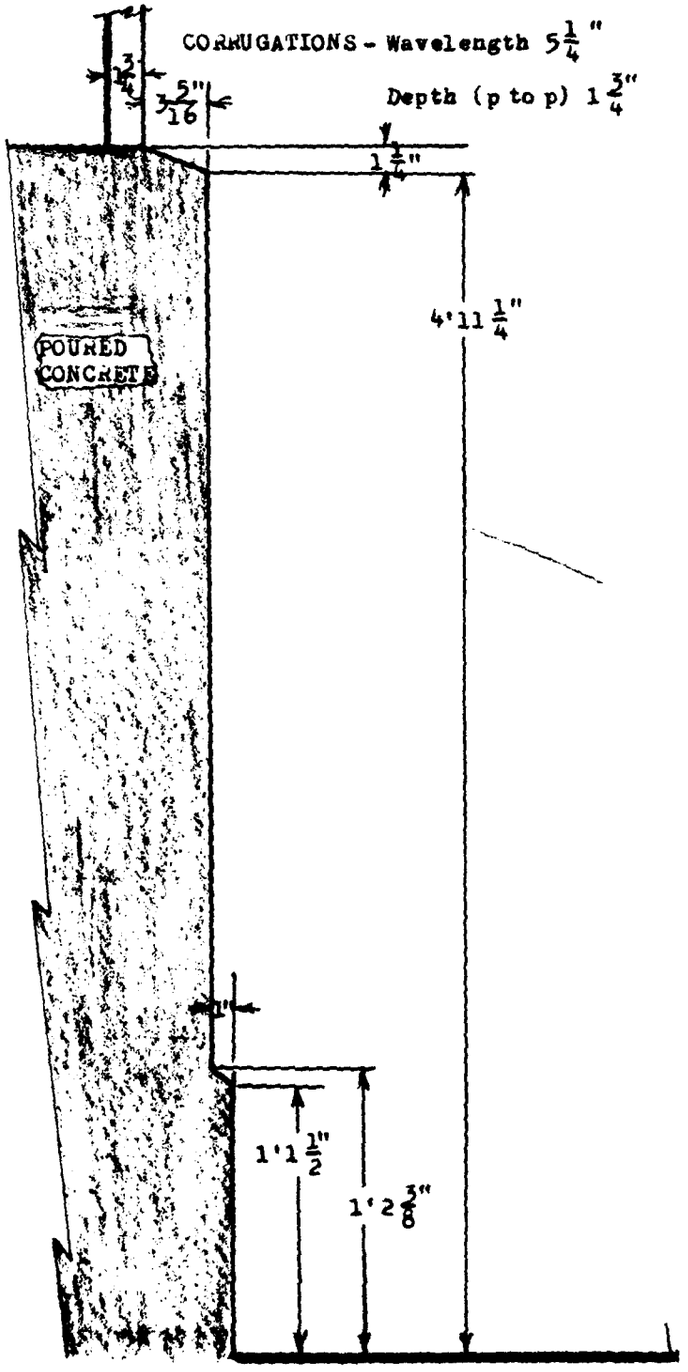

Figure A14 Section Through Building 22
Showing Corrugated Material

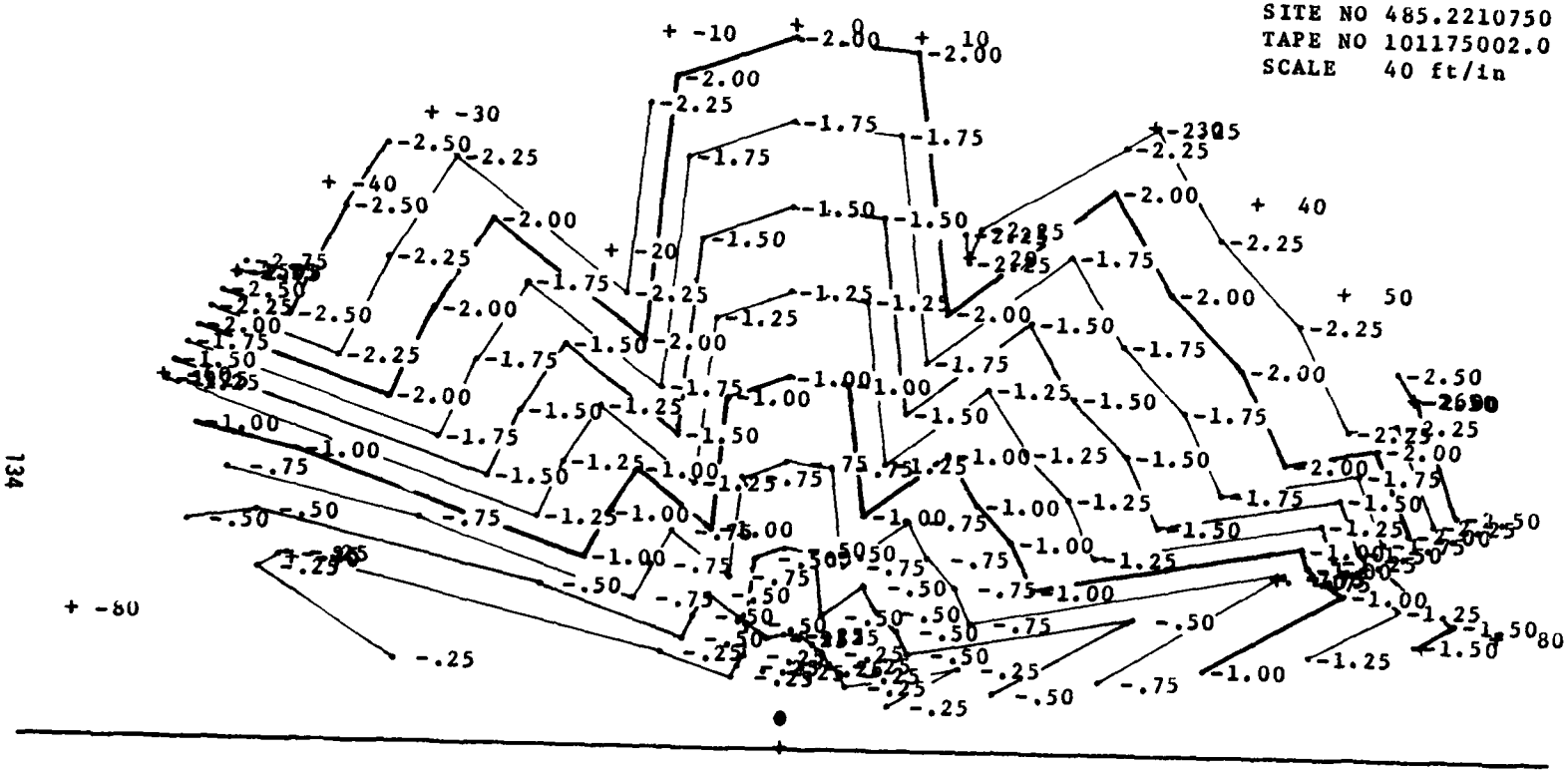

Figure A15 Building 485 Site Contour

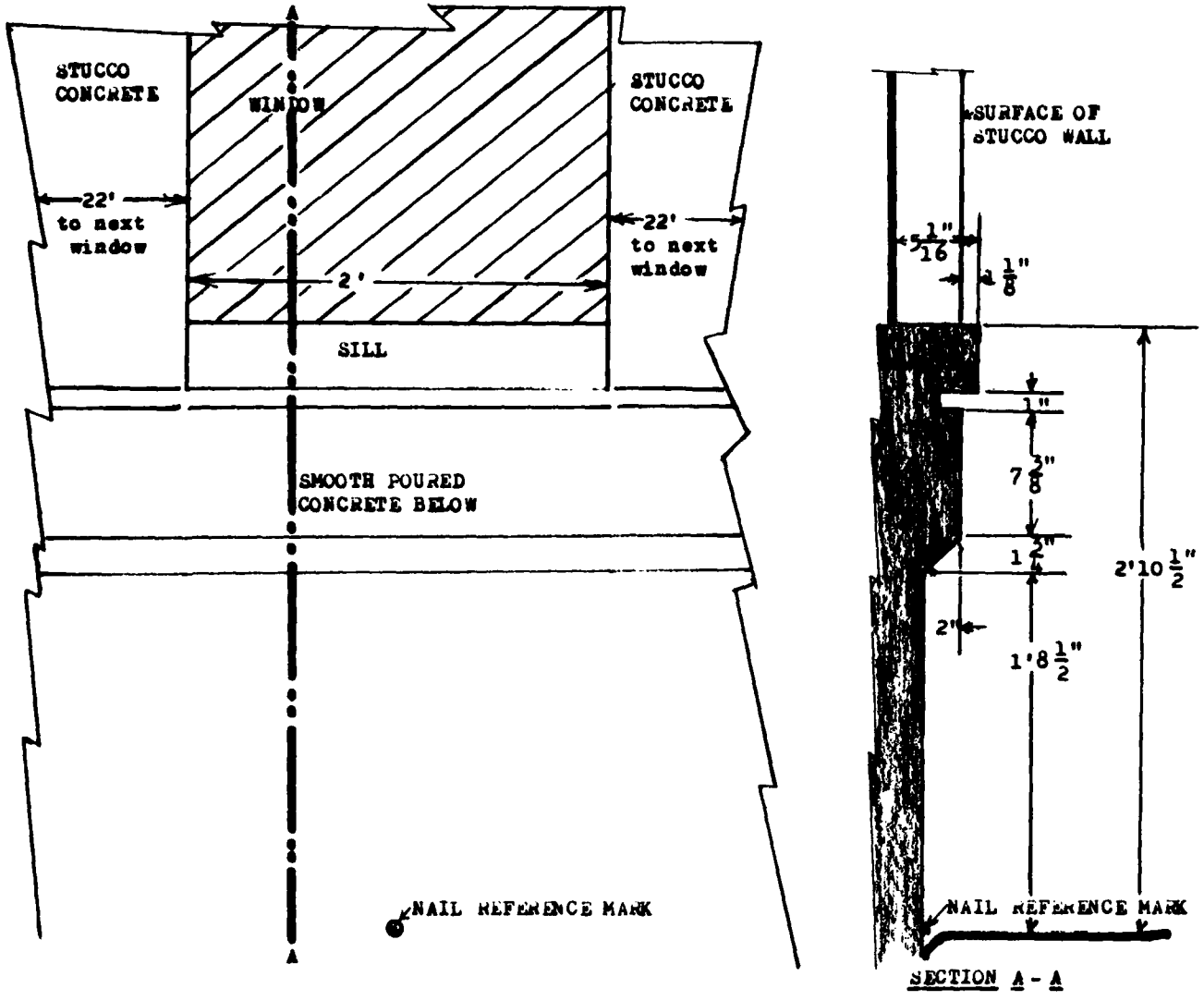

Figure A16 Building 485 Section Characteristics

24 NOV 75

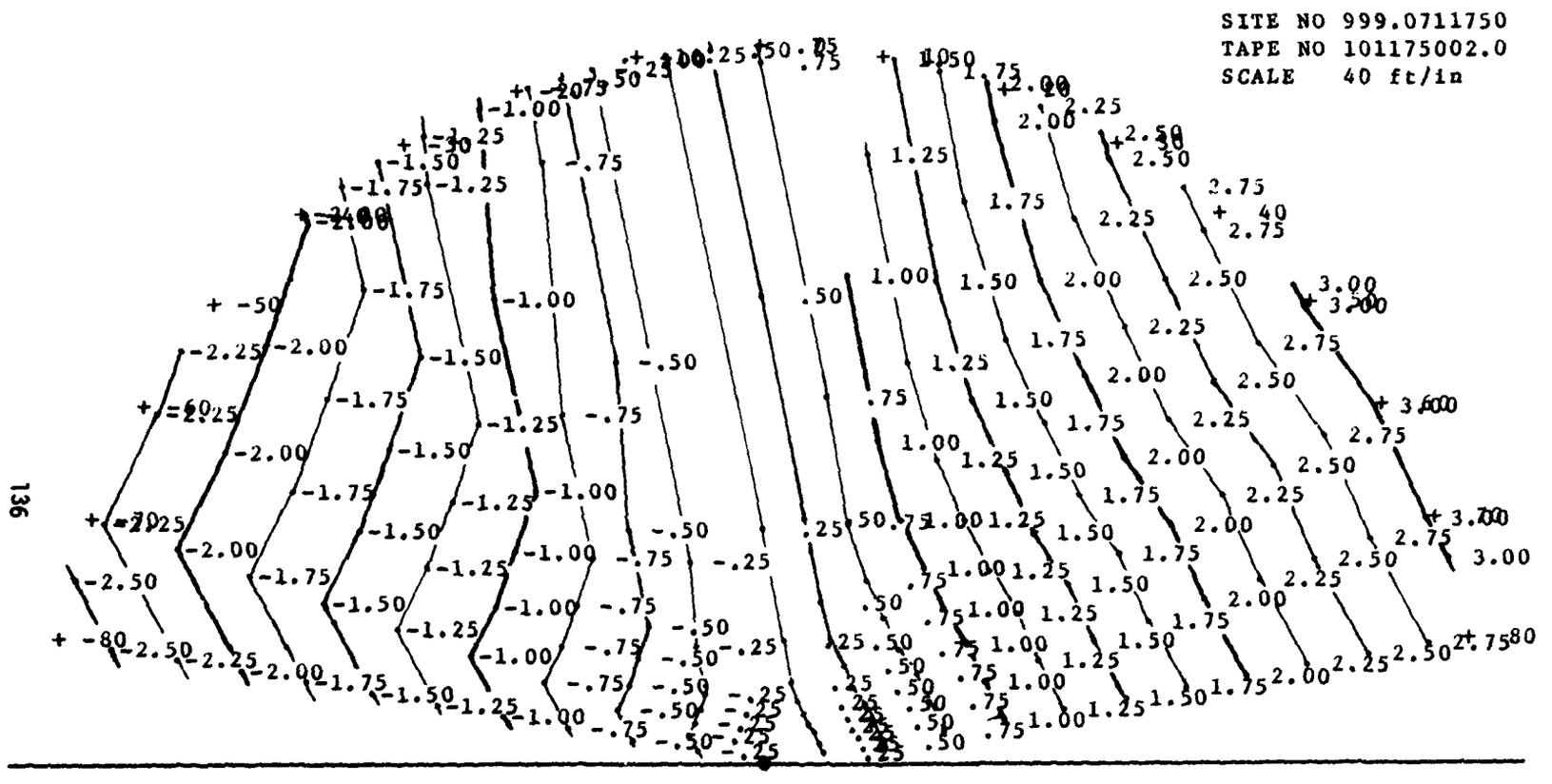

Figure A17 "Ghost" Site Contour at end of Area B runway

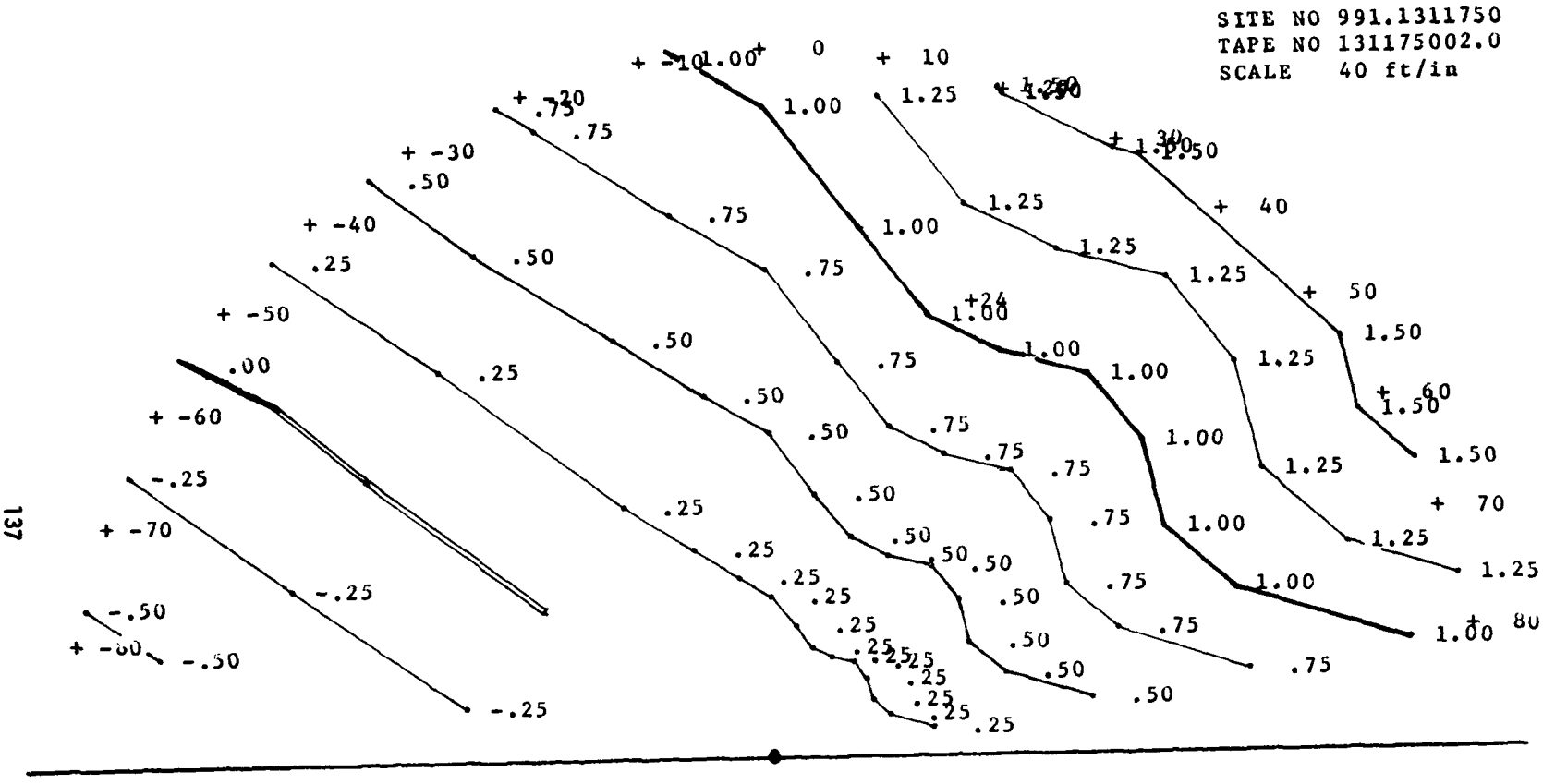

Figure A18 "Ghost" Site Contour Between Bldges 1 and 485

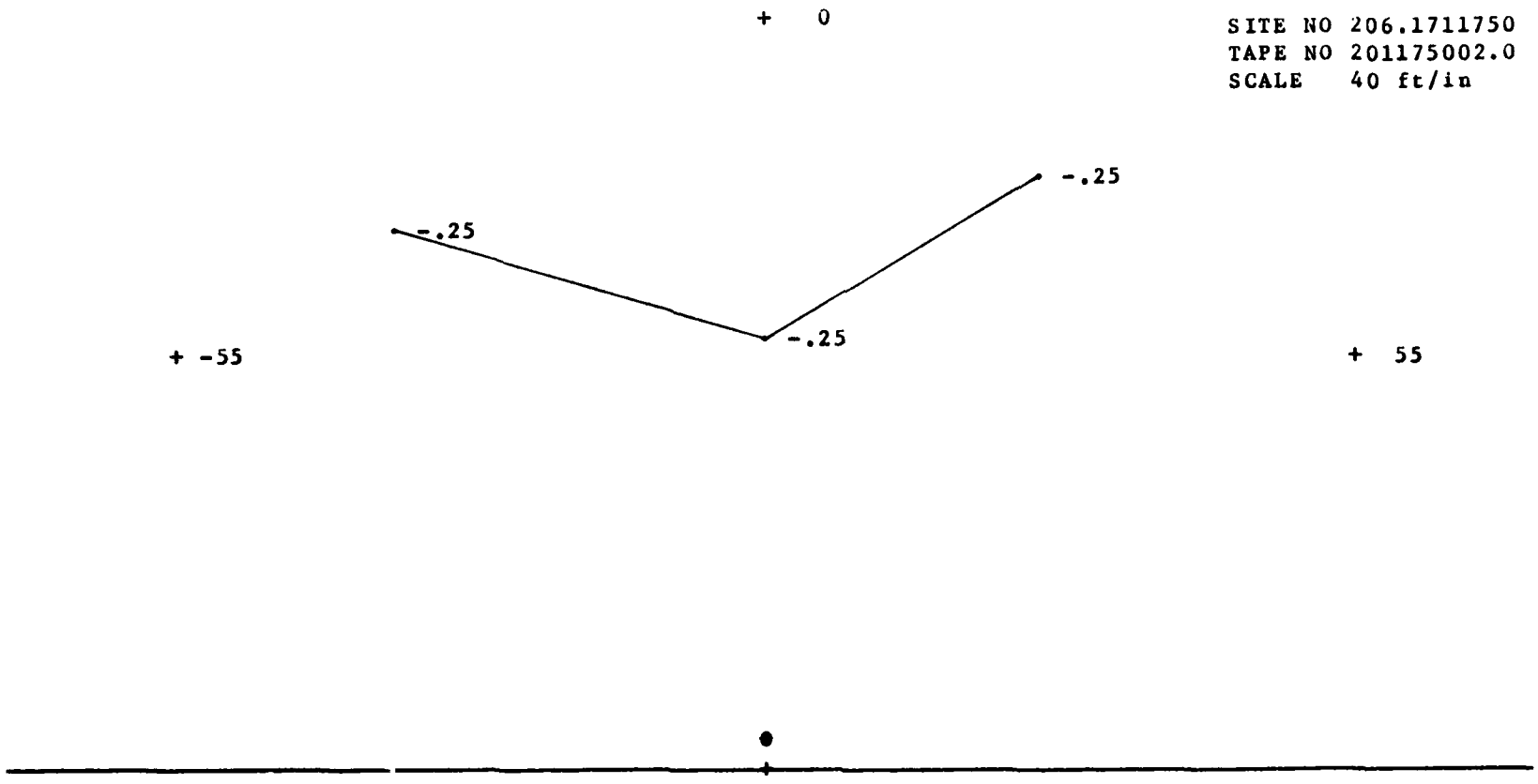

Figure A19 Building 206 Site Contour

APPENDIX B

Geometric Considerations

Introduction

An important aspect of test planning for the present experiments relates to the control of the illumination of the desired reflecting surface. To this end it is desired that incident signal fall uniformly on the homogeneous surface and that the transmitted power be directed mainly into the primary reflecting region with reduced illumination away from it. The main tools for exercising such control are: 1) first Fresnel zone, 2) illumination spot, and 3) antenna heights. This appendix is concerned with the first two of these items insofar as they may have impact on the present experimental program. In particular it is of interest to see how they behave for shallow grazing angles.

Fresnel Zone

For a given frequency (or wavelength) a Fresnel ellipsoid may be defined, with respect to two given points in space, as the locus of points such that sum of the distances from a point in the locus to the two given points in greater than the distance between the two given points by an integral number of half wavelengths.

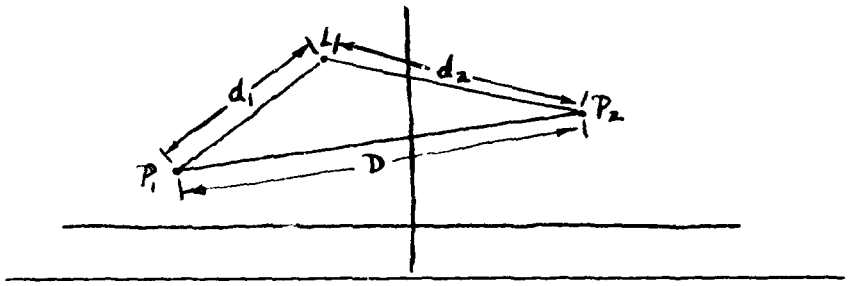

If $d_1 + d_2 = D + \frac{n\lambda}{2}$

Then L is in the nth Fresnel Ellipsoid

The condition may be viewed in the plane as shown, but of course it holds as well for three dimensions. The locus is an ellipsoid of revolution about the axis connecting P_1 and P_2. When a reflecting surface is involved the locus is somewhat more complex, but a useful planar representation is still feasible.

Again, if $d_1 + d_2 = D + \frac{n\lambda}{2}$

L is in the nth Fresnel Ellipsoid.

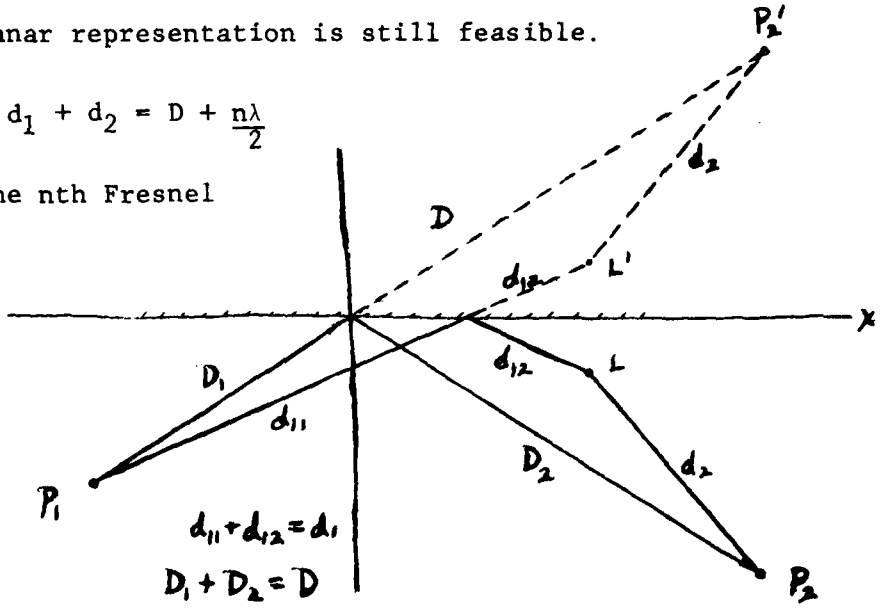

Here the X axis represents the reflecting surface. P_2' is the geometric image of P_2 and L' of L. Clearly, the point P_2 may be replaced, for ease of computation, by P_2' generate those points of the locus which coincide with the reflecting surface. These points constitute a plane figure which may be shown to be an ellipse. That figure is a Fresnel zone at the reflecting surface. When n=1 the first Fresnel zone is defined. For present purposes, this is the Fresnel zone of interest.

Now consider the case shown in the third figure

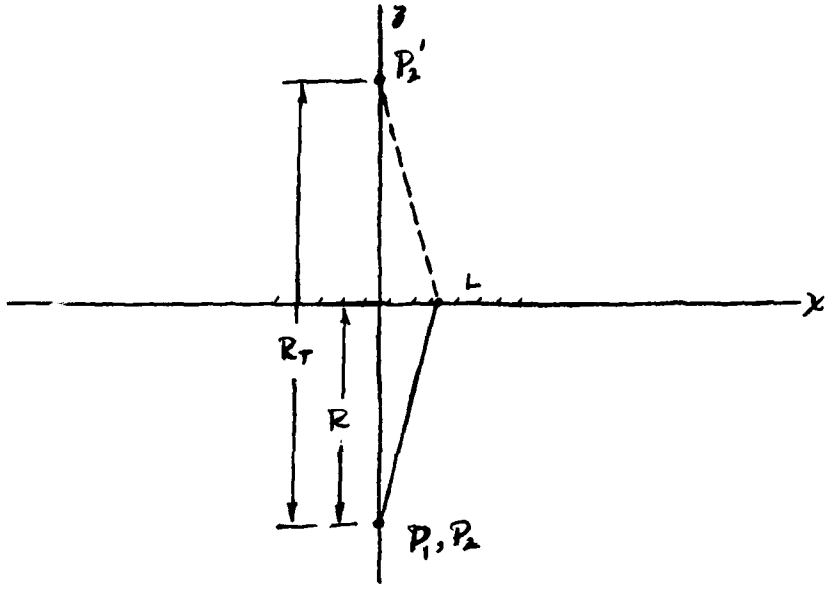

For this geometry the ellipsoid reduces to a simple mathematical form.

$$\frac{x^2}{B^2} + \frac{y^2}{B^2} + \frac{z^2}{A^2} = 1$$

where $A = \frac{R_T}{2} + \frac{\lambda}{4}$ and $B = \sqrt{\frac{R_T\lambda}{2} + \frac{\lambda^2}{16}}$

The first Fresnel zone, at the reflecting surface, can be found simply by setting z = 0. The result is a circular region of radius B. In general $R_T \neq 2R$, but rather $R_T = R_1 + R_2$. This situation may be accommodated by a translation in z. Also in general, the incidence angle will be something greater than zero. This situation may be handled by means of a rotation of the ellipsoid in the x-z plane. For the translation it is necessary only to substitute z + a for z. For the rotation the following substitutions are necessary.

$$\left.\begin{aligned} x &= u\cos\phi - v\sin\phi \\ y &= \zeta \\ z &= u\sin\phi + v\cos\phi \end{aligned}\right\}$$ ϕ corresponds to the angle of incidence*

Effecting both of these substitutions gives

$$\frac{(u\cos\phi - v\sin\phi)^2}{B^2} + \frac{\zeta^2}{B^2} + \frac{(u\sin\phi + v\cos\phi + a)^2}{A^2} = 1$$

But the intersection of the ellipsoid with the $u - \zeta$ plane (which now corresponds to the reflecting surface) occurs when $v = 0$. Also, the origin of this plane is pierced by the direct path between P_1 and P_2'.

Hence,

$$\frac{u^2\cos^2\phi}{B^2} + \frac{\zeta^2}{B^2} + \frac{u^2\sin^2\phi + 2au\sin\phi + a^2}{A^2} = 1$$

After collecting terms and completing the square, this expression may be worked into the following form.

$$\frac{(u - Y)^2}{\Lambda^2} + \frac{\zeta^2}{\Omega^2} = 1$$

where

$$Y = \frac{a B^2 \sin\phi}{A^2\cos^2\phi + B^2\sin^2\phi}$$

$$\Lambda^2 = A^2 B^2 \left[\frac{(A^2 - a^2)\cos^2\phi + B^2\sin^2\phi}{(A^2\cos^2\phi + B^2\sin^2\phi)^2}\right]$$

$$\Omega^2 = B^2 \left[\frac{(A^2 - a^2)\cos^2\phi + B^2\sin^2\phi}{A^2\cos^2\phi + B^2\sin^2\phi}\right]$$

But $A \simeq \frac{R_T}{2}$ i.e. $\frac{R_1 + R_2}{2}$

$B \simeq \sqrt{\frac{(R_1 + R_2)\lambda}{4}}$ i.e. $\sqrt{\frac{R_T\lambda}{4}}$ See previous page

* This is the complement of "grazing angle".

and $a = R_1 - A$ or $A - R_2$ so that

$$a = \frac{R_1 - R_2}{2}$$

Finally, grazing angle, θ, is equal to $\frac{\pi}{2} - \phi$.

Substituting these values gives

$$Y = \frac{\frac{(R_1 - R_2)}{2} \cdot \frac{R_T\lambda}{4} \cdot \cos\theta}{\frac{R_T^2}{4}\sin^2\theta + \frac{R_T\lambda}{4}\cos^2\theta}$$

$$\boxed{Y = \frac{(R_1 - R_2)\,\lambda \cos\theta}{2(R_T \sin^2\theta + \lambda \cos^2\theta)}}$$

$$\Lambda^2 = \frac{\frac{R_T^2}{4} \cdot \frac{R_T\lambda}{4} \cdot}{\frac{R_T^2}{4}\sin^2\theta + \frac{4R_T\lambda}{4R_T}\cos^2\theta} \left[\frac{\frac{4R_1R_2}{R_T}\sin^2\theta + \frac{4R_T\lambda}{4R_T}\cos^2\theta}{\frac{4R_T^2}{4R_T}\sin^2\theta + \frac{4R_T\lambda}{4R_T}\cos^2\theta}\right]$$

$$\boxed{\Lambda^2 = \frac{R_T\lambda}{4(\sin^2\theta + \frac{\lambda}{R_T}\cos^2\theta)} \left[\frac{\frac{4R_1R_2}{R_T}\sin^2\theta + \lambda\cos^2\theta}{R_T\sin^2\theta + \lambda\cos^2\theta}\right]}$$

Similarly

$$\boxed{\Pi^2 = \frac{R_T\lambda}{4} \left[\frac{\frac{4R_1R_2}{R_T}\sin^2\theta + \lambda\cos^2\theta}{R_T\sin^2\theta + \lambda\cos^2\theta}\right]}$$

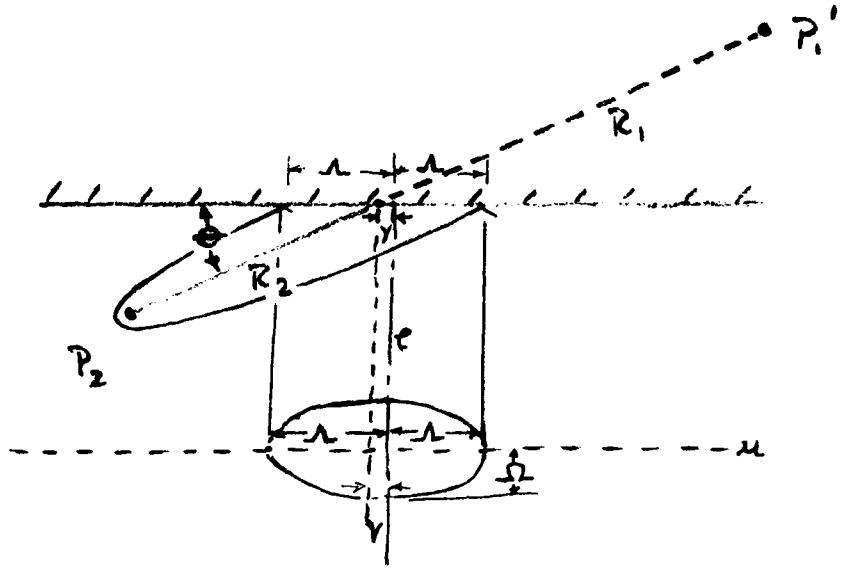

Useful forms of these equations, for the short range geometries considered in the present experiment, take advantage of the fact that $R_1 = R_2$. Consequently

$$Y = 0$$

$$\Lambda^2 \cong \frac{R_T \lambda}{4 \sin^2 \theta}$$

$$\Omega^2 \cong \frac{R_T \lambda}{4}$$

$R_T \simeq 2000$

$R_1 = R_2$

3°

Illumination Spot

Consider illumination of a vertical reflector with RF energy from a pencil beam (of circular cross section). The beam axis is in the horizontal plane, and pierces the reflector at the aim point forming an incidence angle, ϕ, also in the horizontal plane.

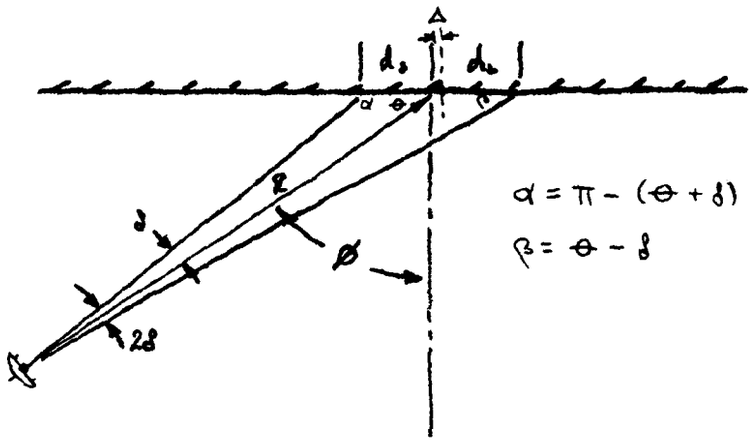

If the illuminated spot is considered to be within the 3db beamwidth, 2δ, of the antenna, it can be seen that on the reflector the illuminated spot will form an ellipse with horizontal major axis.

The center of the major axis will be displaced away from the antenna boresight intersection.

$$\Delta = \frac{d_L - d_S}{2}$$

By the law of Sines

$$\frac{d_S}{\sin\delta} = \frac{R}{\sin(\theta + \delta)} \quad \text{and} \quad d_L = \frac{R}{\sin(\theta - \delta)}$$

$$d_S = \frac{R \sin\delta}{\sin(\theta + \delta)} \qquad d_L = \frac{R \sin\delta}{\sin(\theta - \delta)}$$

and

$$\Delta = \frac{R \sin\delta}{2}\left[\frac{1}{\sin(\theta - \delta)} - \frac{1}{\sin(\theta + \delta)}\right]$$

$$\Delta = R \sin\delta\left[\frac{2\cos\theta \sin\delta}{\cos(2\delta) - \cos(2\theta)}\right].$$

Similarly, the semi-major axis is given by $L = \frac{d_S + d_L}{2}$

$$L = R \sin\delta\left[\frac{2\sin\theta\cos\delta}{\cos(2\delta) - \cos(2\theta)}\right].$$

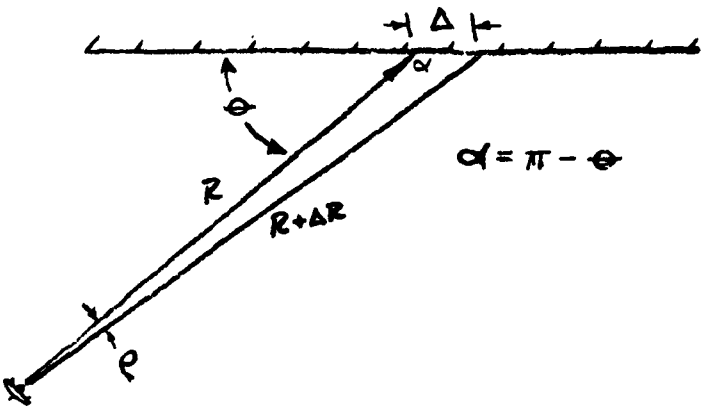

This geometry characterizes the problem of determining the semi-minor axis, S, of the illumination ellipse.

$$S = (R + \Delta R)\tan\delta\cos\rho$$

By the Law of Cosines

$$(R + \Delta R)^2 = R^2 + \Delta^2 - 2R\Delta\cos(\pi - \theta)$$

$$= R^2 + \Delta^2 + 2R\Delta\cos\theta$$

$$= R^2\left(1 + \frac{\Delta^2 + 2R\Delta\cos\theta}{R^2}\right)$$

and $$(R + \Delta R) = R\left(1 + \frac{\Delta^2 + 2R\Delta\cos\theta}{R^2}\right)^{\frac{1}{2}}$$

$$(R + \Delta R) \simeq R\left(1 + \frac{\Delta^2 + 2R\Delta\cos\theta}{2R^2}\right)$$

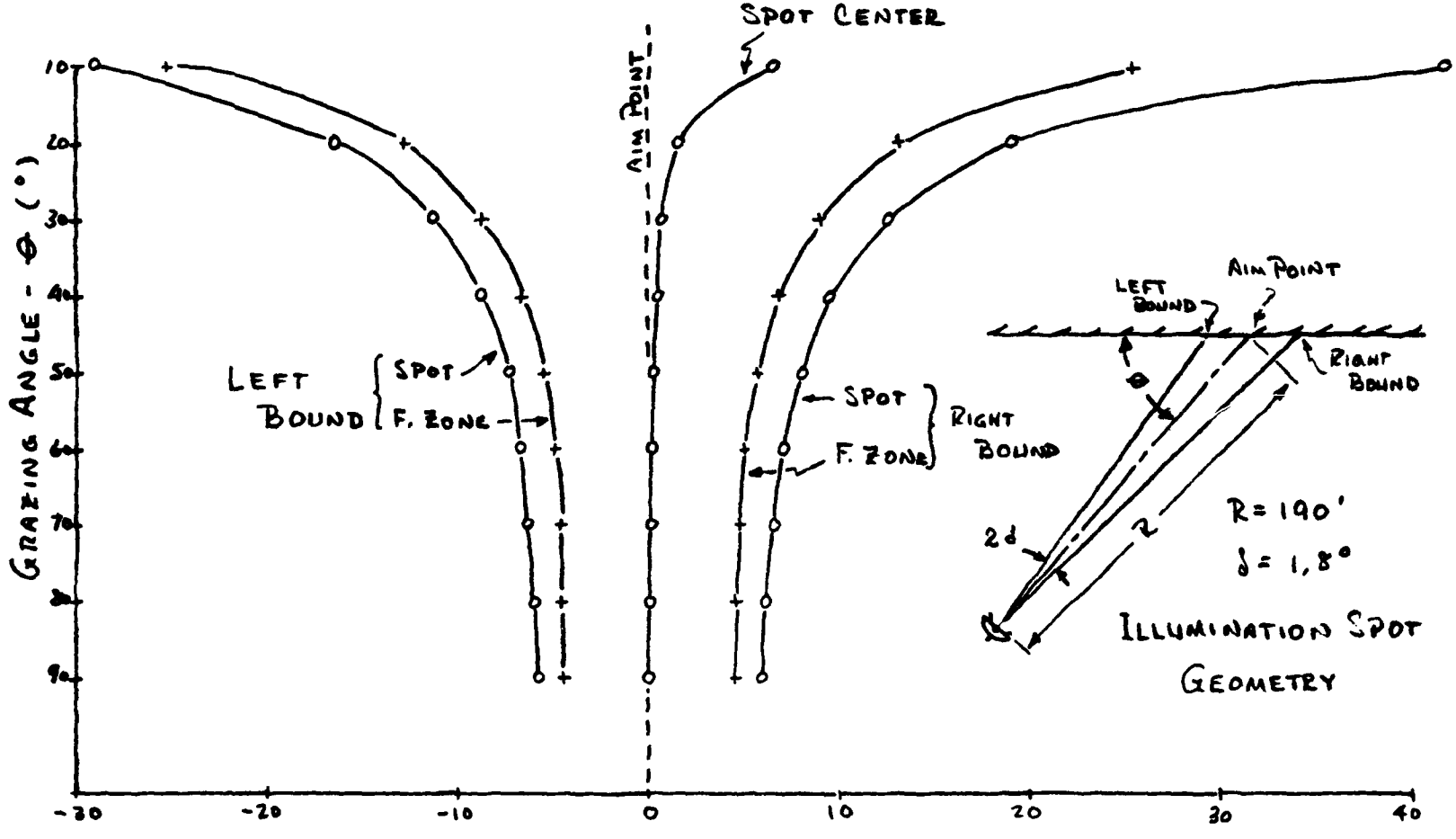

Figure B1 SPOT & FRESNEL ZONE BOUNDS (FT)

$$(R + \Delta R) \simeq R + \Delta \cos\theta + \frac{\Delta^2}{2R}$$

Also $$\rho \simeq \frac{\Delta \sin\theta}{R} \quad \text{radians}$$

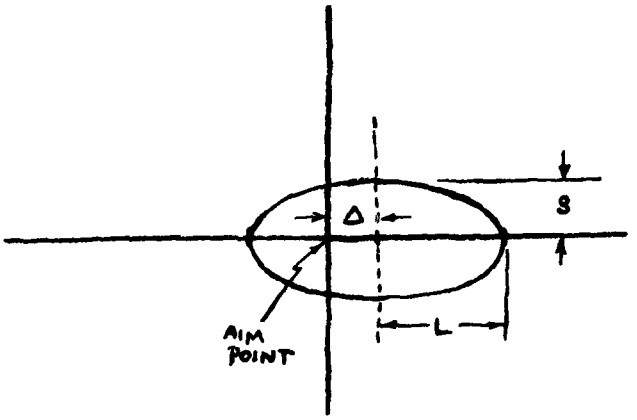

And in summary:

$$= R \sin\phi \left[\frac{2 \cos\theta \sin\phi}{\cos(2\phi) - \cos(2\theta)} \right]$$

$$L = R \sin\phi \left[\frac{2 \sin\theta \cos\phi}{\cos(2\phi) - \cos(2\theta)} \right]$$

$$S = (R + \Delta R) \tan\phi \cos\rho \begin{cases} (R + \Delta R) \simeq R + \Delta\cos\theta + \dfrac{\Delta^2}{2R} \\ \rho \simeq \dfrac{\Delta \sin\theta}{R} \text{ radians} \end{cases}$$

For the experimental range and beamwidth, these various relations are summarized for the full range of grazing angles. It should be noted that, for shallow grazing angles, even though the Fresnel zone is all within the 3 db spot, illumination will vary because of the range differentials. These are largely compensated by the increased range on the remainder of the reflected path. In fact, at the bounds of the Fresnel zone, the total difference from path length through the aim point is only one half wavelength. This wavelength amounts to about 2.5 inches at C Band and roughly an inch at Ku Band.

☆ U. S. GOVERNMENT PRINTING OFFICE: 1976 — 657-630/963